UC Berkeley
UC Berkeley Electronic Theses and Dissertations

Title
Enclosed Microfluidic Platform Realizing Enhanced Stem-cell Survival

Permalink
https://escholarship.org/uc/item/40j4h0mn

Author
Zhang, Yolanda Yue

Publication Date
2011

Peer reviewed|Thesis/dissertation

eScholarship.org Powered by the California Digital Library
University of California

Enclosed Microfluidic Platform Realizing Enhanced Stem-cell Survival (EMPRESS)

By

Yue Zhang

A dissertation submitted in partial satisfaction of the

requirements for the degree of

Joint Doctor of Philosophy

with University of California, San Francisco

in

Bioengineering

in the Graduate Division

of the

University of California, Berkeley

Committee in charge:

Professor Matthew V. Tirrell, Chair
Professor Albert P. Pisano
Professor Tejal A. Desai

Fall 2011

ABSTRACT

Enclosed Microfluidic Platform Realizing Enhanced Stem-cell Survival (EMPRESS)

by

Yue Yolanda Zhang

Joint Doctor of Philosophy

University of California, Berkeley
with University of California, San Francisco

Here we present a microfluidic culture platform for enhancing single stem cell survival. Traditional plate culture is inadequate for large scale single cell studies because of (1) less than 40% single stem cell survival leading to (2) possible inaccuracies in the biostatistics in single cell studies from lack of sufficient data. This platform mitigates these issues by doubling overall survival rates as well as increasing the available data points by two orders of magnitude, both factors which improve statistical certainty. The platform is fabricated using widely accepted biocompatible polymers and incorporates the novel integration of an enclosed microwell array with an upstream linear gradient generator. The device can selectively trap single cells, tightly control intercell spacing, and change the chemical microenvironment around the stem cells in real-time. In this dissertation, we first characterize the performance of the platform in improving single cell survivability. Subsequently, the system was tested using two difference stem cell types: mouse embryonic stem cells (mES) and induced pluripotent stem cells (iPS). Using this platform we are able to highlight the thresholds of leukemia inhibitory factor concentrations which lead to metastable gene expression of Nanog, a key stem cell pluripotency regulator in mES cells. The enhanced survival of single cells has also enabled the statistically significant observation of Nanog+, non-proliferative, single mES cells which are previously unreported in literature.

Table of Contents

CHAPTER 1: INTRODUCTION

This dissertation presents the design, fabrication, characterization and application of a pump-free, rapidly manufacturable microfluidic platform which enhances survival of single stem cells for single cell studies. The platform is an integrated culture system composed of an upstream linear gradient generator and an enclosed microwell cell trapping array and is optimized to enhance survival of single stem cells for single cell clonal culture studies.

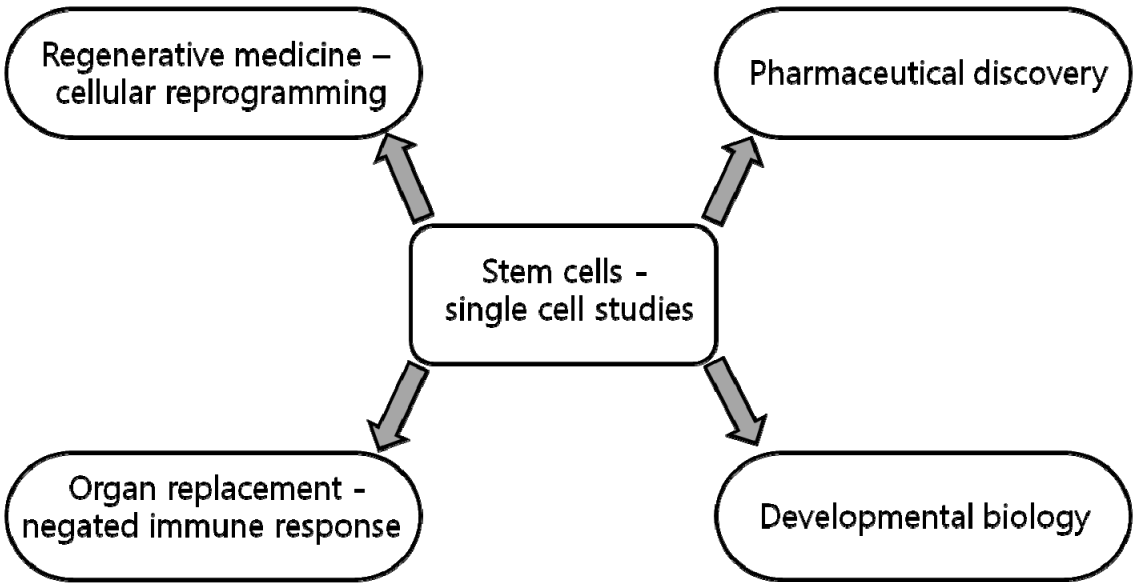

Figure 1. Single cell studies of stem cells to discover novel subpopulations have great impact on clinical and basic science research fields such as regenerative medicine, developmental biology, pharmaceutical discovery, and organ replacement therapy.

The discovery of novel stem cell subpopulations has garnered great interests from fields including developmental biology, phamaceutical discovery, and regenerative medicine (Figure 1). However, the discovery of new stem cell subpopulations can only be achieved utilizing single cell studies, currently a difficult process due largely to high cell mortality rates. The low stem cell survival rate when they are dissociated into single cells (~10-40%) is a fundamental challenge as it significantly impacts the quality of the data obtained. Oftentimes, the researchers cannot eliminate obfuscating factors that select for cell survival and therefore influence the outcome of the experiment; especially if the study examines the expression of genes known to influence cell survival and proliferation. It is unfortunately common practice to disregard from consideration all cells/wells which did not survive until the endpoint of the experiment. Such circumstances give rise to inadvertent skewing of the data from selection pressures and could result in misplaced confidence in the conclusions. For instance, a researcher would not be able to determine whether 80% of the total cell population truly expresses high levels of gene X, or only 80% of the *surviving subpopulation* (a fraction of the total) that was selected for under the specific experimental conditions. In such cases, the

biostatistics of the study could be greatly improved if the survival rate of the entire population is increased, reducing the effect of unknown factors on cell survival and experimental outcome (Figure 2).

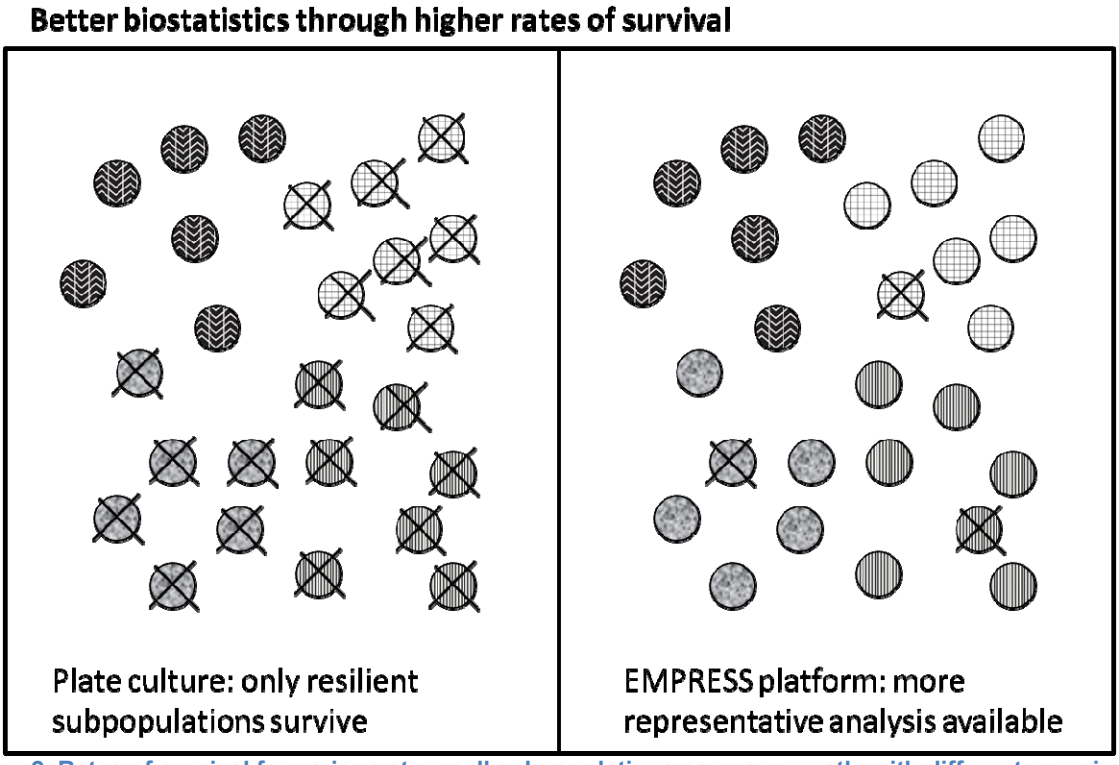

Figure 2. Rates of survival for various stem cell subpopulations can vary greatly with different experimental conditions. Current protocols for single stem cell culture suffer from heavy selection pressure against all but the strongest of cells (left). Our platform increases overall survival rates of the general stem cell population such that more representative data may be obtained (right).

The study of rare cells such as stem cells and progenitor cells does not lend itself to high-throughput population-based protocols due largely to the small quantities of cells available. In addition, using bulk analysis techniques such as RT-PCR or Western Blot will mask the difference between a normally distributed population and a bimodal or some other complex distribution (Figure 3). This distinction is especially important for stem cell studies since recent results suggest that the cross-regulatory interactions between core transcription factors and their target genes responsible for directing pluripotent cell identity are metastable, allowing a dynamic range of expression states[12]. Specifically, experiments examining the fate of single cells have proven to be crucial in examining stem cell self-renewal capacity and lineage restriction, and in identifying factors influencing proliferation and differentiation.[12, 13] Unfortunately, the analysis of individual stem cells within standard multiwell formats can be inefficient and time consuming and may not provide the necessary quantity and quality of data required.

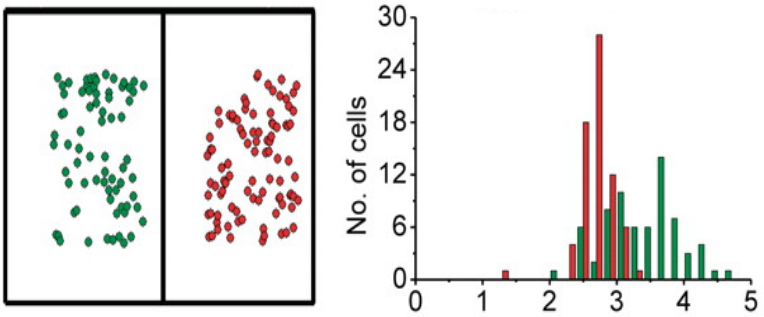

Figure 3. Bulk analysis will often mask the presence of subpopulations which exhibit differing behavior. Such population heterogeneity is of particular interest in the field of stem cell research where the desired phenotype is only a small fraction of total cells.

We present in this dissertation a novel microfluidic platform which is engineered to simultaneously optimize the survival of single stem cells of various subtypes, as well as increase available data points which can be mined from a limited starting population. The behavior of stem cells is extremely sensitive to elements in their local chemical and physical microenvironment such as soluble growth factors, matrix components, cell–cell contact, and the three-dimensional architecture of the niche itself, which shapes and restricts the delivery of these cues. The dilution of paracine and autocrine signaling molecules in standard plate culture not only creates a microenvironment that is drastically different from that in nature, but is very likely insufficient to sustain cell survival. We aim to use microfluidic engineering to control the local chemical and physical elements to maximum cell survival as single cells.

We hypothesize that the survival of single stem cells could be greatly improved by concentrating the intercellular secreted signals (survival cytokines) by significantly reducing the fluidic volume surrounding the cells (Figure 4). Traditional plate culture technique requires a minimum fluidic volume to be deposited into each well in order to minimize the effect of the meniscus on (1) cell distribution along the bottom, and (2) soluble molecule distribution. By taking advantage of the small fluidic volumes required by microfluidic systems, the volume surround each cell is reduced by more than 40-fold. We expect to enhance single cell survival of these delicate stem cells, and thus enable biological experiments previously hindered by extremely low cell survival rates.

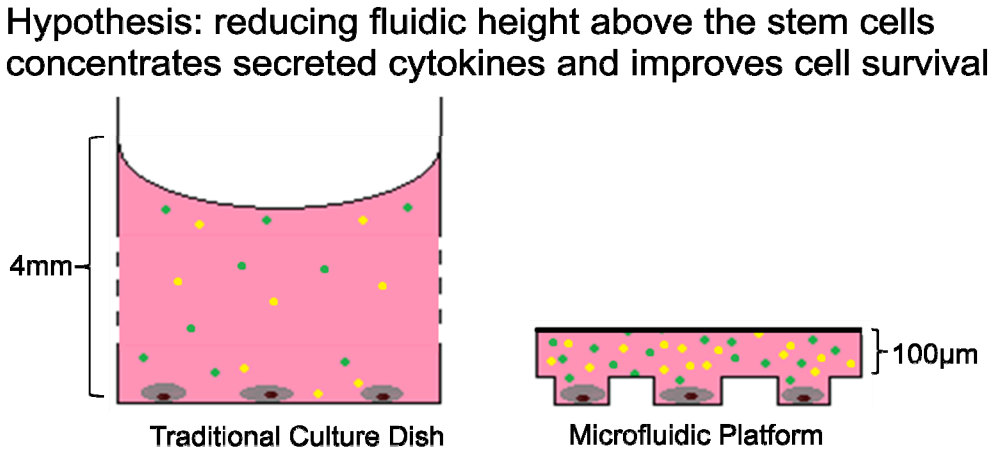

Figure 4. We design a microfluidic platform to reduce the fluidic "dead-volume" above adherent single cells by a factor of 40-fold (from 4mm to 100µm). A reduction in fluidic volume into which secreted cytokines can diffuse will increase local concentrations of survival cytokines, enhancing single cell survival.

This thesis is divided into six chapters including the introduction. The second chapter is a literature review of how microfluidics devices have contributed to stem cell studies so far. The third chapter characterizes the enhanced single stem cell survival which can be achieved on our platform. We demonstrate that this culture platform improves cell survival rates of mouse embryonic stem cells compared to previously published work on standard well plates, and that the number of data points generated is increased by at least an order of magnitude. The fourth chapter then describes the application of the platform on mouse embryonic stem cells to study interesting metastable gene expression behavior when placed in a concentration gradient of leukemia inhibitory factor (interleukin-6 cytokine family). We also note the statistically significant observation of a previously unreported single stem cell subpopulation. Chapter five covers the expansion of our platform into culture of induced pluripotent stem cells and the transfer to a new substrate polymer in order to accommodate surface chemistries necessary for cell attachment. Finally, chapter six summarizes the research performed on the development of EMPRESS, and future directions for which this technology could be applied.

CHAPTER 2: BACKGROUND

2.1. Microfluidics Advantages for Stem Cell Analysis

One of the major challenges facing ES cell researchers is developing technologies to culture cells under controlled homogenous conditions; as homogenous culture conditions is critical in ensuring consistent behaviors of a stem cell population. The behavior of these cells is extremely sensitive to elements in their local chemical and physical microenvironment such as soluble growth factors, matrix components, cell to cell contact, and the three-dimensional architecture of the niche itself, which shapes and restricts the delivery of these cues[14, 15]. Established methods primarily allow biologists the ability to manipulate the environments around populations and clusters of cells in isolated culture wells/dishes, but such experimental conditions require large amounts of expensive reagents, are often labor intensive and hinder time-dependent studies as it is difficult to perform rapid solution exchanges. The advantages of microfluidics for single stem analysis can be broken down into the following four main categories:

2.1.1. Controlled chemical/physical microenvironment

Microfluidics are based around the principle of increased volumetric resolution and precision though the use of microfabricated fluidic channels and chambers. For example, studies of cellular responses to chemical gradients have been hampered by the inability to properly shape the gradient in both time and space, an issue that microfluidic technology is well-suited to tackle. Additionally, the chemicals fed into these chambers can be precisely metered through passive or active feedback systems based on conditions detected in these microstructures by methods as straightforward as fluorescence read-out. The integration of multiple components has enabled the development of complex systems with minimal footprint. Stem cells require strict control of their microenvironments since their culture is quite difficult and slight chemical imbalances can cause dramatic changes to cell behavior, such as unwanted differentiation, proliferation and even cell death.[16] Because microfluidics can reliably control the physical and chemical characteristics of both the growth substrate as well as the surrounding medium at all times, microfluidics enables repeatable and careful culture of stem cells, opening up many avenues for their study.

2.1.2. Manipulation of cell distribution

Microfluidics offers unique advantages for precisely controlling the spatial distribution of cells on a 2D or 3D culture substrate. Using hydrodynamic focusing, physical trapping, adhesion molecule stamping, or a combination thereof, researchers can

reliably create arrays of single cells for single cell studies, doublets to study cell-to-cell communication, or arbitrarily sized clusters to study group dynamics. Such spatial control is not available using standard cell culture techniques which rely purely upon the random distribution of cells as they fall out of suspension.

2.1.3. Sample size reduction

Due to the need for large data sets for conclusive, statistically significant results, multiple experiments with many harvested cells are often required. This procedure is a primary contributor toward the high costs in pharmaceutical discovery and biological research. Single cell analysis using microfluidics significantly reduces these costs by requiring fewer cells for a given set of assays. A gradient with of a signaling molecule can be applied simultaneously to an array of single stem cell cultures (which develop into clonal colonies) resulting in thousands of data points collected in each experiment performed resulting in fewer experiments necessary for generating the data. This lends itself to very high-throughput data mining for experimental conditions as well.

2.1.4. Concentration of secreted molecules

Leveraging microfabrication techniques, microfluidic culture chambers and wells are often on the same size-scale as cells and enclosed. This leads to a de facto concentration of secreted soluble factors from the stem cells resulting in simpler extraction of target molecules of interest and imaging of low concentration molecules. These advantages have driven the development of microfluidic lab-on-a-chip assays for stem cell analysis. To maximize the application of these platforms and enable new stem cell research where one or more of these traits are necessary to generate and image the wanted perturbations, this field has been slowly moving toward single cell stem cell analysis devices which will be discussed later.

2.2. Microfluidic Technology for Stem Cell Analysis

2.2.1. Spot microarrays

Cells of a developing embryo integrate a combination of local and long-range signals that act in concert with intrinsic signals to influence developmental decisions. To systematically investigate the effects of molecular microenvironments on cell fate decisions, it is necessary to expose cells to diverse combinations of extracellular signals. Previous work on patterning extracellular matrix protein combinations in microfluidic culture chambers was done by Hattori *et al*.[17]

In order to identify biomaterials that support appropriate cellular attachment, proliferation and gene expression patterns, Anderson *et al.*[18] developed a nanoliter-scale spot microarray of different biomaterials and characterized their interactions with human embryoinic stem cells (hESCs). They were able to simultaneously characterize over 1,700 material-hESC interactions and identify a host of unexpected materials effects that offer new levels of control over human embryonic stem cell behavior. Flaim *et al*.[19] was able to expand upon that work to study the effects of 32 different combinations of five extracellular matrix molecules (collagen I, collagen III, collagen IV, laminin, and fibronectin) on cellular differentiation in two contexts: maintenance of primary rat hepatocyte phenotype indicated by intracellular albumin staining and differentiation of mouse embryonic stem (ES) cells toward an early hepatic fate.

In order to define parameter boundaries for the use of embryonic stem cells in screening studies, Peerani *et al*.[20] patterned fibronectin/gelatin patches of various size and pitch in order to study how niche size controls endogenous signaling thresholds in mouse embryonic stem cells. They showed how direct and indirect transcriptional targets of Stat3, including members of the Jak-Stat pathway and pluripotency-associated genes, were controlled by colony size and separation. Similar work with spatiotemporally patterned human embryonic stem cell colonies was done by Abhyankar *et al*. [21]

Sasaki *et al.*[22] was able to use maskless micropatterned surfaces that comprised cell-adhesive hydrophobic domains and non-cell-adhesive hydrophilic domains (100–400 μm in diameter) to study the effect of stem cell cluster size on controlling cardiac differentiation. They found that the optimal diameter of micro-domains was 200 μm, with the resulting cardiomyocyte concentration reaching ~1.5%, which falls within the range of reported values by the conventional hanging drop method. The present method is useful for the simple and reproducible mass preparation of ESC-derived differentiated cells and high-throughput assays.

To systematically investigate the effects of molecular microenvironments on cell fate decisions, Soen *et al.*[23] cultured primary human neural precursor cells on contact printed microenvironment arrays composed of mixtures of extracellular matrix components, morphogens, and other signaling proteins. Quantitative single cell analysis revealed striking effects of some of these signals on the extent and direction of differentiation. They found that Wnt and Notch co-stimulation could maintain the cells in an undifferentiated-like, proliferative state, whereas bone morphogenetic protein 4 induced an 'indeterminate' differentiation phenotype characterized by simultaneous expression of glial and neuronal markers.

Trkov et al. [24] investigated the vasculogenic potential of human mesenchymal stem cell (MSC) populations while co-culturing them in a novel spatially controlled three-dimensional (3D) fibrin hydrogel model. Using microfluidic patterning, they localized hydrogel-encapsulated HUVECs and MSCs within separate channels spaced at 500, 1000 or 2000 μm. They concluded that bone marrow-derived MSCs (but not umbilical vein or artery derivedMSCs) showed strong distance-dependent migration toward

HUVECs and supported the formation of stable vascular networks resembling capillary-like vasculature.

2.2.2. Mechanical strain effects on stem cell differentiation

Mechanical forces have been reported to induce proliferation and/or differentiation in many cell types, but the role of mechanotransduction during embryonic stem cell fate decisions was unknown. To ascertain the role of mechanical strain in human embryonic stem cell (hESC) differentiation, Saha *el al*. [25]used a commercially available culture plate setup to measure the rate of hESC differentiation in the presence and absence of biaxial cyclic strain which was applied to a deformable elastic substratum upon which the hESC colonies were cultured. They concluded that the frequency of mechanical strain application had little effect on extent of differentiation. hESCs cultured under cyclic strain retained pluripotency, evidenced by their ability to differentiate to cell lineages in all three germ layers. Mechanical strain is not sufficient to inhibit differentiation, however, in unconditioned medium. Thus, while mechanical forces play a role in regulating hESC self-renewal and differentiation, they must act synergistically with chemical signals.

To study osteogenesis by hMSCs (human mesenchymal stem cells), Sim *et al*.[26] designed a chip to apply compressive pressure to a pneumatic actuator with a flexible diaphragm which consists of an air chamber and cell chambers. Their results suggest that cyclic mechanical stimulation is attributed to the different phenomenon of cultured hMSCs in cell proliferation and differentiation after one week.

2.2.3. Genomic studies on-chip

The gene expression of human embryonic stem cells (hESC) is a critical aspect for understanding the normal and pathological development of human cells and tissues. Single-cell gene expression profiling from early embryos showed transient expression of critical regulatory genes. Current bulk gene expression assays rely on RNA extracted from cell and tissue samples with various degree of cellular heterogeneity.

Chen *et al*.[27] and Zhong *et al.*[28] details a RTV silicone microfluidic device which can simultaneously process 50 individual cells into cDNA within 3 hours. Their device can extract total mRNA from individual single-cells and synthesize cDNA on the same device with high mRNA-to-cDNA efficiency. Their results indicate that gene expression data measured from cDNA of a cell population is not a good representation of the expression levels in individual single cells. Within the G0/G1 phase pluripotent hESC population, some individual cells did not express all of the 3 interrogated genes in detectable levels. Consequently, the relative expression levels, which are broadly used in gene expression studies, are very different between measurements from population cDNA and single-cell cDNA. The results underscore the importance of discrete single-

cell analysis, and the advantages of a microfluidic approach in stem cell gene expression studies.

2.2.4. Stem cell pairing and fusion

For ethical reasons revolving around the use of embryonic stem cells, the frontiers of stem cell biology have pushed towards reprogramming of somatic cells through either cell fusion, or the creation of induced pluripotent stem cells (iPS). Through cell fusion, embryonic stem (ES) cells can erase the developmental programming of differentiated cell nuclei and impose pluripotency on previously somatic cells.[29, 30] Yet cell fusion requires consistent placement of one cell against another, something which is generally achieved through glass pipettes, a labor-intensive and low throughput endeavor. Microfluidics is uniquely poised to make breakthroughs in enabling high-throughput cell fusion by taking advantage of the ability to manipulate cell placement through passive fluidic physics. Lee *et al*.[31] first introduced cell-cell pairing in microfluidics through the use of two parallel rows of pipette-like channels where negative pressure could be used to perform suction trapping of mammalian cells floating by. Skelley *et al*.[32] expanded upon a design published by Di Carlo *et al*. to use cup-shaped traps in combination with fluidic backflow as a method of placing one cell type reliably on top of another. Single cell pairs were created by Frimat *et al*.[33] using a combination of differential fluidic resistance trapping method with a novel cellular valving principle. Differential fluidic resistance was used for sequential single cell arraying, with the adhesion and flattening of viable cells within the microstructured environment acting to produce valves in the open state. Reversal of the flow was used for the sequential single cell arraying of the second cell type.

Dielectric cell trapping and fusion was reported by Gel *et al*.[34, 35] Device operation was verified by observation of dye transfer between mouse fibroblasts (NIH3T3) placed in membrane contact.

2.2.5. Embryoid body culture and analysis on-chip

Directed embryonic stem (ES) cell differentiation is a potentially powerful approach for generating a renewable source of cells for regenerative medicine. Typical in vitro ES cell differentiation protocols involve the formation of ES cell aggregate intermediates called embryoid bodies (EBs), which recapitulate early stages of embryonic development. EBs are typically made from suspension cultures and shaped using hanging drops, resulting in a wide range of sizes and shapes. Because the differentiation efficiency of ES cells is dependent on the size of embryoid bodies, being able to reproducibly prepare size-controlled EBs in a scalable manner is a powerful tool for stem cell biology. One method to control the size of ES cell clusters is to entrap them in 3-D microwells of a preset size. Karp *et al*.[5, 36] made polymeric microwells from poly(ethylene glycol) (PEG) which have been used to trap and culture ES cells for multiple days. Intact EBs could be easily retrieved from the microwells with high viability

(>95%) using mechanical disruption. Despite these promising results, the previously developed technology was limited as it was difficult to reproducibly obtain cultures of homogeneous EBs with high efficiency and retrievability. Moeller *el al*.[37] was able to improve the platform by optimizing a number of features: material composition of the microwells, cell seeding procedures, and aggregate retrieval methods. Adopting these modifications, they demonstrated an improved degree of homogeneity of the resulting aggregate populations and establish a robust protocol for eliciting high EB formation efficiencies.

Human embryonic stem cells (hESCs) are generally cultured as cell clusters on top of a feeder layer formed by fibroblast cells which secretes growth factors and extracellular matrix (ECM) into the local microenvironment. Great care is required to maintain undifferentiated hESC cultures since spontaneous differentiation often occurs in culture, presumably resulting from a combination of soluble factors, cell–cell signaling, and cell–matrix contact. Mohr *et al*.[38]developed a 3-D microwell-based method to maintain undifferentiated hESC cultures for weeks without passaging using physical and extracellular matrix patterning constraints to limit colony growth. Over 90% of hESCs cultured in microwells for 2–3 weeks were viable and expressed the hESC transcription marker Oct-4. Upon passaging to Matrigel-coated tissue culture-treated polystyrene dishes (TCPS), microwell cultured hESCs maintained undifferentiated proliferation. Khademhosseini *et al*.[39, 40] was able to improve upon the basic microwell by making polymeric microwells which were able to coculture hESCs with mitotically inactivated murine embryonic fibroblasts (MEFs). Because this more closely mimics standard tissue culture microenvironment, differentiation of these clusters can be directly compared to results from previous publications on culture dishes.

Kamei *et al*.[41] was interested in being able to perform single cell profiling of the levels of protein expression in human pluripotent stem cells in embryoid bodies. They used a PDMS-based microfluidic culture array where each chamber can perform immunocytochemical analysis under discrete culture conditions, with medium changes every 12 hours for over a week. Post-culture analysis of protein expression was done using microfluidic image cytometry.

Embedment of cells in hydrogels introduces operational complexity, potentially hinders mass transfer, and is not suitable for establishing cell-dense, ECM-poor constructs. Ong *et al*.[42] used a combination of transient inter-cellular polymeric linker and micro-fabricated pillar arrays for the *in situ* formation and immobilization of 3D multi-cellular aggregates of primary bone marrow mesenchymal stem cells.

Cell–cell signaling is an important component of the stem cell microenvironment, affecting both differentiation and self-renewal. However, traditional cell-culture techniques do not provide precise control over cell–cell interactions, while existing cell-patterning technologies are limited when used with proliferating or motile cells. To address these limitations, Rosenthal *et al.*[43] created the Bio Flip Chip (BFC), a microfabricated polymer chip containing thousands of microwells, each sized to trap down to a single stem cell with patterning efficiencies >75%. The chip is designed to be

compatible with a variety of substrates—a cell-culture dish patterned with gelatin, a 3-D substrate, and even another layer of cells. Since it traps the stem cells in a patterned spatial configuration with preset cluster sizes before the cells are dropped onto the culture substrate, the BFC allows incremental and independent control of contact-mediated signaling. Using this tool, the authors were able to provide quantitative evidence that cell–cell contact plays an important role in depressing mESC colony formation, and show that E-cadherin is involved in this negative regulatory pathway.

2.2.6. Control of stem cell differentiation with microfluidics

Organized cellular alignment is critical to controlling tissue microarchitecture and biological function. Although a multitude of techniques have been described to control cellular alignment in 2D, recapitulating the cellular alignment of highly organized native tissues in 3D engineered tissues remains a challenge. While cellular alignment in engineered tissues can be induced through the use of external physical stimuli, there are few simple techniques for microscale control of cell behavior that are largely cell-driven. Aubin *et al*.[44] presented a simple and direct method to control the alignment and elongation of fibroblasts, myoblasts, endothelial cells and cardiac stem cells encapsulated in microengineered 3D gelatin methacrylate (GelMA) hydrogels, demonstrating that cells with the intrinsic potential to form aligned tissues in vivo will self-organize into functional tissues in vitro if confined in the appropriate 3D microarchitecture. The presented system may be used as an in vitro model for investigating cell and tissue morphogenesis in 3D, as well as for creating tissue constructs with microscale control of 3D cellular alignment and elongation, that could have great potential for the engineering of functional tissues with aligned cells and anisotropic function.

Tourovskaia *et al*.[45] demonstrated a microfluidic perfusion system suitable for a long-term (>2 week) culture of muscle cells spanning the whole process of differentiation from myoblasts to myotubes. By delivering fluorescent markers using heterogeneous laminar flows, it was possible to confine a membrane receptor labeling assay to a region smaller than a myotube. Their results showed that there were no differences in differentiation between microfluidic and traditional cultures using muscle cell-specific differentiation markers and the timing of fusion for comparison.

To study apipocyte differentiation, Ni *et al.* [46] grew human mesenchymal stem cells (hMSCs) on-chip using a normal culture medium for one day. Then, the differentiation of hMSCs into adipocytes was successfully induced by the perfusion of a differentiation medium for 14 days. The results showed that the differentiation rate of hMSCs in the chip critically depends on the initial cell density. When the cell density increases from 800 to 5000 cells/cm^2, the differentiation rate increases from 21% to 41%.

Zhang *et al*. [47] studied osteogenic differentiation of human mesenchymal stem cells (hMSCs) on-chip by using two types of nutrient feeding methods. The first one was with a hydraulic pressure which allows controlling the flow rate with a large dynamic range.

The second one was with integrated reservoirs of relative large volumes, providing a quasi stationary culture condition (regular medium change has to be done once per day). In both cases, cells survived for several weeks but showed different behaviors of cell proliferation and differentiation. In hydraulic pressure controlled chambers, cells grow fast but the formation of calcium nodes is less efficient. Under quasi stationary conditions with an optimal initial cell density, staining images show a better osteogenic differentiation. To illustrate the capability for individual culture chamber control, Gomez-Sjoberg *et al*. [48] built a fully automated cell culture screening system based on a microfluidic chip that creates arbitrary culture media formulations in 96 independent culture chambers and maintains cell viability for weeks. They studied how long of an osteogenic stimulus is required to induce hMSC differentiation, by examining the effect of eight different durations of osteogenic stimulation (0, 3, 6, 12, 24, 48, 96, or 168 hr) on the osteogenic differentiation and motility of hMSCs.

The study of cardiogenesis from different sized EBs was performed by Hwang *et al*.[49] They used microengineered hydrogel microwells to direct ES cell differentiation and determined that cardiogenesis was enhanced in larger EBs (450 μm in diameter), and in contrast, endothelial cell differentiation was increased in smaller EBs (150 μm in diameter). Their data suggests that EB size could be an important parameter in ES cell fate specification via differential gene expression of members of the noncanonical WNT pathway.

2.2.7. Stem cell culture on-chip with small molecule gradients

In early embryonic development, spatial gradients of diffusible signaling molecules play important roles in controlling differentiation of cell types or arrays in diverse tissues. Thus, the concentration of exogenous cytokines or growth factors at any given time is crucial to the formation of an enriched population of a desired cell type from primitive stem cells in vitro. Microfluidic technology has proven very useful in the creation of cell-friendly microenvironments. Such techniques are, however, currently limited to a few cell types. Improved versatility is required if these systems are to become practically applicable to stem cells showing various plasticity ranges.

Chung *et al*.[50] describes a gradient-generating microfluidic platform for optimizing proliferation and differentiation of neural stem cells (NSCs) in culture. Their platform exposes cells to a concentration gradient of growth factors under continuous flow, thus minimizing autocrine and paracrine signaling. Human NSCs (hNSCs) from the developing cerebral cortex were cultured for more than 1 week in the microfluidic device while constantly exposed to a continuous gradient of a growth factor (GF) mixture containing epidermal growth factor (EGF), fibroblast growth factor 2 (FGF2) and platelet-derived growth factor (PDGF). Proliferation and differentiation of NSCs into astrocytes were monitored by time-lapse microscopy and immunocytochemistry. The NSCs remained healthy throughout the entire culture period, and importantly, proliferated and differentiated in a graded and proportional fashion that varied directly with GF concentration. A minimal handling culture platform was developed by Park *et*

al.[51] who built a microfluidic platform in which cells can be exposed to stable concentration gradients of various signaling molecules for more than a week with no external power source. They cultured an enriched population of neural progenitors derived from human embryonic stem cells in the microfluidic chamber for 8 days under continuous cytokine gradients.

Figallo and Cimetta [52, 53] developed a microbioreactor to control the attachment and hydrodynamic shear around a variety of stem cell lines. They established correlations between the expression of smooth muscle actin and cell density for three different flow configurations. Futai *et al*.[54] created a palm-sized microfluidic recirculation system for the long term culturing of C2C12 myoblasts and MC3T3-E1 osteoblasts for over 2 weeks in ambient atmosphere without medium exchange. The method opens up new possibilities for portable cell culture and for long-term continuous visual monitoring of cells. To characterize the effect of flow rate on stem cell proliferation, Kim *et al.*[55] demonstrated culture of murine ESCs (mESCs) in continuous, logarithmically scaled perfusion for 4 days, with flow rates varying >300× across the array. Cells grown in the slowest flow rate did not proliferate, while colonies grown in higher flow rates exhibited healthy round morphology.

2.2.8. Stem cell - single cell studies

Chin *et al*.[56] reported a simple, versatile, and efficient micropatterned arraying system conducive to the culture and dynamic monitoring of stem cell proliferation. Because the platform incorporates a photoresist-coated glass coverslide, they were able to track individual cell fates over time and correlate differentiated progeny with founder clones. To achieve these goals, they used microfabrication techniques to create an array of 10,000 microwells on a glass coverslip, which was then coated with adhesive proteins. The entire system was enclosed for the duration of the experiment, allowing gas exchange only through the device sides. Since the enclosure precluded nutrient refreshment, culture duration was limited to the nutrition supply contained within the initial loading volume (3mm of medium over cells, comparable to dish culture).

Lindstrom *et al*.[57] developed a similar glass-based microwell system which could screen 700,000 substances in less than two days. Their system is not an enclosed system like Chin's, but considered each well to be fluidically independent. High-throughput cell placement and medium screening was performed by a combination of FACS (fluorescently activated cell sorter) and automatic pipetter machines.

2.3. Conclusions

While microfluidic tools have been shown to contribute to stem cell biology, improvements can still be made in the area of single cell culture. The work presented in this dissertation has improved the efficiency of single cell trapping beyond what is shown in published literature (by Chin and Lindstrom, discussed in section 2.2.8) by

confining the microwell size to less than two cell diameters in width and height. Rapid fabrication of the platform is also possible due to the use of polydimethylsiloxane (PDMS) as a microwell substrate instead of coverslide glass, which requires costly and hazardous reagents. Published systems focus not on the enhancement of cell survival but the high-throughput trapping of single cells into arrays, culture of trapped cells into colonies (Chin), and testing a library of small molecule compounds (Lindstrom). Also, no previous published work has combined an enclosed single cell array with an upstream gradient generator to enable high-throughput concentration screening.

CHAPTER 3: ENHANCED SINGLE STEM CELL SURVIVAL ON-CHIP

3.1. Introduction

One of the major challenges facing ES cell researchers is to develop technologies to culture cells under controlled homogenous conditions to ensure consistent behavior of a stem cell population. Such control is critical for achieving predictable and uniform control over stem cell differentiation in many systems and is of immense practical importance in regenerative medicine. Limitations in established methods are due to the combination of (1) poor single cell survival rates, (2) lack of spatial resolution in cell placement, and (3) dissociation of immediate genetic relatives during cell sorting. Without control over all of these factors, the biostatistics of clonal studies are inadvertently skewed towards certain subpopulations which can withstand unknown survival selection pressures or whose behavior were influenced by poorly controlled microenvironment changes, resulting in misleading confidence in the conclusions.

The novel design of our microfluidic platform addresses these challenges by controlling the spatial distribution of the cells, doubles single cell survival, and generates two orders of magnitude more data than 96-well clonal culture. The improved single cell survival (>50%) compared to plate culture (Chambers[12] 30%, Zandstra[13] 12-40%) produces more representative data of the entire population versus selection of particular subpopulations.

3.2. Microfluidic Platform Design

3.2.1. Single cell trap array

Our microfluidic platform to perform long term stem cell culture has several design objectives. The first is the ability to trap individual single stem cells into an ordered array to control the cell-to-cell distance. It has been postulated that cell-to-cell distance is a very important variable in cell-to-cell signaling since diffusion of secreted cytokine factors is a direct function of distance.[16] Normal single cell culture on plates relies merely upon dilution of the suspended cell solution, whereupon the spatial distribution of the cells at the end are a Poisson function, and a wide variety of cell-to-cell distances are observed with little to no control on the part of the experimenter. Specifically, since mouse embryonic stem cells have the potential to spontaneously and non-homogenously differentiate due to small differences during normal culture procedures; it is important to develop methods which can improve the homogeneity of culture conditions – a topic that is pertinent to the field but seldom discussed. Using single cell microwells we show that it is possible to pattern mES cells to generate large numbers of

isolated clonal colonies within an array, with controlled sizes and shapes; a method that significantly reduces the heterogeneity of initial cell seeding distribution.

The microfluidic platform contains a total of 67,704 microwells, divided into two main trapping regions: 15μm x 15μm, or 20μm x 20μm (Figure 5). Two different microwell sizes are fabricated to accommodate a range of stem cell subtype diameters. Characterization and optimization of the necessary microwell geometries is shown in Figure 7. Trapping of the largest percentage of single mouse embryonic stem cells occurred when the trap diameter (20μm) is just a little larger than cell diameter (~15-18μm), and the trap height is 1.5x cell diameter (32μm) such that the trap could not contain two cells trapped cells, yet a trapped cell would not be removed with a lateral wash. To aid in image cytometry, the microwell array is broken up into squares labeled with a unique identification tag (Figure 6). Since each square fits perfectly within the field-of-view of a 10x microscope objective, it is possible to automate the microscope stage and fluorescent shutters for data acquisition.

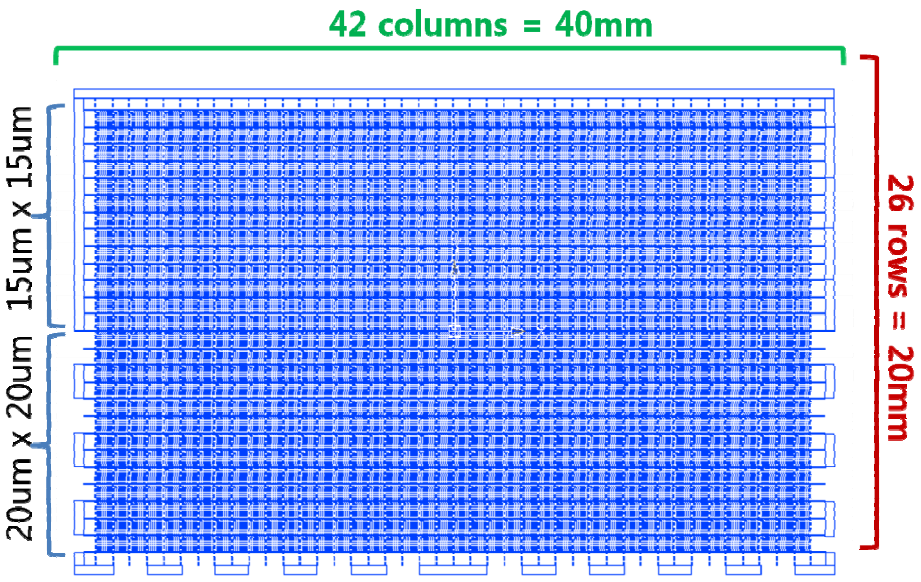

Figure 5. Microwell array breakdown into two main cell trapping regions: smaller 15x15um wells, and larger 20x20um wells.

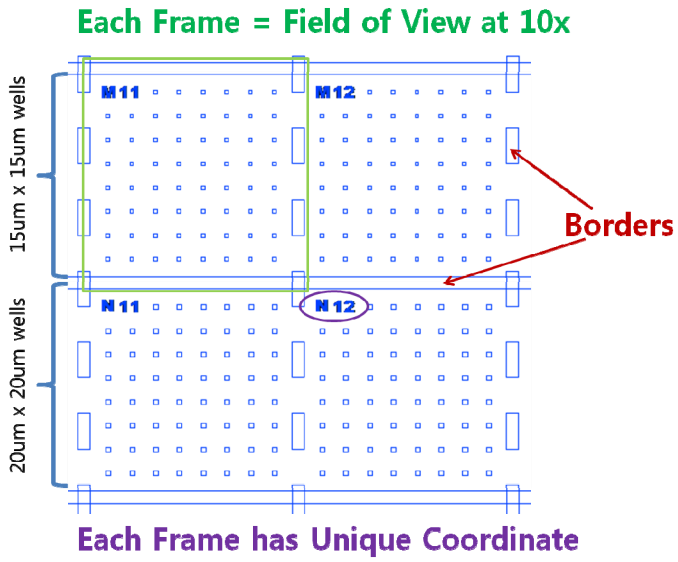

Figure 6. Closeup view of microwell cell trapping array with different sized microwells. The array is broken down into squares framed by borders and given a unique identification coordinate. Since each square fits within the field of view of a 10x microscope objective, image cytometry can be performed with an automated stage and shutter setup.

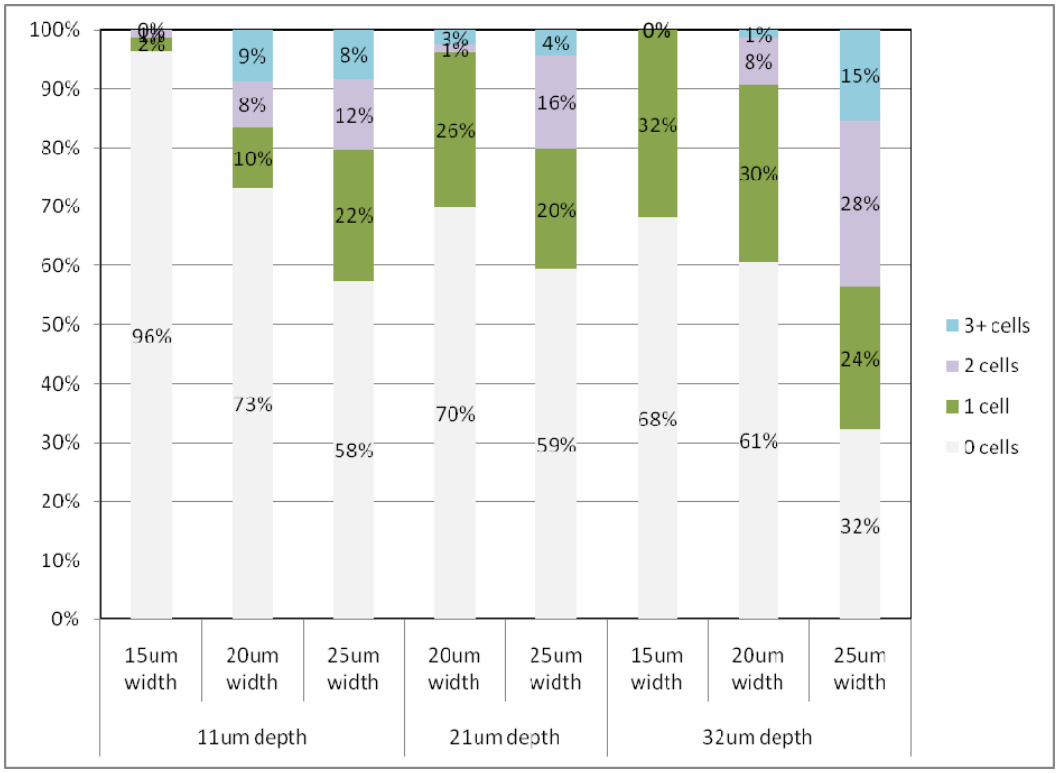

Figure 7. Mouse stem cell loading efficiency for microwells with different geometries. Wells of 32µm depth and 20x20µm square width and 15x15µm square width trap single cells with the highest efficiency. Efficiency can be increased with additional load rounds and higher initial cell concentration.

3.2.2. Growth substrate

The second design objective is to have a stem cell compatible culture substrate. For cell culture, the physical stiffness and chemical surface properties of the substrate material are very important variables which often affect cell behavior.[58-69] Thus it is of paramount importance that the substrate chosen has the necessary stiffness and chemical side-groups. In this study, we used soft lithography to fabricate microwells made from polydimethylsiloxane (PDMS) which are then sandwiched between two pieces of glass. The PDMS microwells are then pretreated with gelatin before stem cells are introduced, ensuring the proper chemical and physical properties are available. The two glass pieces are disregarded from consideration since they are not in direct contact with the stem cells.

3.2.3. Reduction of fluidic volume

The third design objective is to reduce the fluidic dead-volume which resides above the adherent cells on the growth substrate by at least one order of magnitude. One of the key experimental parameters which control stem cell behavior is the chemical microenvironment of the culture medium which immediately surrounds each cell. Of particular note are the dissolved autocrine and paracrine survival factors which stem cells are known to depend upon for survival and proliferation (Figure 8).[16, 70-74]

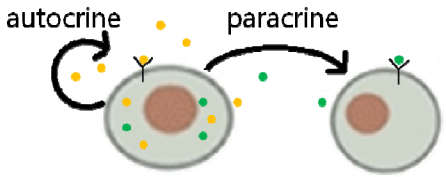

Figure 8. Autocrine signals are secreted and received by the same cell. Paracrine signals are secreted by one cell and received by another.

It has been hypothesized that the reason culture of stem cells as separated individuals using traditional plate technique has such low efficiency (<50% survival)[13] is the severe dilution of the secreted survival factors into the dead-volume of the static medium in the culture plate. Standard plating volumes requires ~4mm of fluidic height in order to ensure that the meniscus effect of the media against the well walls does not interfere heavily with the cell distribution at the bottom. As such, any small molecules secreted by the stem cells are severely diluted in a traditional culture plate. Our microfluidic platform limits the fluidic dead-volume to 100μm of fluidic height, a 40x decrease in the dead-volume, and subsequently, increasing the concentration of any secreted factors by 40x, which is hypothesized to increase stem cell survival within the microwells.

3.2.4. Perfusion culture

A fourth design objective is the refreshment of gas and nutrient supply. Traditional cell culture technique depends entirely upon natural diffusion of gases between the incubator interior and the culture media. Since our microfluidic platform is sandwiched between two non-permeable glass slides, all oxygen and nutrient refreshment must be delivered by perfusion flow, which is more biologically relevant than static culture. Perfusion culture of stem cells has already been shown to have different effects than static culture, which is standard for plate or flask culture[55, 75]. The variables under consideration are 1) optimize oxygen supply, 2) minimizing the dilution of secreted autocrine and paracrine factors (see design objective three), 3) avoiding shear force on the stem cells growing out of the microwells and onto the surface, 4) using the least pumping mechanism possible to increase experimental robustness and eliminate tubing entering the incubator. Balancing those considerations, gravity-driven flow has just enough fluidic velocity to refresh the media at a rate necessary for gas exchange while remaining flow enough to minimize survival factor dilution, and eliminates the necessity for an external pump.

Gravity driven flow also has the advantage that the fluids in the inlet reservoirs can be exchanged very quickly for a new solution, enabling rapid chemical microenvironment changes for time-course studies. Such time course experiments are of interest to biologists since temporal patterns of chemical signaling are often found in nature, especially in embryo development.[76, 77] However, time-course experiments are difficult to perform using standard plate culture since the medium in every well must be removed and replaced with a new medium mix, a very time- and labor-intensive task. Even with the aid of automated machinery, changing the chemical microenvironment in a set of culture plates is much more difficult than changing the solutions within the inlet reservoirs, a task which takes less than a minute to accomplish. The microfluidic platform has the added advantage of having the built-in gradient generator, which reduces the number of required solution replacements to two per temporal leg.

3.2.5. Gradient generation

The fifth design consideration is the addition of a linear-tree gradient generator to the microfluidic platform. Gradient perfusion culture is believed to be more physiologically relevant to the development of embryos than the static chemical microenvironment in tissue culture plates because stem cells within embryos are normally exposed to a gradient of differentiation factors.[50, 51] An additional benefit to having an in-built gradient generator is the ability to produce much finer gradation of molecular concentrations than can be realistically achieved with standard plate culture, where every molecular concentration is prepared separately from each other. Usual standard plate culture is limited to around twelve different experimental conditions with several replicates, whereas our microfluidic platform uses natural diffusion dynamics to create very fine concentration gradations over a large number of cells for sample data points.

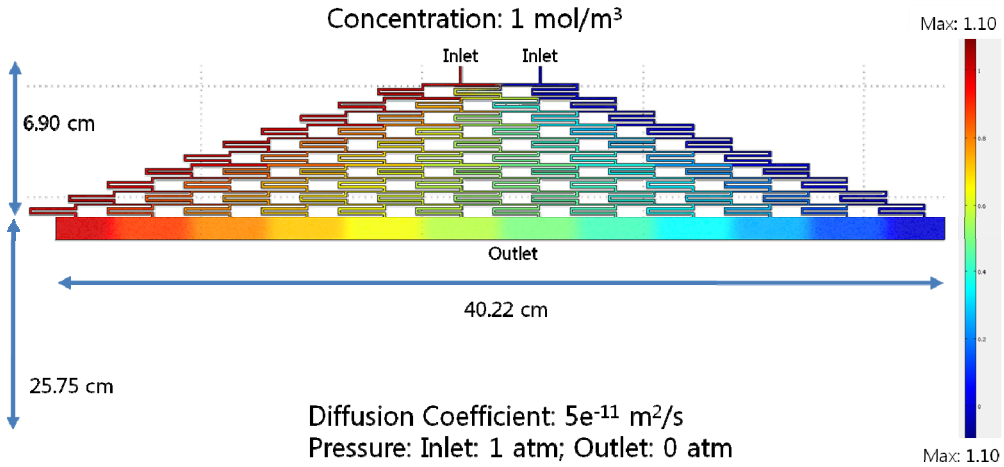

Figure 9. Simulation of gradient generation using a linear gradient tree. Diffusion Coefficient is quoted for a molecule the size of fluorescein.

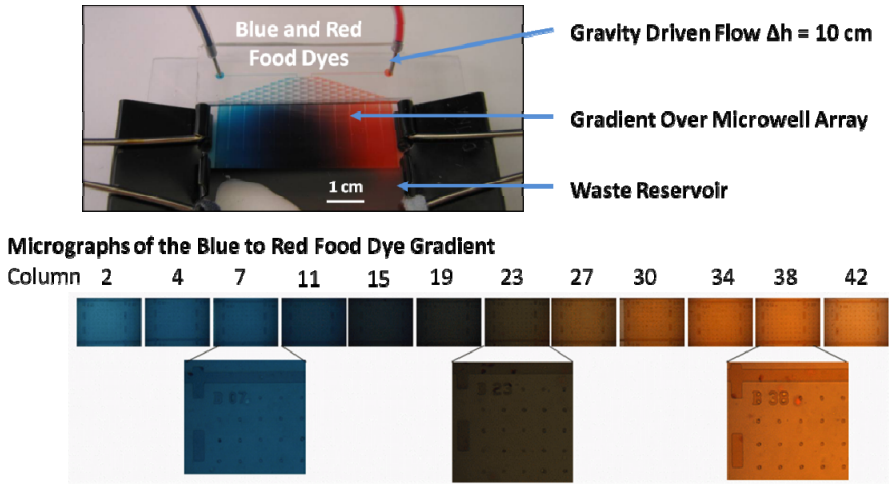

Figure 10. Representation of the gradient over the microwell array using food dye.

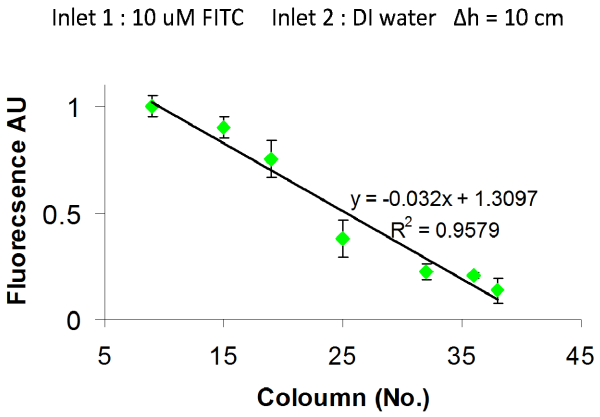

Figure 11. Characterization of linear gradient generation using fluorescein concentration as indicator.

3.2.6. Finalized design

Combining all of those design criteria, we finalized a four layer device (Figure 12) composed of a glass slide on the bottom for structural support, the microfluidic cell trapping and culture layer, a gasket to cap the gradient generator and contain the media, a glass coverslide to constrain the fluidic volume on top of the cells, and two inlet reservoirs. The media reservoirs were chosen so that their height could generate the correct velocity (~10μm/s) for gravity-driven media perfusion. The microfluidic device has a large outlet reservoir to minimize wall effects on the fluid flow and the gradient.

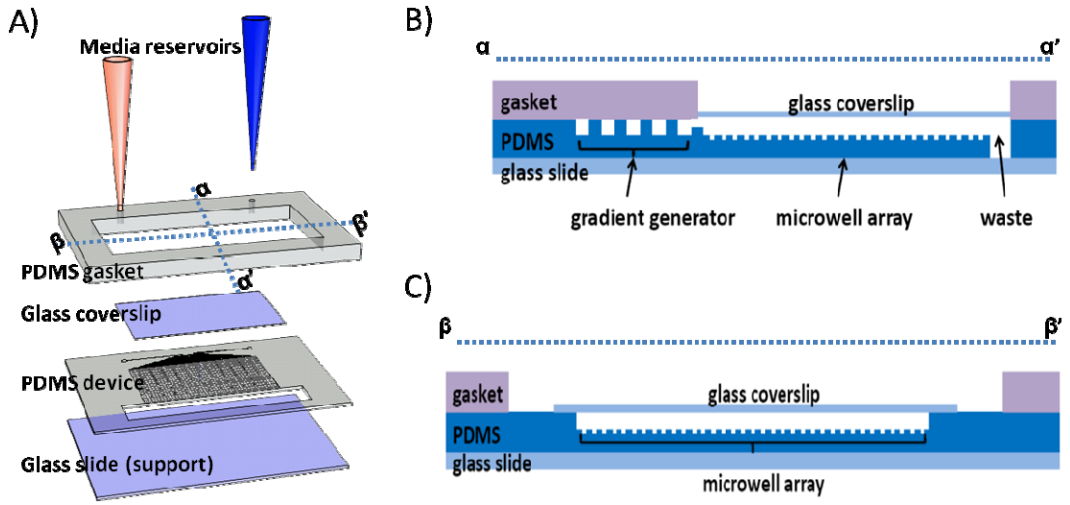

Figure 12. (a) Schematic of the different layers of the device and how they stack together. (b-c) Cross-sectional views of the device after assembly. Relative positions of the layers in the overall device can be seen.

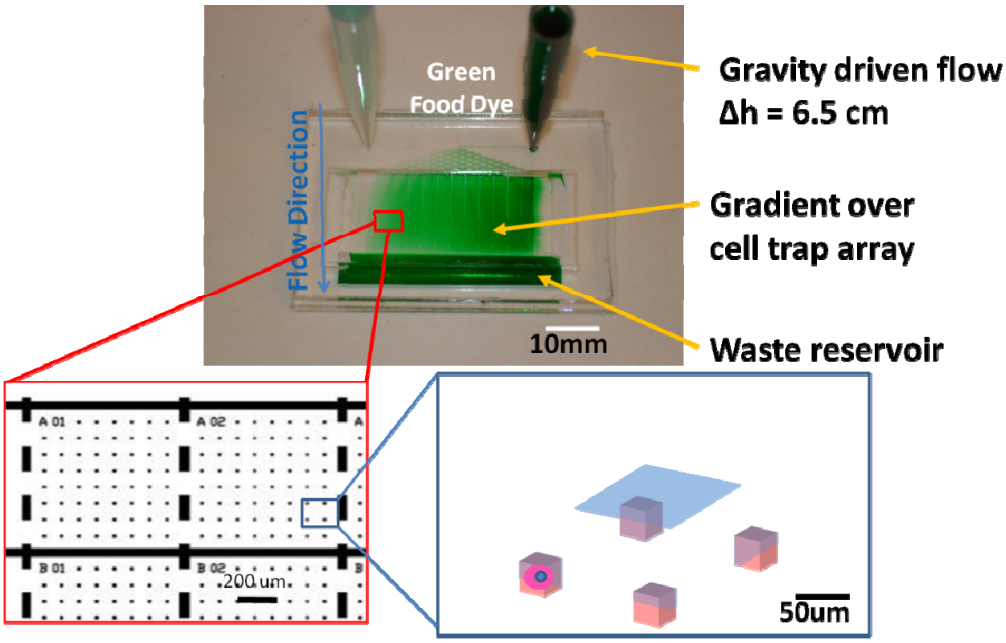

Figure 13. To-scale 3D schematic illustrating the height of the cell medium fluidic height compared to stem cell diameter.

3.3. Experimental Design

3.3.1. Fabrication of the microfluidic platform

Our microfluidic device is a two layer design composed of the microwell trapping layer (35μm in height), and a main fluidic flow layer (100μm in height). Fabrication protocol of the master mold using SU-8 photoresist on silicon wafer is presented in Chapter 7. One disadvantage of having a microfluidic device of such large surface area (~40mm x 60mm) is the lack of surface adhesion between the SU-8 photoresist and the silicon substrate; peeling of the SU-8 occurs often when trying to replicate the microfluidic device using Polydimethylsiloxane (PDMS) elastomer (Sylgard 184). To address this problem, we decided to adopt the use of plastic as the master mold instead of SU-8 on silicon (Figure 14).[80] Use of the plastic master has the added advantage of being able to personalize the device casting master with a slot to hold the glass slide which composes the platform bottom layer. Casting the PDMS and glass bottom together on the plastic master has the dual advantage of eliminating alignment and bonding issues, as well as ensuring that every device cast has the exact same PDMS thickness, reducing noise from the GFP fluorescence analysis. Fabrication protocol for the plastic master is presented in Chapter 7. Another benefit of using a plastic master instead of the traditional SU-8/silicon mold is the softening of the plastic at 60°C, enabling the user to bend the master and release the PDMS device easily. Surface tension against the PDMS microwells can be further reduced with the addition of 5ml of isopropanol between the plastic master and the PDMS device.

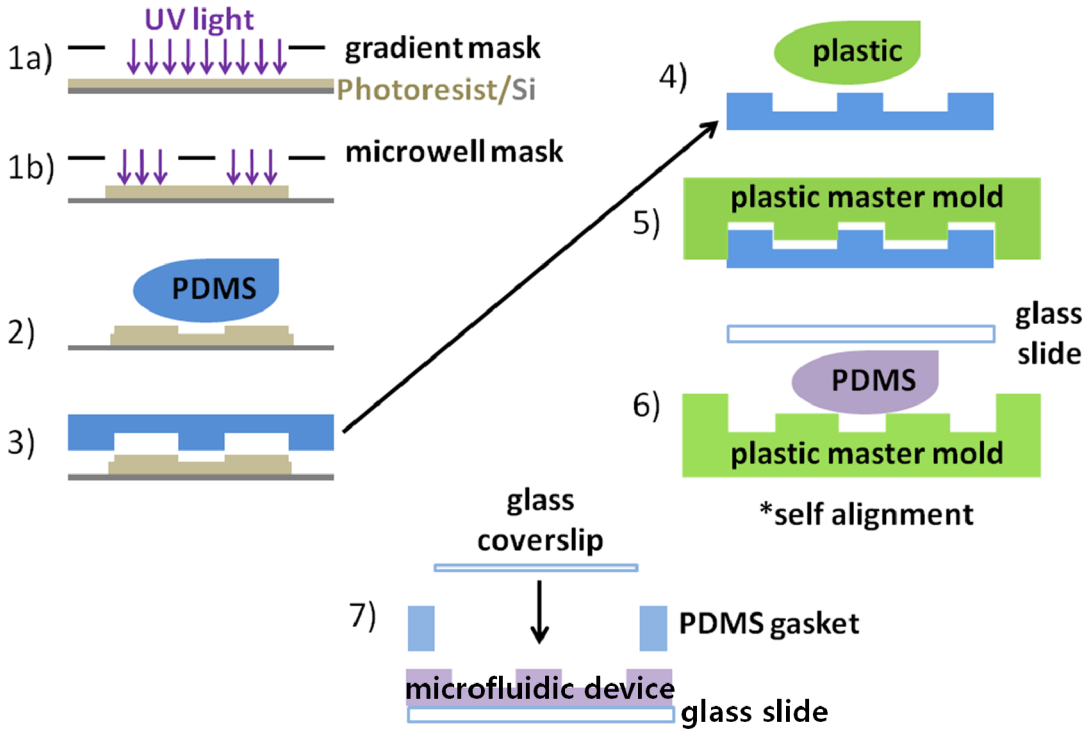

Figure 14. Fabrication process for the microfluidic platform. Steps 1-2 show the fabrication of the initial PDMS device. Steps 3-5 show the fabrication of the plastic master mold. Steps 6-7 show the final casting and assembly of the platform.

3.3.2. Device preparation

Once the microfluidic device and gasket PDMS pieces have been removed from the plastic master molds, the first step is to align the gasket piece to the microwell piece such that the gasket piece completely seals the entire gradient generator. Holes to accommodate the inlet reservoirs are then punched into the gasket piece using 2mm diameter punching tool. Following gasket punching, the two PDMS pieces are permanently bonded using oxygen plasma (50mW, 60sec).

Sterilization of the microfluidic devices requires the devices to be wrapped in aluminum foil, like chocolate bars, and placed within an autoclavable secondary container. Standard autoclave protocol is used (125°C, dry cycle) for 35min. The heat of the autoclave has the added benefit of finalizing any partially formed bonds between the two PDMS pieces by evaporating the water byproduct. UV sterilization, within the biohood, of up to 60min still resulted in bacterial contamination in 33% of experiments by 48hrs of culture, so sterilization by autoclaving is highly recommended. Post-sterilization, the devices are opened and handled exclusively within the biohoods.

Before mouse embryonic stem cells can be trapped and cultured, the growth substrate must be modified to be compatible with stem cell attachment. Standard culture protocol for mES cells incubates a 0.2% w/v bovine gelatin solution on tissue-culture treated polystyrene dishes for 20min. After characterization of various coating chemistries (Figure 37) on PDMS and glass, the protocol chosen was direct addition of 0.2% gelatin solution to the PDMS microwells since the gelatin performed just as well as the Matrigel and costs 100x less. Because of the natural hydrophobicity of PDMS, wetting of the microwells required that the devices be prevacuumed within a sterile bell chamber (40min, house vacuum) before gelatin solution (0.2% gelatin w/v in phosphate buffer saline) is added. Prevacuuming[81] is hypothesized to make the PDMS act like a presqueezed sponge, absorbing the gas bubbles trapped within the microwells as the PDMS re-expands to equilibrium. In addition to absorbing the trapped gas bubbles within the microwells, the vacuum also likely helps the floating gelatin molecules adsorb onto the PDMS surface, promoting an even coating of gelatin everywhere. Devices can be stored (wet with gelatin solution) in a sealed container at 4°C for at least three days with no loss in function.

3.3.3. Stem cell loading

Standard mouse embryonic stem cell subculture protocol is found in Chapter 7; experimental protocol diverges after addition of trypsin-substitute. Normal subculture protocol does not recommend breaking up the cell clumps into single cells because the shear rates necessary to accomplish single cells suspensions are very detrimental to cell survival. Subculture survival of small clumps (2-5 cells) is over 85% while survival of single cells is ~50%. To generate the largest number of surviving single stem cells as possible, the standard protocol is modified so that the exposure time to trypsin solution (chemical cell dissociater) is carefully monitored under the microscope and cell dissociation is controlled by lateral hitting force against the culture flask instead of shear force using stereological pipettes. Cell dissociation is followed by media inactivation of the trypsin and centrifugation (1000rpm, 5min) to concentrate the cells for removal of residual trypsin. The stem cells are then carefully resuspended in full experimental media (avoiding excessive shear force) at a concentration of $1x10^6$ cells/ml, a concentration which optimizes the density of cells while minimizing cell-cell adhesion and clumping. The cells are allowed to fall by gravity onto the microfluidic platform before a lateral wash is performed to remove all cells not trapped within the microwells. The calculated settling time for the cells in the chamber was determined from the equation for the sedimentation velocity of a sphere in an infinite fluid.[82] From the maximum height of 3 mm (initial fluid height), the maximum time to settle is ~7–

15min, where the density of a cell is 1.06 g/mL and the cell diameter ranges from 10–15μm. Usual final loading efficiency within the microwells is ~75% microwells, in accordance with literature.[83] The experimental process flow can be seen in Figure 15 detailing how the stem cells are introduced into the device, and when the perfusion gradient is added. Further detail on colony growth and analysis will come in later sections.

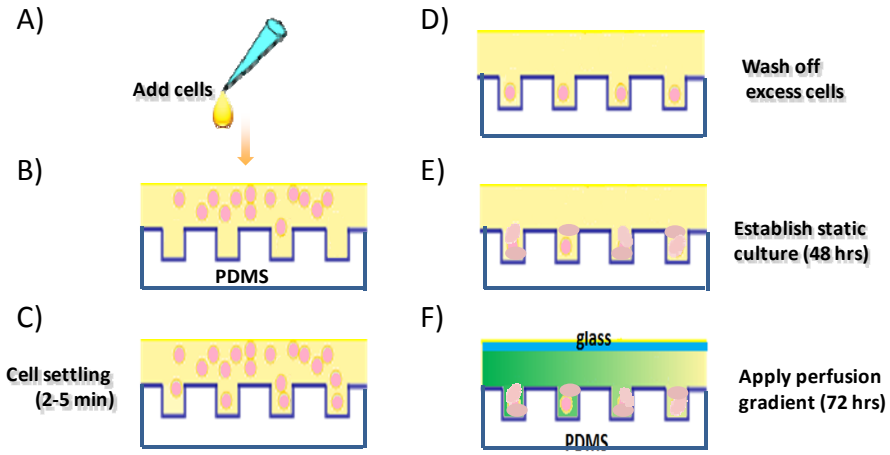

Figure 15. Experimental procedure detailing how the (A) stem cells are released from culture plate and (B) loaded as cell suspension, (C) allowed to settle into the microwells, (D) removal of excess cells on top surface and (E) static culture for 48 hrs to allow the stem cells to establish themselves. (F) Perfusion gradient can then be applied for up to an additional 72-120 hrs.

3.3.4. Stem cells have same growth and differentiation behavior on-chip

Once the mouse embryonic stem cells been trapped inside the microwells, they are given 24-48hrs to establish and adhere themselves to the microfluidic substrate. Normal colony proliferation is confirmed using standard culture medium before a gradient of leukemia inhibitory factor (LIF), is introduced via perfusion flow. The entire microfluidic platform functions as a completely contained set of culture experiments (positive and negative controls included), with different regions exposed to different concentrations of LIF. Positive control of stem cell growth is when the cells are cultured in an overabundance of LIF and there is minimal pressure towards a differentiated fate. Cells cultured in high LIF conditions are expected to maintain normal proliferation doubling times as plate culture (Figure 16), increase in colony size (Figure 18), and have consistent levels of average Nanog expression across the population over time (Figure 19). Negative controls are cells growing in zero LIF medium, which are expected to universally differentiate, lose their Nanog-controlled puromycin resistance, and then are killed by the selective antibiotic puromycin. Since every gradient experiment has one side of the microwell array growing at 100% LIF concentration (1000 U/ml) and the other side growing at 0% LIF concentration, both positive and negative controls are accounted for. Control experiments were also performed without the presence of selective antibiotic to ensure that the colonies were not reacting to the growth substrate with higher or lower rates of differentiation. The colonies growing on the gelatinized PDMS exhibited normal amounts of differentiation at the perimeter of the colonies (Figure 17), in agreement with standard flask culture.

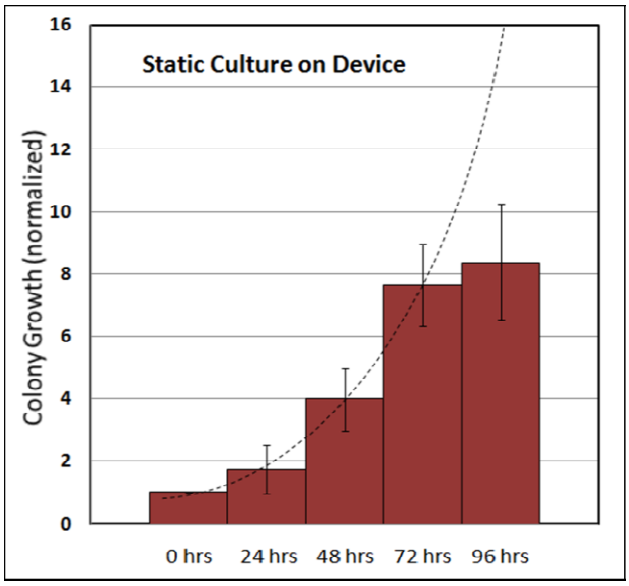

Figure 16. Positive control experiment showing that gelatin-coated PDMS as a growth substrate has the same doubling time as standard plate culture (dotted line). The drop-off in colony growth on Day 4 is hypothesized to be due to lack of nutrition because the culture medium was not refreshed for the duration of the experiment.

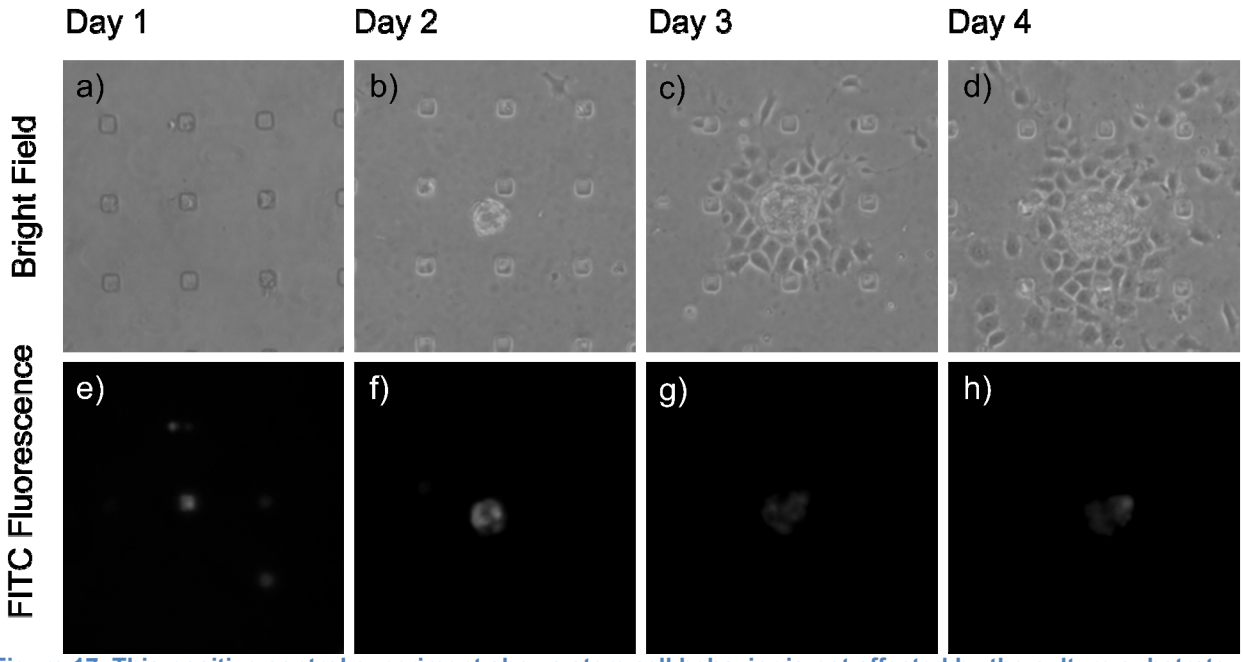

Figure 17. This positive control experiment shows stem cell behavior is not affected by the culture substrate of gelatin-coated PDMS since the stem cell colonies experience a normal amount of cell differentiation at the colony edges (all cobblestone-looking cells). This experiment cultured the stem cells without the selective antibiotic in the medium, which in future experiments will kill all differentiated cells. The fluorescence images confirm that only the undifferentiated stem cells in the middle of the colony exhibit Nanog gene expression, as expected.

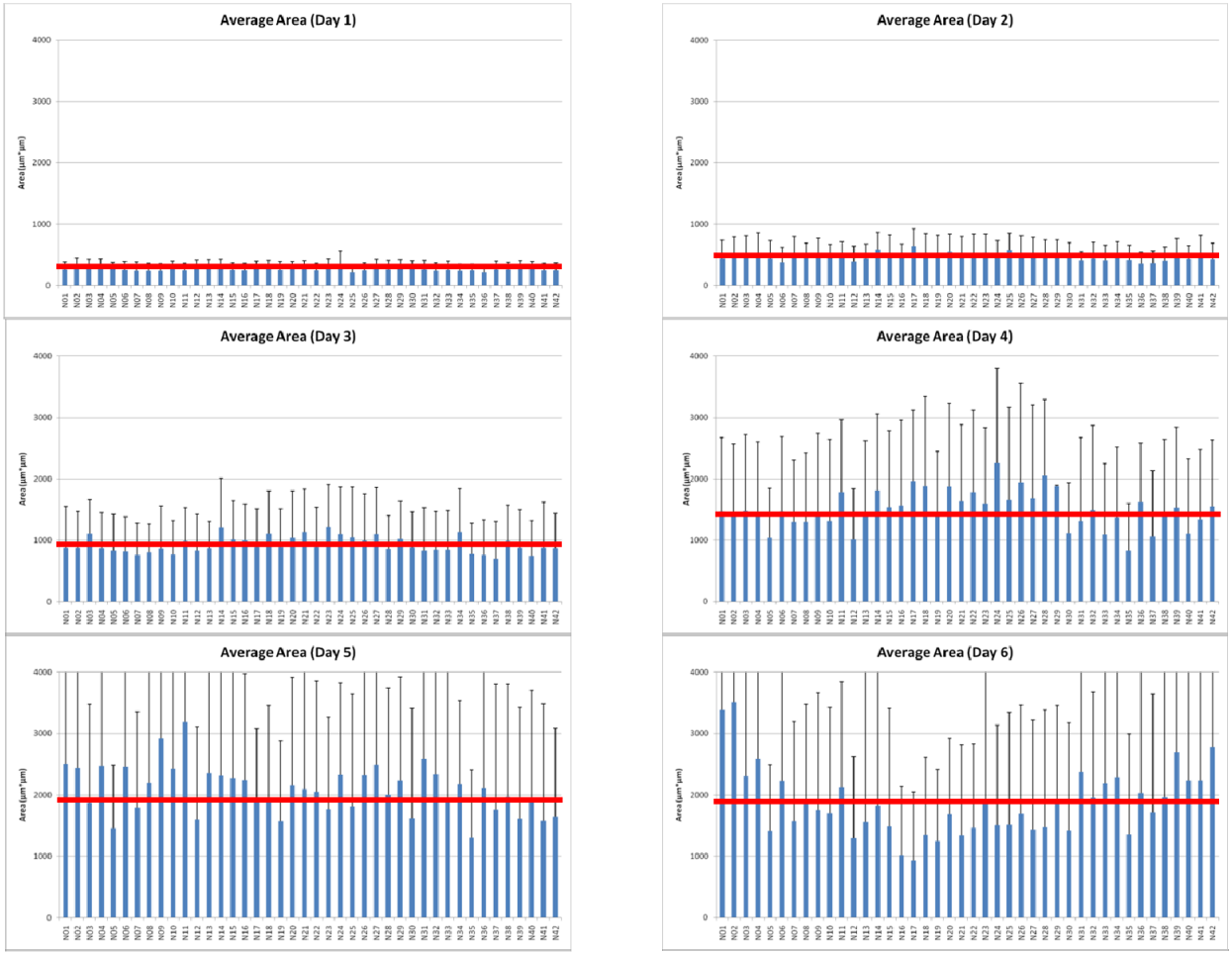

Figure 18. This positive control experiment shows that the use of medium perfusion does not have a detrimental effect on stem cell survival on our microfluidic platform. Average colony area from Day 1 to Day 6 from left (N01) to right (N42) across the same row with no LIF gradient present. While cell size is very tightly correlated on Day 1 (24hrs after cell loading), colony size fluctuates as culture time increases, although general colony size (average = red line) is increasing.

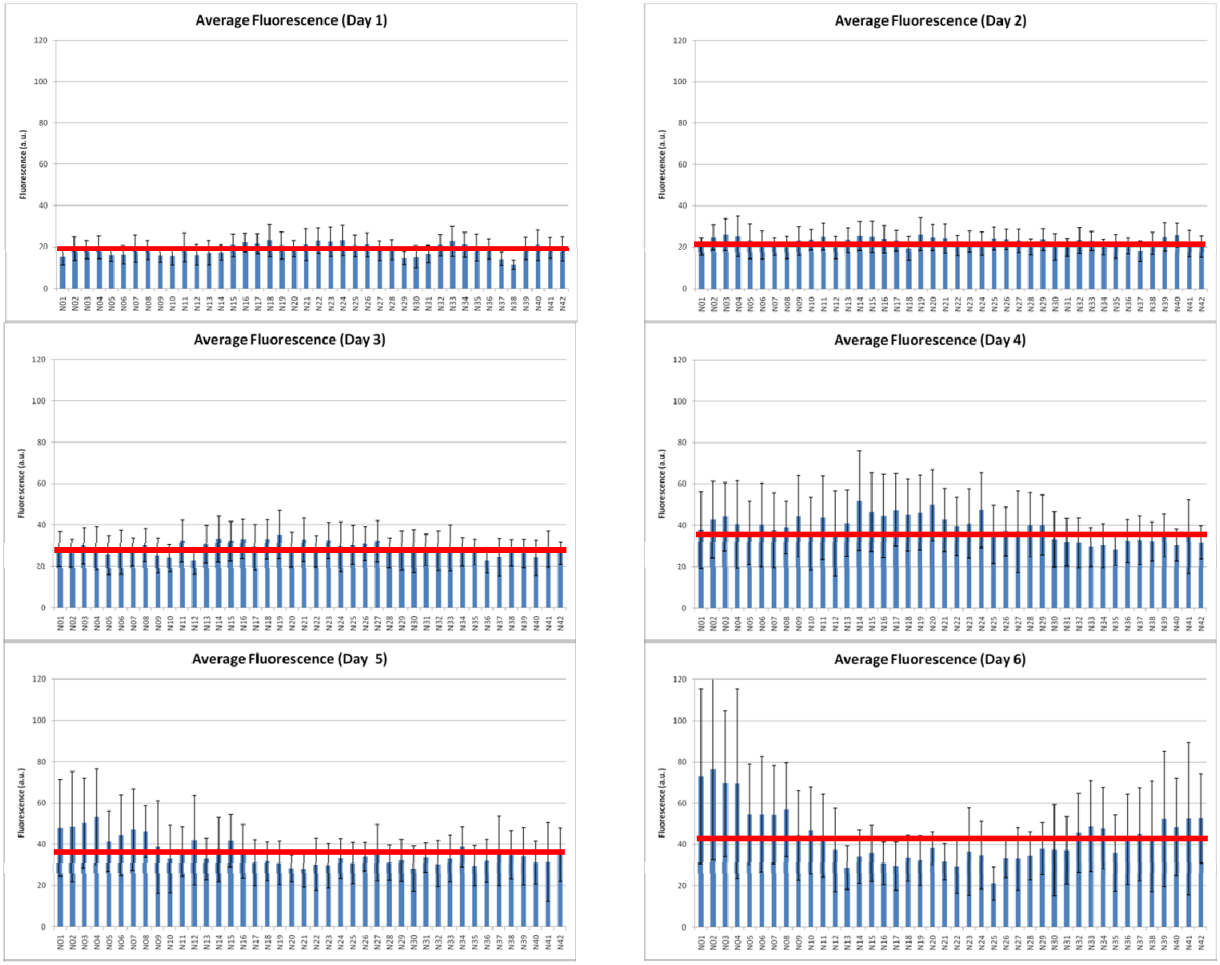

Figure 19. This positive control experiment shows that medium perfusion has no effect on Nanog gene expression levels. Average colony Nanog expression from Day 1 to Day 6 from left (N01) to right (N42) across the same row with no LIF gradient present. Levels of GFP expression (directly correlated with Nanog levels) fluctuates as culture time increases, although general colony gene expression appears to be increasing because the cells are growing on top of each other.

3.3.5. Conditioned medium has no advantage

While single cell culture on the microwell array has better survival rates than comparable cell densities on standard flask, higher survival rate at 48hrs past plating would still be desirable. If the cells are dying, we hypothesize, because they do not acquire enough paracrine signal from the bulk media, one possible solution to improve cell survival past the critical 48hr mark would be to use conditioned medium (medium taken from flask cultures with established colonies). Conditioned medium is commonly used in biology as a means to deliver undefined/unknown cell secretions as a behavioral signal. One example of the use of conditioned medium is the classical use of fibroblast feeder layers under stem cell colonies. It was known that stem cell survival (before the discovery of LIF) needed some mysterious secretions which the fibroblasts provided. But, to exclude fibroblast cell DNA from genomic analyses, it was more expedient to use medium which the fibroblasts had already secreted into (i.e.

"conditioned") to feed the stem cells. We decided to try a similar tactic of using conditioned medium to try to improve cell survival, none of which succeeded. The experiments varied the age of conditioned medium (how many days old the original donor flask was), the freshness of the conditioned medium (ideally, fresher the better to minimize molecular degradation), and the dilution ratio of conditioned medium to new medium (1:1 to 1:4). Since the use of conditioned medium from a donor flask did not provide improved survival, we tried to provide "fresh conditioned medium" through the use of heavy cell seeding in a portion of the microwell array. If the trench full of donor cells did indeed manage to secrete large amounts of survival factor, the stem cell survival rate would decrease exponentially as a function of distance away from the "cell feeder" region. Unfortunately, while the survival of the stem cell mass within the trench was high, there was no visible effect on single cell survival elsewhere on the microarray. Based upon these results, we discarded the idea of using conditioned medium for future experiments.

3.4. Conclusions

We demonstrate that our microfluidic platform is made from biocompatible culture substrates, contains microwells sized to efficiently trap single stem cells into an ordered spatial array, and maintains a steady gradient using pump-less perfusion flow. Our culture system is able to prove our hypothesis that we can greatly increase survival of single stem cells (Figure 19) by concentrating secreted survival cytokines to a very limited fluidic space. Without sufficient population survival, the biostatistics of clonal studies are inadvertently skewed towards certain subpopulations which can withstand unknown survival selection pressures or whose behavior were influenced by poorly controlled microenvironment changes, resulting in misleading confidence in the conclusions. The novel design of our microfluidic platform addresses these challenges by controlling the spatial distribution of the cells, doubles single cell survival, and generates two orders of magnitude more data than 96-well clonal culture. The improved single cell survival (>50%) compared to plate culture (Chambers[12] 30%, Zandstra[13] 12-40%) produces more representative data of the entire population versus selection of particular subpopulations.

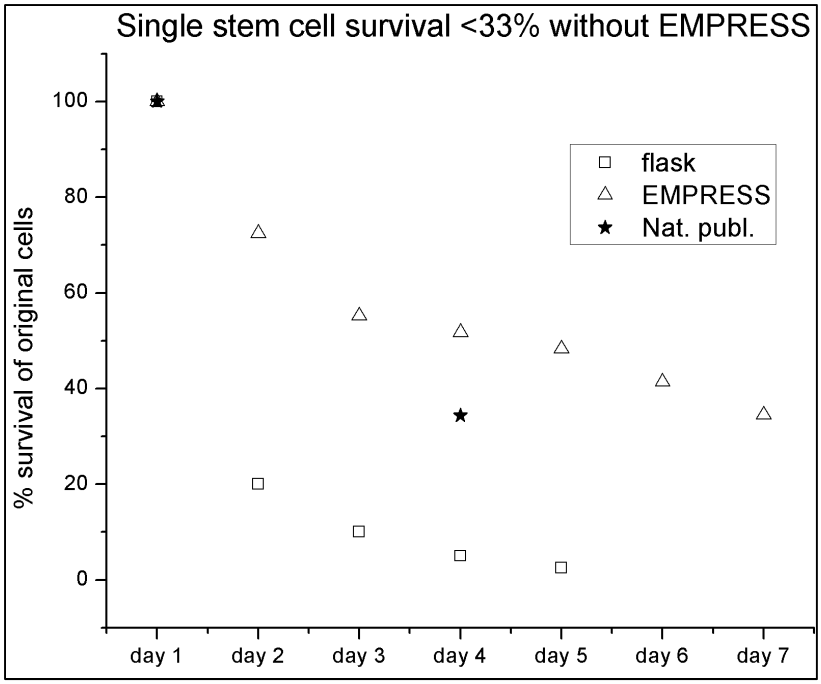

Figure 20. Stem cells have very low survival rates at low plating densities as single cells. Direct comparison of single stem cell survival, at the same 2D density, using traditional culture flasks versus EMPRESS system clearly shows that the EMPRESS system more than doubles single stem cell survival. Solid stars show survival of the single stem cells within a 96-well plate as published by the original cell line creator.

CHAPTER 4: MOUSE STEM CELL CULTURE ON-CHIP

4.1. Abstract

Using this platform, we have identified the LIF (leukemia inhibitory factor) concentration thresholds where mouse embryonic stem cells differentiate readily into the metastable behavior that is important in the study of cross-regulatory interactions between core transcription factors and their target genes. We were also able to track in real-time the clonal colonies derived from single cells to study gene expression fluctuation within cells which started in the same genetic state, something unachievable by conventional cell sorting methods which dissociate cells of immediate genetic relation. Our platform has also enabled the observation of non-proliferative, Nanog+ cells which have not been noted in literature before.

4.2. Biological Hypothesis: Nanog Expression is Metastable at Low LIF Concentrations

Our objective is to test this hypothesis of stem cell gene expression metastability (Figure 21) by visualizing the dynamic operation of the pluripotency transcription factor network in individually trapped stem cells. Chemical microenvironment changes such as altering the local concentration of small-molecule inducers (e.g. leukemia inhibitory factor) will serve as systemic perturbators which will affect the cells' levels of Nanog expression (Figure 22). Our experiments will visually record changes in cell survival, colony proliferation, colony movement, colony size, and levels of Nanog gene expression as a function of time. If the stem cells truly exhibit metastable gene expression of Nanog when the chemical microenvironment pushes towards differentiation, we expect to observe cells which enter into a low-Nanog expression state, and then with time, recover back to high-Nanog expression state with subsequent full stem cell potential. The questions under consideration are 1) what percentage of cells appear to differentiate, but then recover back to stem cell morphology (proof of metastableness), and 2) can we determine which environmental factors are key effectors to stem cell recovery from metastableness to full pluripotency.

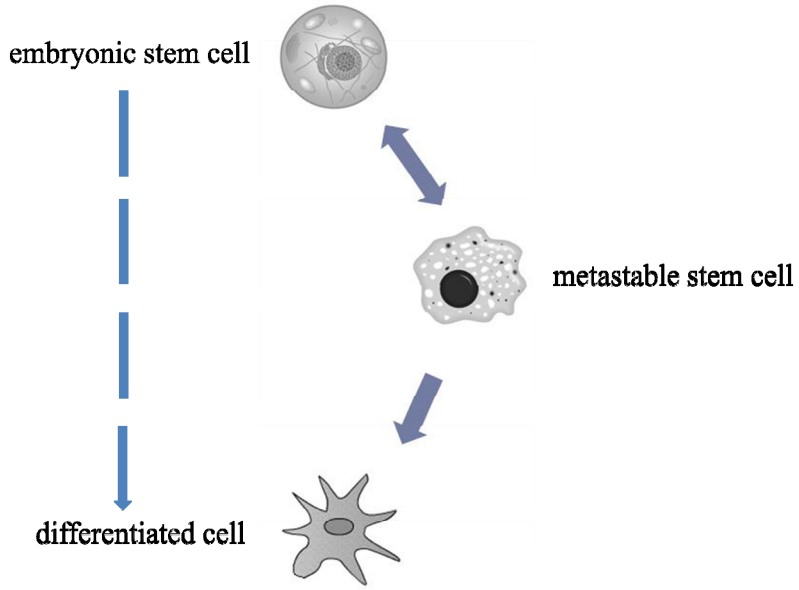

Figure 21. Embryonic stem cells are hypothesized to enter a metastable state in between full pluripotency and full differentiation, where recovery back to full pluripotency is still possible. Differentiated cells, however, enter a terminal fate.

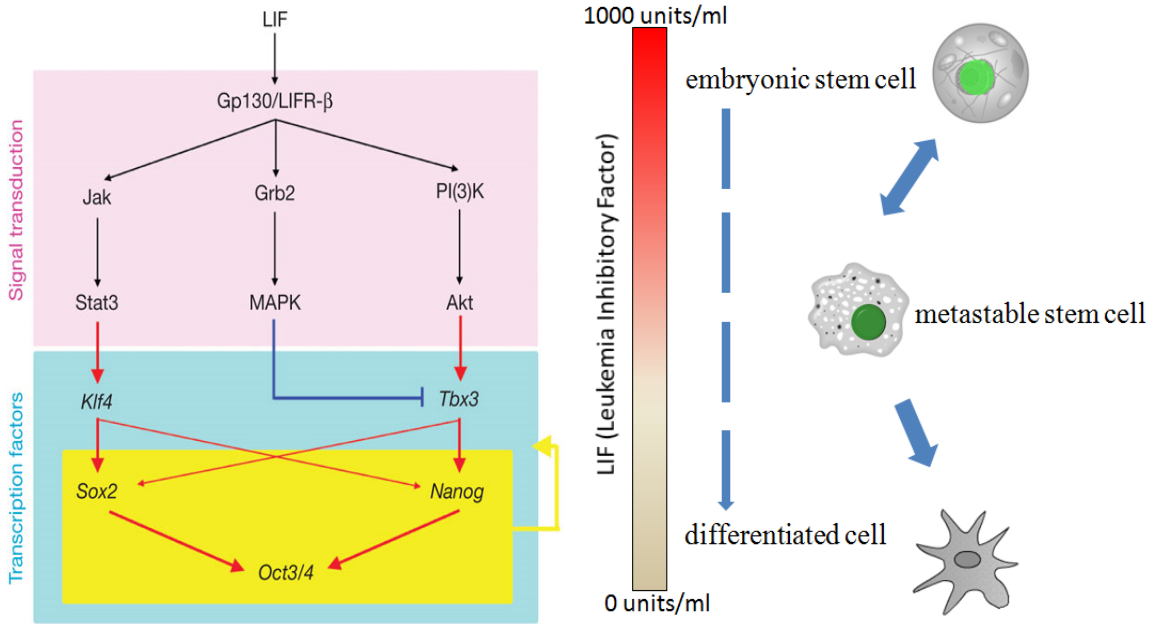

Figure 22. Signal transduction network between external small molecular signal (LIF) and nucleic gene expression of key stem cell gene Nanog. LIF is capable is sustaining a mouse embryonic stem cell's pluripotency potential without the addition of other cofactors. There is a minimum necessary LIF concentration in the culture medium to maintain cell pluripotency, or else the cells will start to fall into a partial or fully differentiated state.

Another hypothesis of interest is how cells experience gene expression fluctuation within stem cells which started in the same genetic state (i.e. clonal). It is hypothesized that a stem cell's metastability in terms of Nanog expression is more affected by the

stochastic expression of Nanog at a particular moment than by genetic predetermination. This can be experimentally verified by visualizing whether stem cell colonies which grew out of single cell fluctuate their Nanog expression in synchrony, or independently of each other. If the colony fluctuates in synchrony, then Nanog expression is predominantly determined by the genetic state. If cells fluctuate their Nanog expression differently from their clonal neighbors, it is more likely to be determined by other factors. One particular advantage to doing clonal studies on the microfluidic platform instead of a conventional FACS (fluorescence activated cell sorting) is the preservation of spatial information in addition to real-time continuous monitoring of the Nanog gene expression levels.

4.3. The Stem Cell Model

The mouse embryonic stem cells which are used as a model for Nanog genomic metastability is a mouse embryonic stem cell (mES) subclone line called TNG-B (courtesy of Prof. Ian Chambers), which has two genomic modifications that make it very useful for experimentation (Figure 23). Both modifications take advantage of the fact that Nanog is naturally a transcription factor which activates other genes in the genome, i.e. when Nanog is present, both genes' products will be transcribed and translated into protein. The first genetic modification is for the expression of green fluorescent protein (GFP). The result is that when Nanog is present in the nucleus, GFP is being produced in the cytoplasm and remains unsequestered throughout the volume of the cell. This provides a nice visual readout of the relative levels of Nanog present at any point in time. The half-life of unmodified GFP in the cytoplasm is 26 hrs[78] but can be shortened down to 6 hrs with slight modifications. While the particular sequence of this GFP form is unknown to us, observation of the same cell colony over time shows fluorescence fluctuations at higher time frequencies than every 24hrs, so it is believe we have a short-lived form of GFP. It is also important to keep in mind that there is an inherent time lag (~4-8hrs) between changes in genomic expression and the subsequent effect on the cell's protein levels, taking into account mRNA transcription, translation by ribosomes, and any post-translational modifications. The second genomic modification in our stem cells is for resistance against the selective antibiotic puromycin. Normal mES cells are very sensitive to the toxic presence of puromycin, so only cells with high levels of Nanog will be resistance to being killed by this antibiotic which is added to the media. In this way, a pure population of undifferentiated stem cells can be maintained for long term culture and ensure that the stem cells used for experimentation start out with a minimum amount of Nanog activity. Culture protocol for the TNG-B line can be found in Chapter 7.

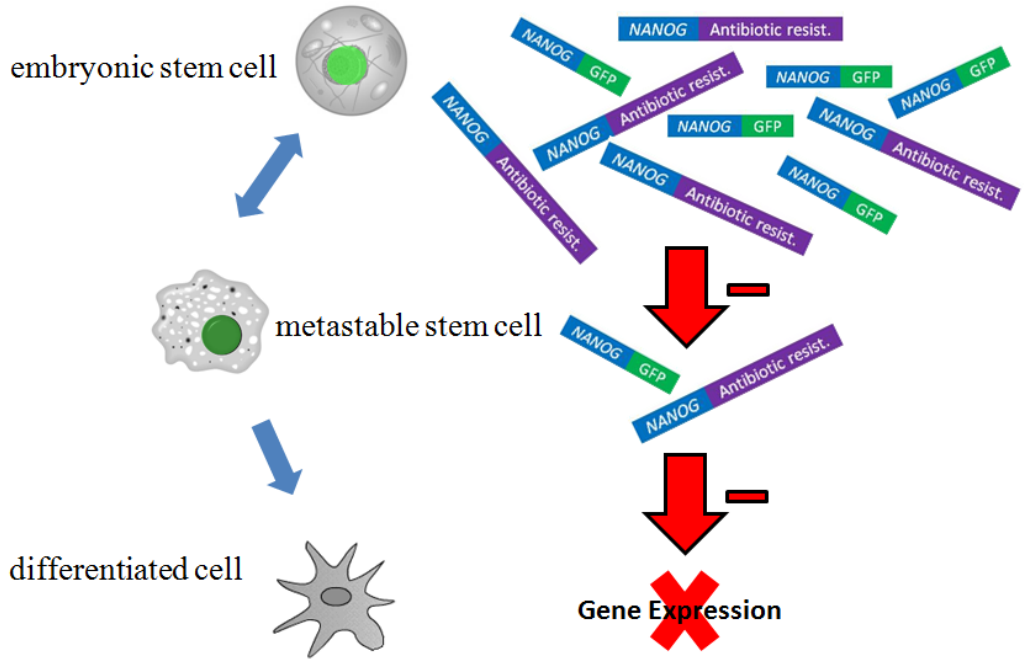

Figure 23. TNG-B subclone has two genetic modifications which respond to the *in situ* Nanog levels within the cell: GFP expression, and antibiotic resistance. Both genetic products are produced if and only if the Nanog protein is present within the nucleus to act as a transcription factor, and can act as direct quantitative readouts of a cell's Nanog levels.

4.4. LIF Gradient Perfusion Results

The biological hypothesis we wish to test using our microfluidic platform is that below a certain LIF threshold, the pressure to differentiate will cause the stem cells to enter into metastable Nanog gene expression behavior, whereupon clonal colonies of genetically identical cells will show different levels of Nanog expression. Determining where that LIF threshold resides, as well as stem cell behavior below that threshold, will give scientists insight into the stochastic fluctuations in the gene expression of key stem cell genes.

The media dead-volume was reduced by dropping a 22x40mm coverglass over the microwell array after aspiration of most of the media volume. The coverglass was gently pushed against the top edge of the gasket near the gradient generator and fluidically sealed by application of fast-drying nail acrylic along the left and right sides of the coverglass where it overlaps with the PDMS. P1000 pipet tips were added onto the inlet ports and used as fluid reservoirs for the relevant medias in the study.

All experiments featuring a gradient had green food dye used as a LIF concentration indicator (Figure 24). Although green food dye (MW=765)[84] and LIF (MW=32-62kD)[85] have different molecular sizes and therefore diffusion coefficients, the color dye gives an easy visual readout of the state of the gradient perfusion flow, and the existence of

any unintentional blockages or flow problems. A calculation of expected lateral diffusion of molecules of similar size to LIF through water solution follows.

Diffusion distance in one-dimension: $X^2 = 2Dt$
Where D is diffusion coefficient ($\mu m^2/s$).

using $D = 2.3 \times 10^{-11}$ m^2/s for FITC-dextran 70kD in phosphate buffer saline.[86]
upon conversion, $D = 23\mu m^2/s$.

The rate of flow we commonly used in our experiments was 20mm in 40min.

$X^2 = 2 * 23\mu m^2/s * (40min * 60s/min) = 110{,}400\mu m^2$
$X = 332\mu m$

A LIF molecule will diffuse 332μm laterally within the amount of time it takes for the medium to flow the length of the microwell array, an insignificant distance (<1%) compared to the 40mm width of the array. We can thus conclude that the LIF gradient generated by the gradient generator tree has fidelity down the length of the device and thus we can directly compare all the rows equally.

One common problem was the blockage of the gradient generator channels by unexpected protein blobs. After testing several hypotheses, it was discovered that the protein blobs resulted from when serum-rich media continuously backflowed and dehydrated out of the inlet holes. The dried protein crust was then scraped off the sidewalls of the inlets when the inlet reservoirs were inserted, and the crust rehydrated and congealed within the channels, blocking flow. This issue was easily resolved by adding the inlet reservoirs from the beginning and prewetting with 500μl of phosphate buffer saline.

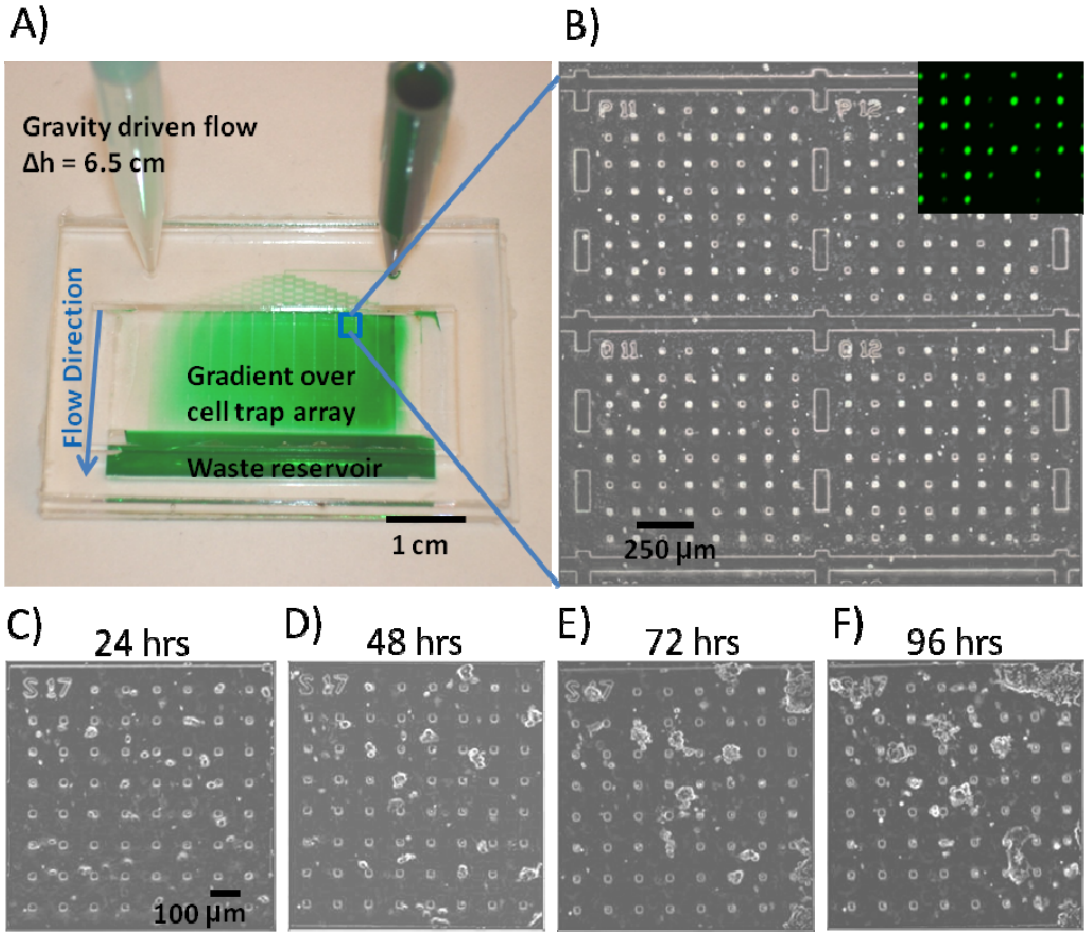

Figure 24. (a) Photograph of assembled device. Gradient generated by the device is visualized using green food dye. Characterization of the gradient generation can be found in Supplementary Fig. 1. (b) Phase contrast image of four squares of the microwell array containing trapped single mouse embryonic stem cells. The device contains 1092 square units. Each square is delineated by borders and a unique identification tag to facilitate ease of repeat imaging. Inset shows green-fluorescence picture of trapped cells inside the microwells. The stem cells are Nanog-GFP positive when first loaded into the device. (c-f) Phase contrast images of stem cells in the same location from day 1-4 (left to right).

4.4.1. Data Analysis

Fluorescent (Nanog+) cells were visualized with appropriate filters under an inverted microscope (Nikon Eclipse TE2000-E). Both phase contrast and FITC fluorescence images were taken of every square in a particular row in order to have the full spectrum of LIF concentrations in one go. Phase contract images had a shutter time of 100ms, FITC images had a shutter time of 3sec, and gain was set to 3. Image processing of the fluorescent images was done using the freely available ImageJ software, protocol found in Chapter 7. The data was compiled in Microsoft Excel and regular QC was done to verify the parameters being used. The colony size and intensity data was divided into 5 groups based on LIF concentration and the mean and variance values were calculated.

As the population size in the different groups varied, we used Welch's T-test was used to calculate the statistical relevance of the variations observed in the data.

4.4.2. LIF Threshold: Experimental Results

Mouse embryonic stem cells are well known to be responsive to the local concentration of Leukemia Inhibitory Factor (LIF), yet the response of individual stem cells has been difficult to study; most studies use population data which averages the response of any individual subpopulations. Our culture platform is designed to illuminate any subpopulations which may exist for a particular experimental condition analyzing the response of single cells separately. For stem cells grown in a LIF gradient, for example, there is a sharp decrease in cell viability as the LIF concentration decreases, as expected (Figure 25). The experimental data suggests that the cells have LIF concentration sensitivity around 400 U/ml, above which threshold the stem cells exhibit colony growth and proliferation, below which the stem cells show differentiation and subsequent death (by puromycin). While it may initially seem intuitive that colony growth would increase linearly with LIF concentration, the data suggests instead that there is a very narrow range of LIF concentration where the stem cell response to the LIF concentration is metastable, with certain cells exhibiting normal growth rates, and other colonies which either maintain their size or die off. This narrow band of LIF concentration resides at 200 to 450U/ml, and would merit further study in order to differentiate possible subpopulation growth behaviors (Figure 26). Future experiments could limit the LIF gradient range from 200 to 500U/ml in order to maximize the number of data points within this region of interest.

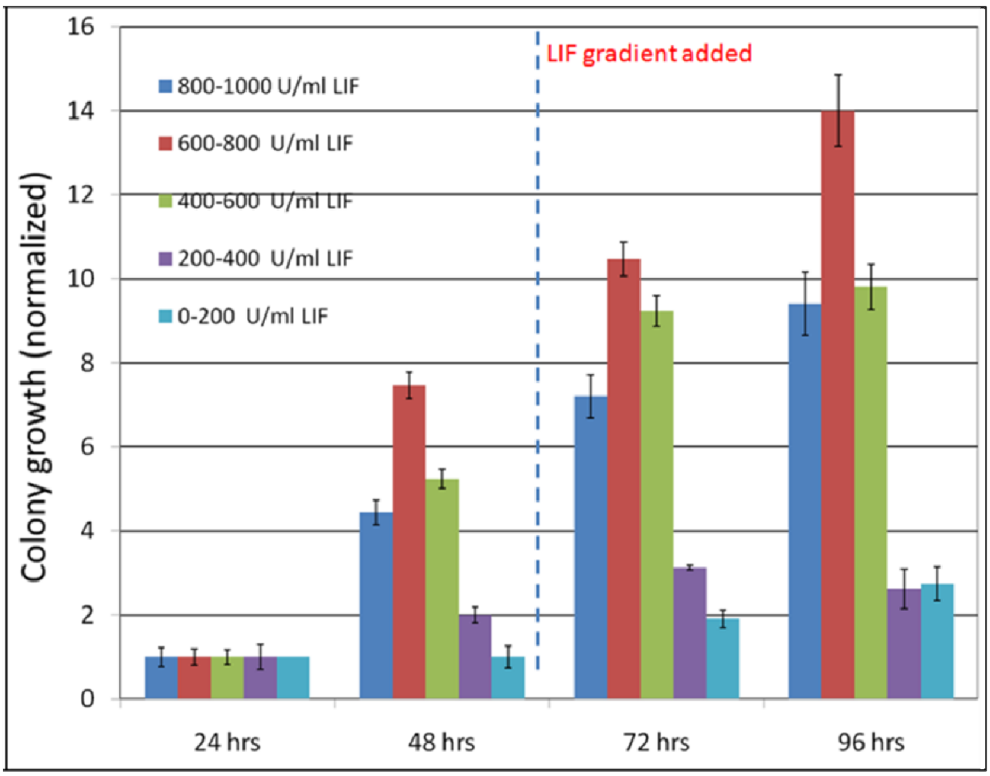

Figure 25. Comparison of stem cell growth under different LIF concentrations. LIF negative media was added to one inlet at 48 hrs to form a perfusion gradient for an additional 48 hrs. Growth of mouse embryonic stem cells exposed to ≥600 U/ml of LIF show steady colony growth. Stem cells which did not proliferate and remained as single cells were excluded from analysis. n≥5 for LIF≤400 U/ml. n≥30 for LIF>400 U/ml.

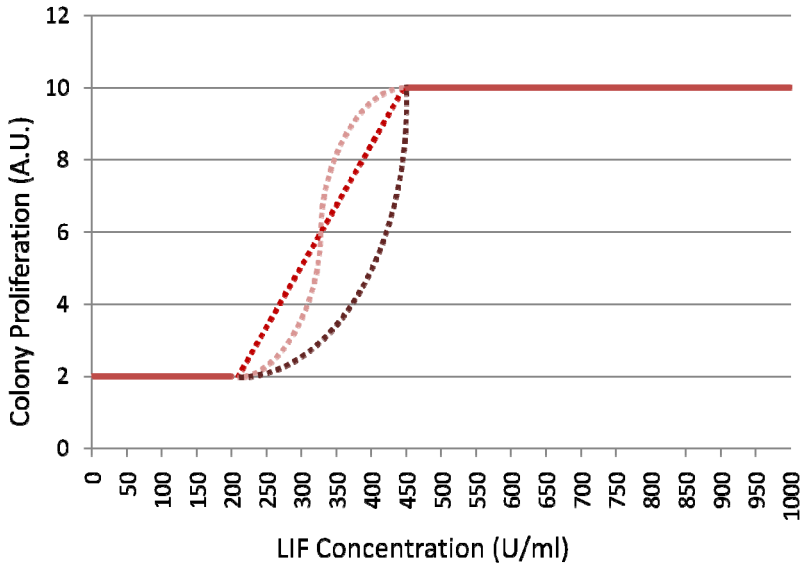

Figure 26. Illustration of three possible growth trends of cell subpopulations within the narrow LIF concentration which generates metastable cell behavior. The microfluidic platform will greatly aid being able to discern these subpopulations from each other since traditional plate culture is not optimized to grow and keep track of stem cell colonies as individuals.

Our original hypothesis was that the mouse embryonic stem cells experience gene expression fluctuation within stem cells which started in the same genetic state (i.e. clonal). It is hypothesized that a stem cell's metastability in terms of Nanog expression is more affected by the stochastic expression of Nanog at a particular moment than by genetic predetermination. This can be experimentally verified by visualizing whether stem cell colonies which grew out of single cell fluctuate their Nanog expression in synchrony, or independently of each other. If the colony fluctuates in synchrony, then Nanog expression is predominantly determined by the genetic state. If cells fluctuate their Nanog expression differently from their clonal neighbors, it is more likely to be determined by other factors. Since our microfluidic platform is optimized to trap single cells and observe the clonal colonies which grow out of those single cells, our experiments are primed to test that hypothesis. Our data strongly suggests that Nanog expression is not predominantly determined by the initial genetic state since the majority of cell colonies within the metastable LIF concentration (see above paragraph) region show a speckled pattern suggesting that each cell's Nanog gene expression is controlled independently of its immediate neighbors (Figure 27). One possible explanation for colony speckling is the death of cells within the colony mass, but that hypothesis is discounted by looking at the phase-contrast images (not shown) which confirm no missing mass within the cell colony. A more certain verification of cell number and location can be obtained with a nuclear stain such as DAPI, but unfortunately, nuclear stains terminate the experiment in progress by causing irreparable damage to the cell's genome and are therefore incompatible with temporal tracking studies.

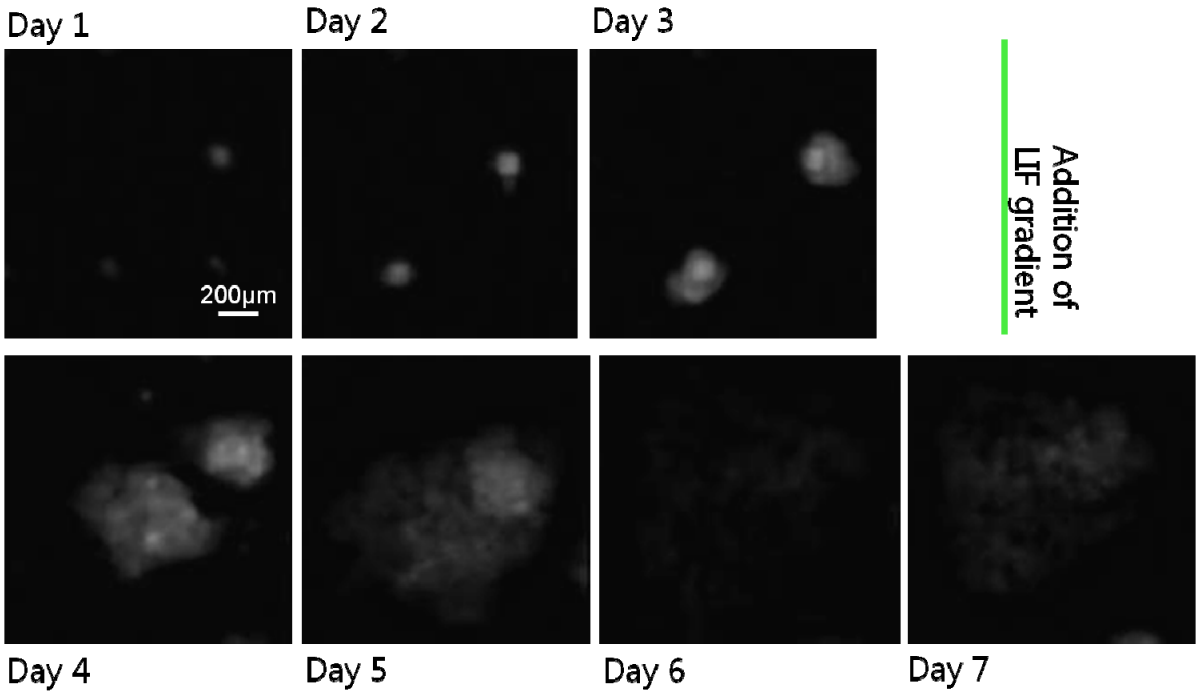

Figure 27. Temporal tracking images of a set of mouse embryonic stem cell colonies cultured for the first three days in 1000U/ml of LIF, followed by another four days in 250U/ml LIF. Fluorescence indication of Nanog expression can be observed to fluctuate greatly between immediate cell neighbors starting on Day 4.

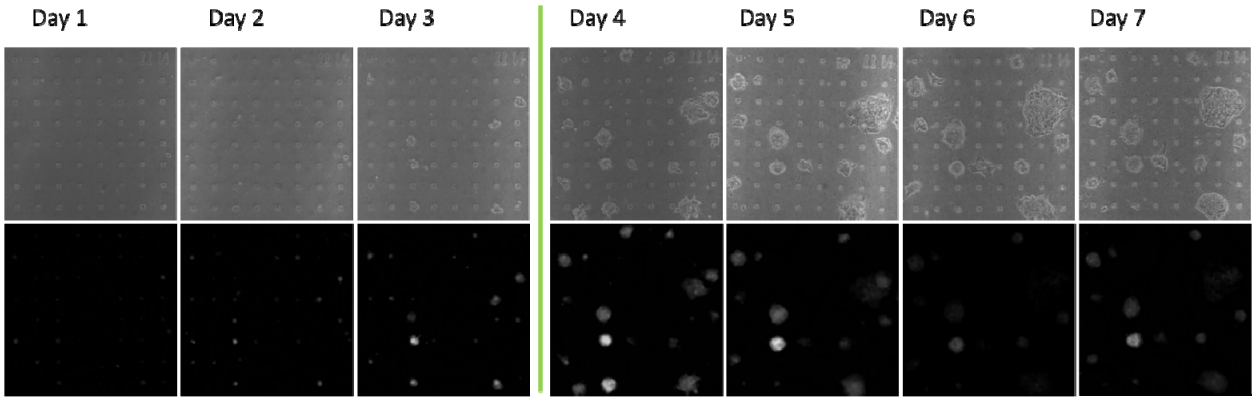

Figure 28. Temporal tracking images of a viewing square of the EMPRESS device. The mouse embryonic stem cell colonies were cultured for the first three days in 1000U/ml of LIF, followed by another four days in 250U/ml LIF. Fluorescence indication of Nanog expression can be observed to fluctuate differently amongst the colonies within secretion distance of each other.

4.5. Single Cells: Mysterious Islands

Another method of looking for growth trends within the stem cell colonies was to plot each colony based on size and average Nanog expression to see if there are discernable subpopulations. From the image cytometry data we collected (Figure 29), the mouse stem cells show a bimodal growth response once they are exposed to a LIF gradient. The cells will either increase in colony size and stabilized Nanog expression (LIF > 600 IU/ml), or cells proliferate at a greatly reduced rate, but increase Nanog expression to compensate for the loss of LIF signaling and overcome differentiation pressure (LIF <200 IU/ml). It is currently unknown what causes a small percentage of stem cells to overcome the differentiation pressure presented by low LIF concentrations and maintain their pluripotency potential and proliferative behavior.

It is well known that there is a significant increase in stem cell differentiation as the LIF concentration decreases below a critical threshold, but surprisingly, there are also some cells which remain undifferentiated and non-proliferative. Please keep in mind that selective antibiotic was present in the medium to eliminate non-Nanog expressing (i.e. differentiating) stem cells. These single stem cells (Figure 30) are expressing Nanog and maintaining high levels of Nanog over 96hrs, so they are overcoming the pressure to differentiate, and yet they are also not exhibiting standard proliferative behavior, another downstream effect of Nanog. By their very existence, these stem cells are contradictory based upon known biological signaling pathways. Post-experimental harvesting and genomic analysis of these single stem cells could yield information on a branch of the Nanog signaling pathway which is currently unknown.

The existence of these non-proliferative, Nanog+ single stem cells was highlighted by the design of our microfluidic platform, which optimizes the trapping of single cells, improves their rate of survival as single cells, and enables repeatable image cytometry over a long time scale. It is of particular note that their existence was not previously noticed by Prof. Chambers' lab, from whom the cells originated. Since traditional plate culture technique does not lend itself to high-efficiency survival of single embryonic stem cells, our platform enabled the discovery of possibly a novel subpopulation of interest to the biological community.

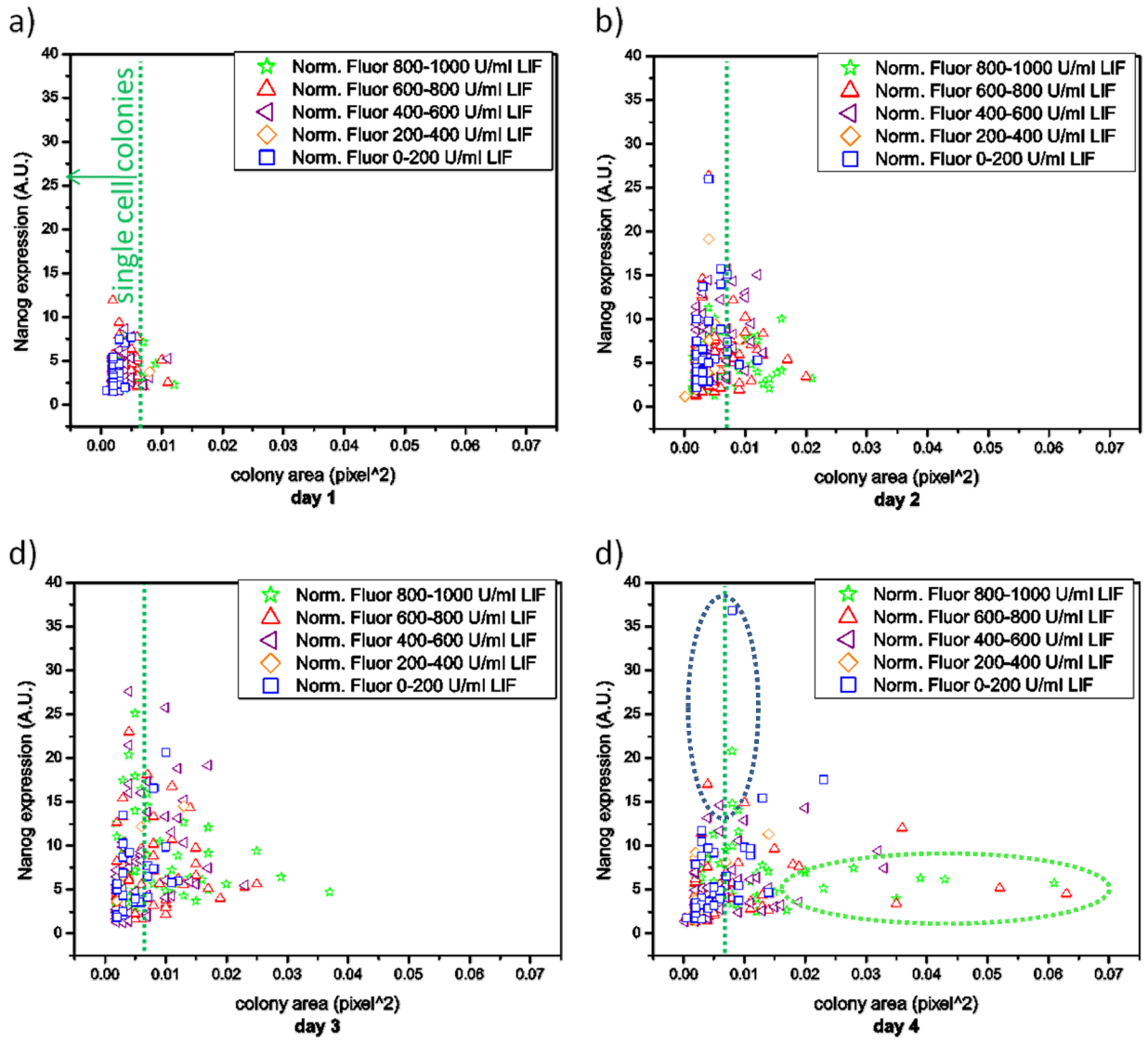

Figure 29. Single colony Nanog expression data for mouse stem cells establishing themselves in 1000 U/ml LIF (Day 1 and 2) and living under a LIF gradient (Day 3 and 4). n≥5 for all conditions. Colonies smaller than 0.007 area are considered to be single cells. (a) all cells which were loaded into the microwells 24 hrs previously (Day 0) have similar levels of Nanog expression and mostly the same colony size. (b) as the stem cells start to proliferate, the colonies show increased scatter in size. (c,d) Once a LIF gradient has been added, the colonies show bimodal response: normal behavior by increasing colony size and stabilized Nanog expression (LIF > 600 U/ml), or trying to overcome differentiation pressure (LIF <200 U/ml). These cells proliferate at a greatly reduced rate, but increase Nanog expression to compensate for the loss of environmental LIF. Selective antibiotic was present to eliminate non-Nanog expressing stem cells, causing all differentiating cells to be killed.

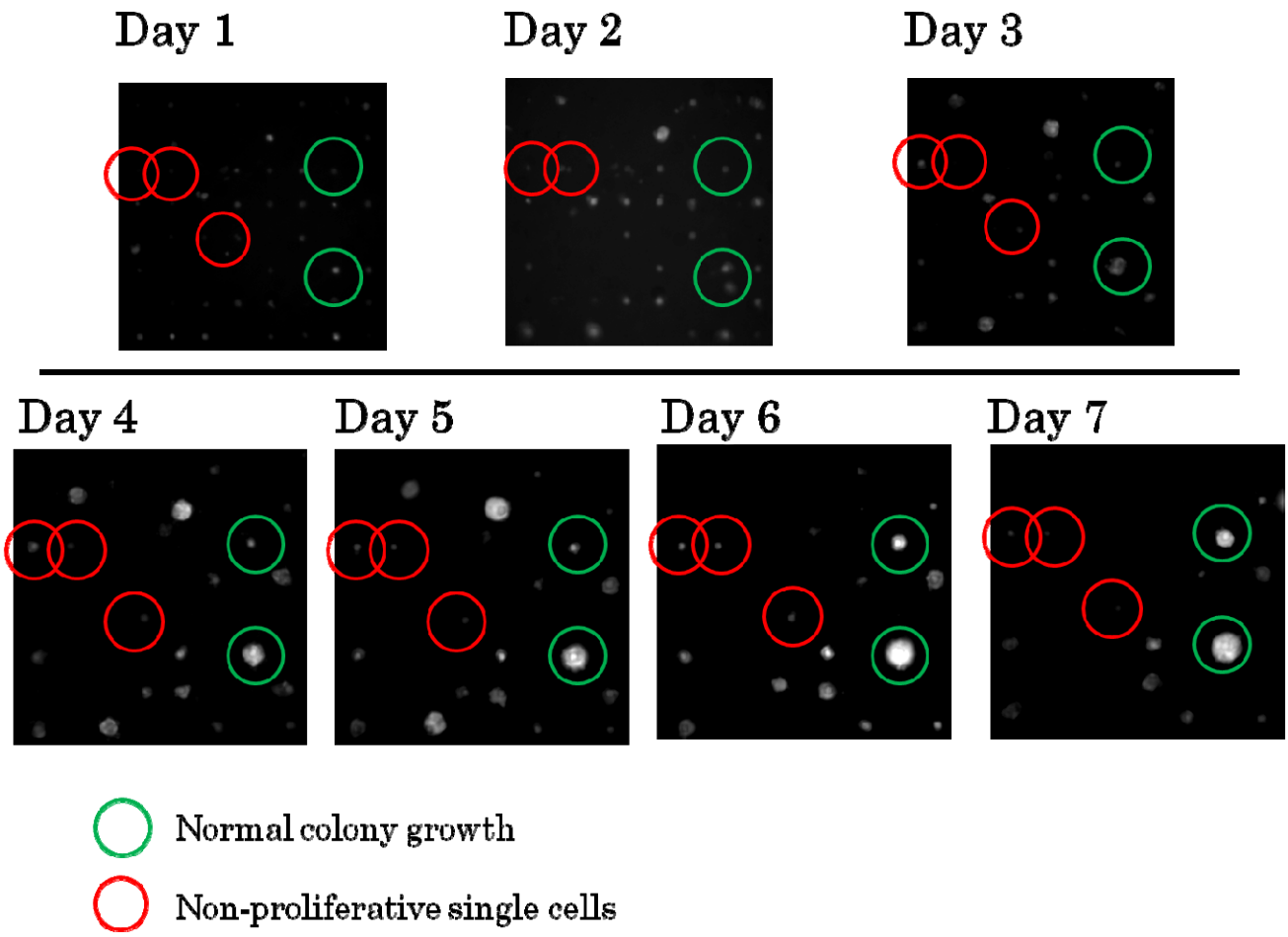

Figure 30. Illustration of non-proliferating single cells where some Nanog+ cell which do not proliferate at all, contrary to normal Nanog effect on gene expression and behavior within mouse embryonic stem cells. The growth medium is 400U/ml of LIF.

4.6. Conclusions

Using this platform, we have identified the LIF (leukemia inhibitory factor) concentration thresholds (200-450U/ml) where mouse embryonic stem cells differentiate readily into the metastable behavior that is important in the study of cross-regulatory interactions between core transcription factors and their target genes. We were also able to track in real-time the clonal colonies derived from single cells to study gene expression fluctuation within cells which started in the same genetic state, something unachievable by conventional cell sorting methods which dissociate cells of immediate genetic relation. Our results indicate that Nanog gene expression is not predominantly controlled by genetic sequence since clonal colonies of daughter cells show marked different levels of Nanog between neighboring cells. Since adjacent cells fluctuate their Nanog levels independently of each other as a function of time, we also postulate that Nanog expression is not controlled by cell-to-cell contact signaling. Our platform has also enabled the observation of non-proliferative, Nanog+ cells which are previously unreported in literature.

CHAPTER 5: INDUCED PLURIPOTENT STEM CELLS

5.1. Abstract

Induced pluripotent cells (pluripotent stem cells created from adult non-stem cells) hold great promise for regenerative medicine because they can potentially bypass the usual immune response against donor tissue. Since the production efficiency of these promising cells is very low (<5%), and the formation process creates a heterogenous population of cells with differing expression levels of the key stem cell genes, there is a lot of interest in being able to isolate single iPS cells and grow clonal colonies for further study. Our microfluidic platform consumes a smaller cell population per experiment than standard plate culture, an advantage when the initial population is limited. Our cytokine diffusion-limiting geometry may also offer higher survival rates of dissociated single iPS cells than is currently achievable on-plate.

5.2. Introduction

For many years, scientists struggled with balancing the ethics of working with human embryonic stem cells with potential clinical breakthroughs. Embryonic stem cells seemed to hold so much clinical potential with their pluripotent power to differentiate into all the tissue types of the adult body, yet animal studies kept on encountering the roadblocking problem of unpredictable teratoma growth. Most stem cells injected into an animal model did not differentiate only into the tissue type of the host tissue, but instead grew into a hodgepodge mixture of different tissue types.[87-91] Such uncontrolled behavior is very dangerous for a patient, and seemed like an insurmountable obstacle for embryonic stem cell treatment to overcome. To circumvent usage of embryonic stem cells, researchers instead tried to find ways to reprogram adult cells back into a pluripotent state. There were some successful pioneering experiments in the 1960s with somatic nuclear transfer[92], whereupon it was shown that the genome of a differentiated somatic cell could be reprogrammed by exposure to egg cytoplasm. Yet, scientists struggled for many years to replicate somatic nuclear transfer reprogramming in mammals, with only a handful of successes.

Instead, in 2006, a seminal paper by Yamanaka[93] reported the creation of ESC-like cells from adult cells, called induced pluripotent stem cells (iPSCs) by the retroviral introduction of four key genes: Oct4, Sox2, Klf4, and c-myc. In principle, human iPSCs could be used as an ethically uncontentious substitute for human embryonic stem cells for the purposes of patient-specific cell therapy, but the retention of exogenous DNA sequences from the retroviral carriers makes current iPSC lines unsuitable for clinical use. Many advances are currently being made to replace retroviral DNA delivery with other, less clinically hazardous methods such as protein delivery, plasmid delivery, and chemical reprogramming.[94-107] In addition to having clinical potential, iPSC lines are also

prospective models of human disease, especially the prenatal phases of human genetic diseases. The most compelling advantages of using iPSCs as disease models is that virtually any disease can be "captured" in the form of potentially malleable iPSC lines.[108-110] A further advantage is that patient-derived iPSC lines can come with the donor's complete clinical history, a benefit that is not available for human embryonic disease models.

5.3. PDMS Substrate Not Compatible for iPS Culture

The golden ticket in induced pluripotent stem cell research is being able to start with a patient somatic cell, reprogramming it into an iPSC, and then reliably differentiating those iPSCs into the tissue type of choice. However, existing methods to grow human pluripotent stem cells are not well suited for genetic manipulation experiments and introduce animal components, increasing the risks of immune rejection. Present methods to grow hES and hiPS cells include growing them on a 'feeder' cell layer of mitotically inactivated mouse embryonic fibroblasts[87, 111-113], on 'feeder free' extracellular-matrix proteins coated onto tissue culture dishes[114-122], or synthetic materials such as hydrogels[123-126]. These have been reported to promote hES cell self-renewal when seeded at a suitably high cell density and have not been demonstrated to efficiently promote clonal growth of single hES cells (efficiencies typically <10%).[127-129], making it a very resource-, time-, and labor-intensive endeavor to create enough cells for clinically relevant experimentation. While the created iPSCs themselves replicate quite readily (doubling time between 24-60hrs), the differentiated cells which are the end fate of the iPSC population do not replicate, which means the researcher must start off with billions of iPSC cells in order to generate enough tissue specific cells for cell replacement therapy.

Because iPSC reprogramming efficiency is so low, there is an interest from Prof. Joseph Wu's lab to use our microfluidic platform to enhance the survival of the few iPSC that are created after the successive rounds of gene transfection. It is hypothesized that the microwell geometry may locally concentrate autocrine or paracine factors which may be secreted by the cells. To elucidate whether our microwells can culture the iPSCs with better survival than standard plate culture, our initial trials tested a serial dilution of cell concentrations from 1 to 1/32 of the minimum known standard plate dilution on microwells coated with Matrigel (the standard growth substrate), with no top encapsulation and no perfusion flow (i.e. static culture on-chip). Our results were inconclusive since all the cells died irregardless of cell dilution. Our initial hypothesis to account for this failure was that the enzymatic dissociation of the original iPSC colonies was more cytotoxic than expected, since standard iPSC culture protocol does not promote the dissociation of colonies beyond small clumps (3-10 cells). To test whether our cell survival was dependent on initial cell seeding clumpiness, we then attempted to culture small clumps on the main surface of our microfluidic device instead of within the microwells where the clumps won't physically fit, and eliminated the lateral wash so that the experimental protocol on-chip closely resembled the protocol for plate culture. Our results were again uniformly negative for cell survival irregardless of initial cell

clumpiness or cell dilution. Since our positive control on a standard 6-well plate used the same Matrigel coating solution and the same iPS cell solution and proliferated normally, it was hypothesized that the main issue was the growth substrate. After discussion with other researchers in the Lee lab with experience working with iPSC on PDMS substrates, it was concluded that either (1) the Matrigel does not coat PDMS well due to unknown surface chemistry, or (2) the physical stiffness of the Matrigel-coated PDMS was not suitable for iPSC culture.

5.4. Polystyrene Microwells More Suitable Culture Substrate

Our solution to the growth substrate challenge was to change out the PDMS microwell layer with a microwell device made from polystyrene, the same material standard culture plates are made from. Changing the microwell material to polystyrene will simultaneously absolve both the lack of Matrigel adhesion and of substrate stiffness. In collaboration with the Albert p. Pisano laboratory, we came up with a protocol to hot-emboss the microwell pattern into precut culture dishes (Figure 31) using PDMS as the embossing master. PDMS can also easily withstand temperatures above the 150-180°C melting temperature of polystyrene.

5.4.1. Polystyrene microwell fabrication

Using PDMS as the embossing master instead of the standard metal-based master has several advantages. The first advantage is the much lower cost associated with not using a machined embossing master. The second advantage is that the PDMS master can easily be fabricated from existing PDMS devices by merely making a negative relief of the microwell features. The third advantage is that PDMS is gas permeable, so air bubbles trapped within the microfeatures have an avenue of escape, a material property not available using metal or plastic-based molding masters. The last advantage is that because PDMS allows the trapped gas to escape from the microfeatures, the weight required to form the features is reduced by several orders of magnitude (0.8 vs 35psi), making the fabrication process compatible with a benchtop hotplate and a few handweights, greatly lowering the barrier to adoption.

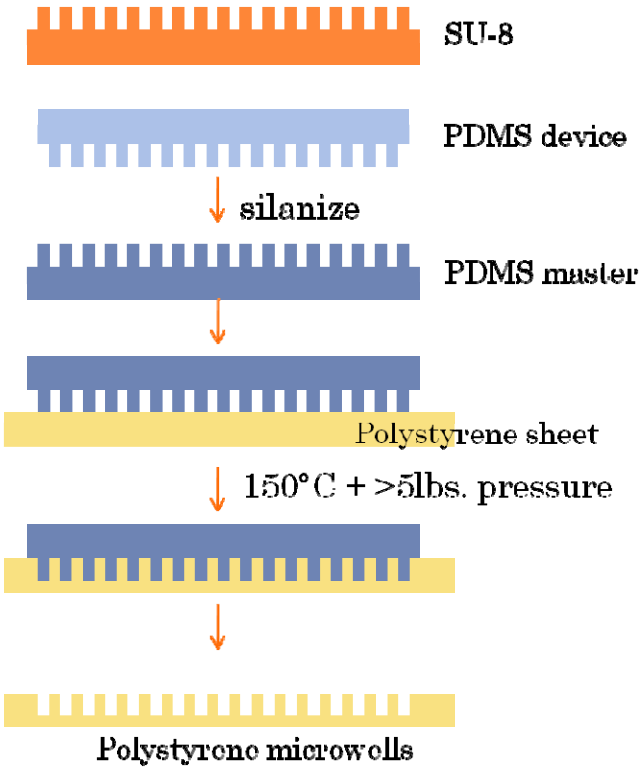

Figure 31. Fabrication protocol for making both the PDMS hot-embossing master and the final polystyrene microwell device. The polystyrene device is then coated with Matrigel following standard iPSC culture protocol.

The feature fidelity of the completed polystyrene devices is excellent, with no distortion in shape or size of the microwells (Figure 32). The microwell walls are sharply defined which minimizes any optical distortion for phase contrast and fluorescence images. While polystyrene does have a very faint autofluorescence, the hot embossing process reduces the thickness of the plastic at the bottom of the microwells from the original 1mm thick to a few hundred microns, dropping the amount of background fluorescence compared to standard plate culture. An unforeseen, but greatly favorable, side-effect is that the hot-embossing process automatically creates a fluidic gasket around the rim of the device with the displaced polystyrene, eliminating the need to separately bond a fluidic gasket as with the PDMS platform.

5.4.2. Polystyrene microwell wetting

The next challenge to overcome was the hydrophobicity and surface tension of the polystyrene. When aqueous solutions are first introduced onto the polystyrene microwells, air bubbles are trapped within the microfeatures, precluding microwell coating by extracellular matrix solutions and the stem cells from falling into the wells. After testing various protocols, the most favorable process prewetted with isopropanol, which has a much lower surface tension than water, followed by water displacement, followed by coating with an extracellular matrix such as gelatin or Matrigel (Figure 33).

Once an extracellular matrix has been successfully applied, the surface properties are permanently altered to hydrophilicity, enabling easy rewetting using aqueous solutions such as medium.

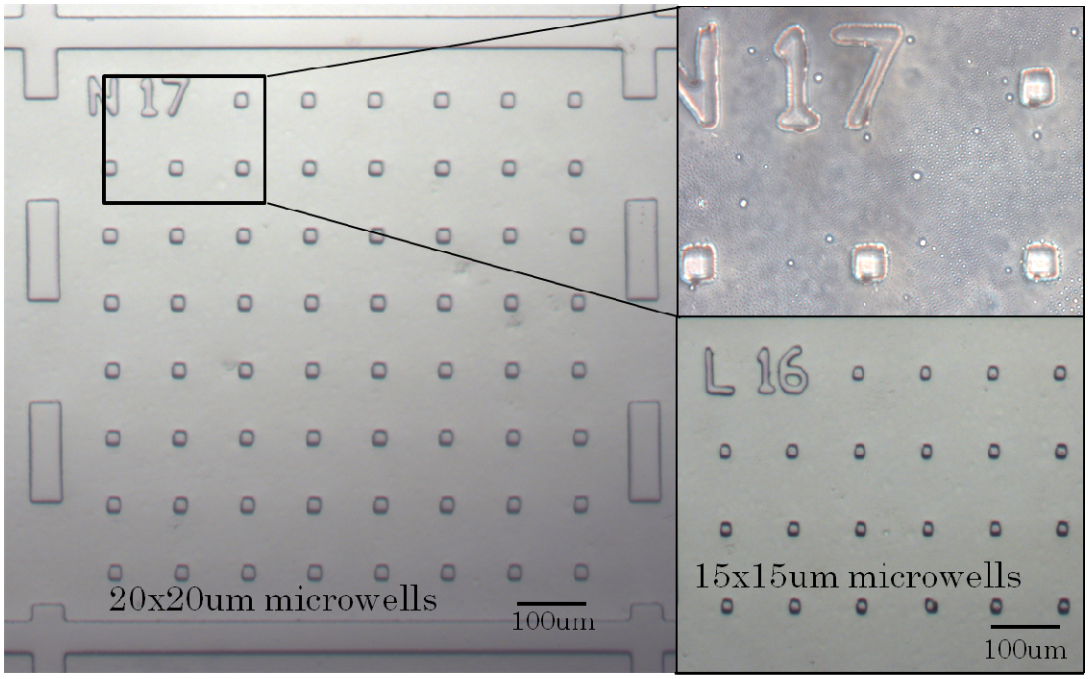

Figure 32. Feature fidelity of the polystyrene device is excellent, with both 15x15µm and 20x20µm microwells showing no distortion or size change compared to the original PDMS mold.

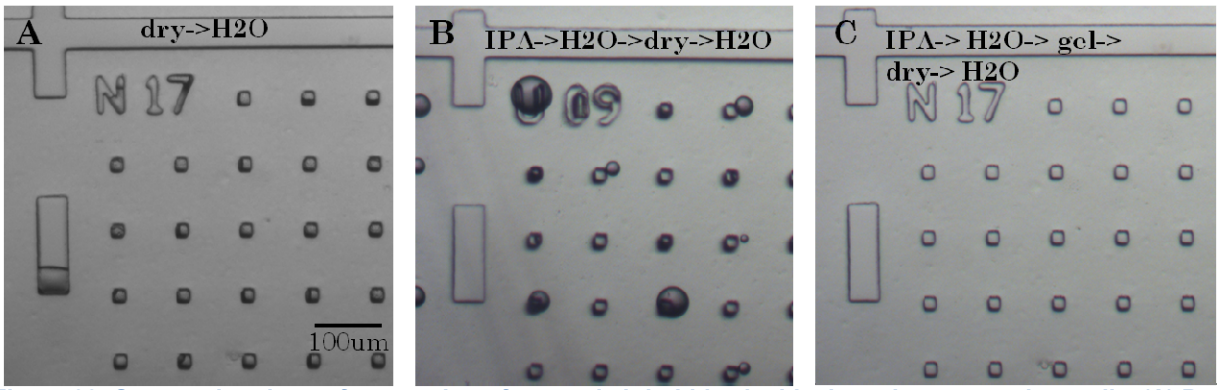

Figure 33. Overcoming the surface tension of trapped air bubbles inside the polystyrene microwells. (A) Bare polystyrene traps air bubbles within all the microfeatures, precluding coating by Matrigel solution or cell trapping. (B) The device can be fully wetted by initial wetting by isopropanol, followed by copious replacement by water; however, once that water has been removed, the surface chemistry reverts back to hydrophobicity. (C) Deposition of an extracellular matrix coat via wet incubation permanently converts the surface chemistry to hydrophilicity, enabling full wetting even upon complete removal of the previous solution.

5.5. Survival of Single iPS Cells

Mouse induced pluripotent stem cells (generously donated by Professor Joseph Wu) are plated at $4x10^5$ cells/100mmTCD and cultured for 5 days before experimentation. The cells are released from the plate with Accutase (Invitrogen Corp., Carlsbad, CA, USA) and triturated gently before centrifugation and resuspension in mTeSR1 medium (Stem Cell Technologies, Vancouver, BC, Canada) at a density of $25x10^3$ cells/ml. Cell solution is then added to microwell array in a protocol similar to Figure 14 and allowed to culture undisturbed for 24hrs. As seen from Figure 32, the iPS cells cultured on the polystyrene EMPRESS system show normal cell morphology to cells cultured on polystyrene dishes. Direct comparison of single cell survival between plate and EMPRESS is currently not available.

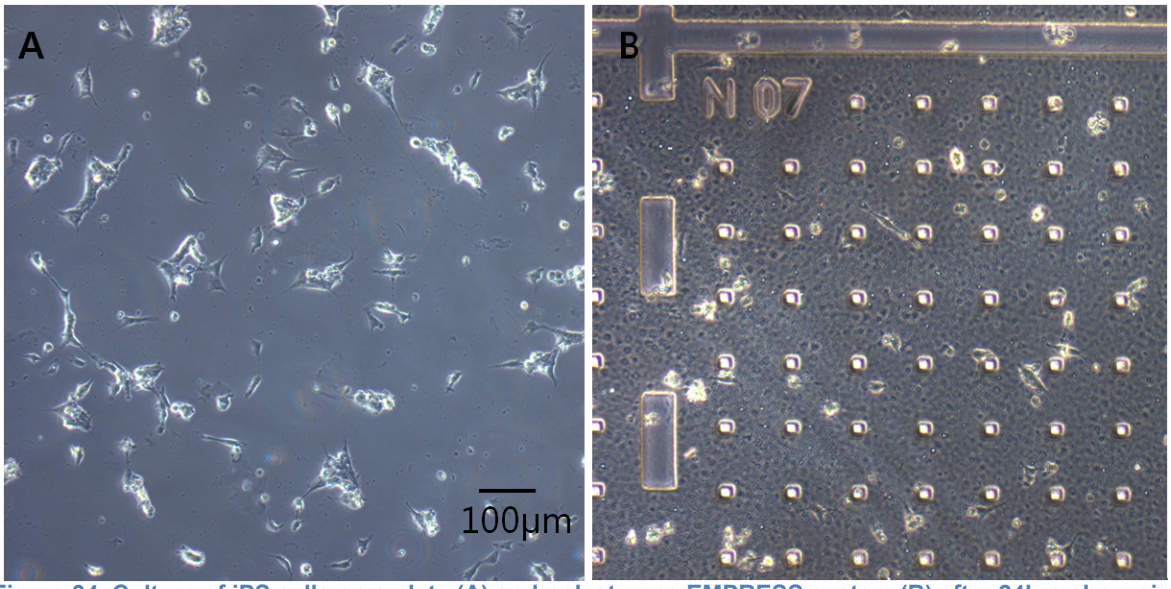

Figure 34. Culture of iPS cells on a plate (A) and polystyrene EMPRESS system (B) after 24hrs show similar cell morphology. The spatial density of the two cannot be directly compared since the EMPRESS system washed away all non-single-cell clumps.

5.5. Conclusions

We demonstrate that PDMS is not a compatible substrate for induced pluripotent stem cell culture due to incompatibility with the necessary extracellular matrix coatings. We then show that polystyrene devices can be easily manufactured using benchtop hot embossing, show excellent feature fidelity, and are amenable to wetting and coating by ECM protein solutions. We also demonstrate survival and normal cell morphology of single iPS cells on the polystyrene EMPRESS system.

CHAPTER 6: CONCLUSIONS AND FUTURE DIRECTIONS

This dissertation presents the creation of a pump-free, rapidly manufacturable microfluidic platform which enhances survival of single stem cells for single cell studies. The platform is an integrated culture system composed of an upstream linear gradient generator and an enclosed microwell cell trapping array. The system is optimized to enhance survival of single stem cells for long-term culture.

One of the major challenges facing stem cell researchers is to culture cells under controlled homogenous conditions to ensure consistent behavior of a stem cell population. Such control is critical for achieving predictable and uniform direction of stem cell differentiation in many systems and is of immense practical importance in regenerative medicine. Limitations in established methods are due to the combination of (1) poor single cell survival rates, (2) lack of spatial resolution in cell placement, and (3) dissociation of immediate genetic relatives during cell sorting. Without control over all of these factors, the biostatistics of clonal studies are inadvertently skewed towards certain subpopulations which can withstand unknown survival selection pressures or whose behavior were influenced by poorly controlled microenvironment changes, resulting in misleading confidence in the conclusions.

The novel design of our microfluidic platform addresses these challenges by controlling the spatial distribution of the cells, doubles single cell survival, and generates two orders of magnitude more data than 96-well clonal culture. The improved single cell survival, compared to plate culture, produces more representative data of the entire population versus selection of particular subpopulations. As discussed in Chapter Three, our device enhances single stem cell survival by trapping the stem cells into specially engineered microwells which physically exclude clusters larger than single cells, but are still shallow enough to allow the colony to subsequently expand outside the microwell for imaging. Inter-well distances are designed so that the wells are spaced close enough to allow sufficient amounts of growth factor to accumulate to aid cell survival and proliferation, yet far apart enough to allow progeny of single cells to be easily distinguished from each other. In addition, the regular spacing of the microwells makes the device compatible with high-throughput image cytometry since the locations of cells are no longer random, greatly decreasing the complexity of analysis.

Using this platform, we have identified the LIF (leukemia inhibitory factor) concentration thresholds where mouse embryonic stem cells differentiate readily into the metastable behavior that is important in the study of cross-regulatory interactions between core transcription factors and their target genes. We were also able to track in real-time the clonal colonies derived from single cells to study gene expression fluctuation within cells which started in the same genetic state, something unachievable by conventional cell sorting methods which dissociate cells of immediate genetic relation. Our platform has also enabled the observation of non-proliferative, Nanog+ cells which have not been noted in literature before.

The microfluidic platform has also been expanded into the culture of induced pluripotent stem cells which have garnered much interest for their clinical potential. Because iPSC reprogramming efficiency is so low, there is an interest to use our microfluidic platform to enhance the survival of the few iPSC that are created after the successive rounds of gene transfection. It is hypothesized that the microwell geometry may locally concentrate autocrine or paracine factors which may be secreted by the cells. Due to culture substrate incompatibility, we shifted the microwell device from polydimethylsiloxane to polystyrene, the material of which standard tissue culture dishes are composed. We show how using a PDMS embossing master has advantages over traditional hot embossing technology, especially in cost and barrier to entry.

In the future, this cell culture platform will have application to other research in the field. For example, we present possible future application of our platform into the field of cancer stem cells, a new paradigm in cancer research. There is convincing evidence that cancer stem cells are one of the key players in tumor proliferation and metastasis potential. As such, these cells are prime targets of study for the pharmaceutical industry whose current products cannot target these rare, resistant cells. Since the rarity and nonexpansion of cancer stem cells is the primary research hurdle, we propose to use our microfluidic platform to maximum the data mining which can be performed with a very limited cell sample size.

CHAPTER 7: METHODS AND PROTOCOLS

7.1. TNG-B Mouse Embryonic Stem Cell Culture Protocol

7.1.1. Thawing cells

1. Coat the base of the new culture flask / dish with prewarmed 0.1% gelatin for an hour.
2. Place 9.5ml of prewarmed media in a universal.
3. Retrieve cells from the liquid nitrogen. It is important that cells are thawed as quickly as possible, this is done by placing them in the 37°C waterbath.
4. Once they are thawed transfer cells to the warm media to dilute out the DMSO in which the cells are frozen. The cells are transferred to the universal using a plugged pasteur pipette.
5. Spin cells down in the bench centrifuge, at 1000rpm for 5 minutes.
6. The media is then aspirated off very carefully to avoid disturbing the cell pellet.
7. Resuspend cell pellet in 10 ml of prewarmed media very gently, as they very fragile at this stage.
8. Transfer to appropriate flask followed by gassing with a CO2/air mixture (5%/95%).
9. The cells are checked under the microscope and then placed in the incubator.
10. Cells should be thawed first thing in the morning and then the media should be changed at the end of the day. This removes any dead cells and dilutes out the rest of the DMSO.

7.1.2. Passaging ES Cells

1. Precoat new culture flasks with 0.1% gelatin.
2. Draw off media using aspirator.
3. Add 5mls of PBS down opposite side of the flask from the cells.
4. Wash cells then draw off PBS using aspirator.
5. REPEAT steps 2 + 3.
6. Add 1ml of trypsin down opposite side of the flask. Ensure trypsin covers cell monolayer. Recap flask and place in the incubator for approximately 30 seconds.
7. Tap flask to dissociate the cells.
8. Check under microscope to ensure cells have dissociated.
9. Add 4mls of media for 1ml of trypsin. The media will stop the action of the trypsin.
10. Transfer cells to a universal and spin down in the bench centrifuge. 5 minutes at 1200rpm.

11. Resuspend cells in 5mls of media, pipetting up and down 2 or 3 times to ensure a single cell suspension. Count cells using hemacytometer.
12. Add 10^6 cells to a $25cm^2$ gelatinized flask. The number of cells added to larger flasks should be adjusted accordingly. All flasks should be clearly labeled with your name, cell line name, passage number and date.
13. A guide for quantity of media to the size of flask is as follows :
    a. 10m/$25cm^2$ flask
    b. 30ml/$75cm^2$ flask
    c. 50ml/$150cm^2$ flask
14. For ES cells add 1µl of LIF / ml of media in the flask.
15. Gas flask with 5%CO2/95% air mixture and close lid tightly.
16. Return to incubator.

7.1.3. Freezing Cells

Freezing Solution
10% DMSO in culture media: Add 2ml of DMSO to 18ml of media to provide a stock solution.

1. Trypsinise as for normal cultures.
2. Once cells have dissociated resuspend in 8.5mls culture media and place in a universal.
3. Add 10% / volume of DMSO to the universal.
4. Spin cells in bench centrifuge at 1000rpm for 5 minutes.
5. Aspirate off supernatant carefully to prevent disturbing the cell pellet.
6. Resuspend in appropriate volume of freezing solution. Mix Gently.
7. Place 0.5ml cell suspension in cryotube, labeled with cell line name, passage number, date, and your initials. The number of vials per flask is dependent on the size of the flask :
   $25cm^2$ flask gives 2 vials
   $75cm^2$ flask gives 4-5 vials
   $150cm^2$ flask gives 8-10 vials.
8. Place the cryotubes in the –80°C freezer overnight and then transfer to cellbank the following day.

7.1.4. Medium Preparation

1x GMEM or 1:1 DMEM:F12 mix	500 ml
Fetal Calf Serum	55 ml
Non-essential Amino Acids	5.5 ml
Glutamine	5.5 ml
Sodium Pyruvate	5.5 ml
Mercaptoethanol	550 µl

Different pipettes should be used for different solutions. Once the medium has been prepared a TESTER should be set up and incubated overnight to ensure sterility. (5ml of media should be added to the 5ml tester)

ALL BOTTLES MUST BE LABELLED WITH INITIALS AND DATED.
**Do not use media if more than one month old.

7.1.5. TVP Formulation

0.05% trypsin/0.53mM EDTA in HBSS	100 ml
PBS, -Mg, -Ca	100 ml
EDTA·2Na, salt	53 mg

7.1.6. LIF Stock Formulation (to yield 1000 U/ml in culturing media)

LIF (Sigma #L5158)	whole volume
PBS, -Mg, -Ca	to make up volume to 500 µl

**Add 10 µl of LIF stock to 10 µl of TNG-B media to make up culturing media. Always add the LIF fresh, do not pre-mix into medium.

7.2. SU-8 Fabrication Protocol

7.2.1. Reagents

MicroChem MCC Primer 80/20
(based on a combination of 20% HMDS and 80% PM Acetate)
MicroChem SU-8 2050
MicroChem SU-8 2025

7.2.2. MCC Primer

Puddle on wafer for 10sec
Spin: 500rpm (accel ↑100 rpm/s, 10sec)
5000rpm (accel ↑300 rpm/s, 30sec)
Bake: 115°C, 3min

7.2.3. SU-8 2050

Spin: 500rpm (accel ↑50 rpm/s, 15sec)
3000rpm (accel ↑100 rpm/s, 45sec)
Bake: 65°C, 2min
95°C, 7min
Expose: 160mJ/cm^2 x 2 / lamp power
PEB: 65°C, 2min
95°C, 7min
Slow cool (turn off hotplate)
Take off edgebead with q-tip and acetone.

7.2.4. SU-8 2025

Spin: 500rpm (accel ↑50 rpm/s, 15sec)
3300rpm (accel ↑100 rpm/s, 45sec)
Bake: 65°C, 2min
95°C, 6min
Expose: 150mJ/cm^2 / lamp power
PEB: 65°C, 1min
95°C, 5min
Slow cool (turn off hotplate)

7.2.5. Develop and Hardbake

Develop: 7min + monitoring every 30sec. Total is ~9-10min
Hardbake: 150°C, 10min (no more, or else will dry out photoresist and lead to massive cracking)
Slow cool (turn off hotplate)

7.3. Plastic Master Mold Fabrication Protocol

7.3.1. Materials

Smooth-Cast 326 (transparent light amber) +Smooth-On release spray
10 or 25ml sereological pipets (2x) + pipettor + Plastic cup
PDMS device master
New petri dish/plastic cup large enough to fit your PDMS master (side height must be >4mm higher than your PDMS master
Strong vacuum chamber

7.3.2. Protocol

1. Cover the device-side of your PDMS with scotch or lab tape. Trim tape so it fits exactly over the top of the device.
2. (a) Put your PDMS master **device-side up** on the bottom half of your petri dish. Use your fingers to squeeze most of the air bubbles out of the bottom so the PDMS is pretty stuck to the plastic. **OR**
3. (b) Cover the other exposed side of your PDMS completely with double-sided tape and trim exactly. Press firmly onto acrylic slide-holder. Put double-sided tape along the outer edges of your acrylic backside, press into clean square petri dish.
4. Inside the chem hood, hold the Smooth-On release spray about 8 inches away from your dish and do a quick burst of spray over the dish. Use your gloved fingers to spread the release agent all along the bottom of the dish and along the sides. Repeat 2-3 times until you are assured all exposed plastic has been covered by the release spray. This is step is important! If you don't apply enough release spray, your urethane will stick to your dish, and the whole mold will be ruined.
5. Remove the tape from the top of your PDMS.
6. Put your dish into the strong vacuum chamber and degas the PDMS for 10min.
7. While waiting for the PDMS to degas, calculate out how much volume you will need to fill the dish. For example, for a 100mm square petri with a PDMS piece 1mm tall, I would need 100x100x3mm=30000mm^3=30cm^3=30ml worth of plastic. Always aim to have about 2 mm of plastic higher than your PDMS top.
8. In a plastic cup, pipet in ½ of your desired volume from the blue bottle (i.e. 15ml). Discard that pipet. To the same cup, pipet in ½ your desired volume from the yellow bottle. Pull the pipet from the pipettor and use as a stir stick. Stir for 2 min until all visible swirls disappear.
9. Pull your petri dish out of the vacuum chamber and immediately pour the mixed plastic over it. Quickly put the petri back into the vacuum chamber and apply vacuum for 1-2min.
10. The plastic stays liquid for ~10min, then hardens very fast, so be sure to pull the petri out of the vacuum before then, or you will harden all sorts of bubble shapes into your plastic mold.
11. Put your petri at room temperature for 1 hr, or 60°C oven for 30min to fully harden the urethane.
12. Squeeze the sides of the petri and push against the bottom of the petri to pop the urethane out like an ice cube from the ice tray.

13. Use tweezers to gently lift a corner of your PDMS from the urethane. Use IPA as necessary to assist the separation. Save the PDMS for future use. Congrats, you have made your plastic mold!

7.3.3. THINGS TO NOT DO:

- Forget to apply release spray.
- Spray the entire dish before putting your PDMS piece down. This causes the PDMS to not stick to the bottom, and it will FLOAT in the liquid plastic once vacuum is applied.
- Forget to take the petri dish out of the vacuum more than 10min after mixing. You will get hardened plastic with plastic foam on top.
- Forget to put your PDMS device-side up.
- Put the petri dish on a hot plate set for 60°C or higher in an attempt to speed up the curing process. This will warp the bottom of the dish.

7.4. Image Analysis Protocol

7.4.1. Image J Processing for Fluorescence Intensity/ Cell Area:

1. ANALYSE → SET MEASUREMENTS → select AREA, MEAN GRAY VALUE
2. IMAGE → TYPE → 8-BIT (16-BIT if specified)
3. PROCESS → SUBTRACT BACKGROUND. Set rolling ball= 50 pixels.

a. Check SLIDING PARABOLOID to deal w/ red(fluorescent) edge.

*Settings must be adjusted for area data:

ANALYSE→ SET SCALE→ Set:

Distance in pixels- 61
Known Distance- 100
Pixel Aspect Ratio- 1.0
Unit of Length- micron Scale: 0.61 pixels/ micron

Check Global so when you open new images the scale is automatically adjusted to this scale.

4. IMAGE → ADJUST → THRESHOLD → RED. Move bottom bar all the way to the right. Move top bar until cells are highlighted w/out noise. Consistency is important b/c this part is very subjective.

*DO NOT CLICK APPLY!!!

5. ANALYSE → ANALYSE PARTICLES → SIZE: 10-Infinity→ CIRCULARITY: 0-1→ SHOW: OUTLINES → DISPLAY RESULTS (raw data for STD), SUMMARIZE (avg. area).
6. Copy all data into MS Excel.
7. In Excel, calculate standard of deviation (STD) and graph data with Error Bars of STD.

7.4.2. PhotoShop Processing for light balance

1. IMAGE → ADJUSTMENTS → AUTO CONTRAST
2. IMAGE→ ADJUSTMENTS→ EXPOSURE. Change exposure till background is even in area of interest
3. IMAGE→ ADJUSTMENTS→ SHADOW

*Sacrificial USB required b/c of viruses

Mean= fluorescence

7.4.3. Macros Automation

Macros can be used to automate most of this procedure.
For PCs, download AutoHotKeys

Code used: (Adjust Pixels to match computer- use AutoIt3 Window Spy)

*For the pixels- first command is On-Screen coordinates; everything after is In Active Window coordinates

```
q::
MouseClickDrag,left, 740,36, 818,396
;clicks background subtractor
Sleep,500
;pause 1 sec
MouseMove 165,229
Click 165,229
;clicks okay
Sleep,1000
;pause
MouseMove 111,36
Click 111,36
;clicks image
MouseMove 131,95
;goes to adjust
Sleep 500
;pause
Click 355,168
;clicks threshold
Return
w::
MouseClickDrag,left, 802,35, 855,83
; clicks Analyze & Analyze Particles
Sleep, 500
;pause  500ms
Click 175,289
;clicks okay
Sleep, 500
;pause
Click 190,656
Return


`::
Click 806,147
;close result window
Sleep,200
;pause
Click 106,98
;clicks no to save
Sleep, 200
;pause
Click 251,134
```

```
;closes summary
Sleep, 200
;pause
Click 320,138
;closes outline
Sleep, 200
;pause
Click 320,122
;close image
Sleep, 200
;pause
```

When using macro- must do first run manually to set scale and other factors (ex background, analyze particle settings)

REFERENCES

1. Kehat, I., Gepstein, A., Spira, A., Itskovitz-Eldor, J. & Gepstein, L. High-Resolution Electrophysiological Assessment of Human Embryonic Stem Cell-Derived Cardiomyocytes: A Novel In Vitro Model for the Study of Conduction. *Circ Res* **91**, 659-661 (2002).
2. van Laake, L.W. et al. Human embryonic stem cell-derived cardiomyocytes survive and mature in the mouse heart and transiently improve function after myocardial infarction. *Stem Cell Research* **1**, 9-24 (2007).
3. Kehat, I. et al. Human embryonic stem cells can differentiate into myocytes with structural and functional properties of cardiomyocytes. *The Journal of Clinical Investigation* **108**, 407-414 (2001).
4. Vats, A. et al. Chondrogenic Differentiation of Human Embryonic Stem Cells: The Effect of the Micro-Environment. *Tissue Engineering* **12**, 1687-1697 (2006).
5. Karp, J.M. et al. Cultivation of Human Embryonic Stem Cells Without the Embryoid Body Step Enhances Osteogenesis In Vitro. *Stem Cells* **24**, 835-843 (2006).
6. Levenberg, S., Golub, J.S., Amit, M., Itskovitz-Eldor, J. & Langer, R. Endothelial cells derived from human embryonic stem cells. *Proceedings of the National Academy of Sciences of the United States of America* **99**, 4391-4396 (2002).
7. Zhang et al. In vitro differentiation of transplantable neural precursors from human embryonic stem cells, Vol. 19. (Nature, New York, NY, ETATS-UNIS; 2001).
8. Kim, J.-H. et al. Dopamine neurons derived from embryonic stem cells function in an animal model of Parkinson's disease. *Nature* **418**, 50-56 (2002).
9. Bjorklund, L.M. et al. Embryonic stem cells develop into functional dopaminergic neurons after transplantation in a Parkinson rat model. *Proceedings of the National Academy of Sciences of the United States of America* **99**, 2344-2349 (2002).
10. Korbling, M. & Estrov, Z. Adult Stem Cells for Tissue Repair -- A New Therapeutic Concept? *N Engl J Med* **349**, 570-582 (2003).
11. Wang, R., Clark, R. & Bautch, V.L. Embryonic stem cell-derived cystic embryoid bodies form vascular channels: an in vitro model of blood vessel development. *Development* **114**, 303-316 (1992).
12. Chambers, I. et al. Nanog safeguards pluripotency and mediates germline development. *Nature* **450**, 1230-1234 (2007).
13. Viswanathan, S., Benatar, T., Rose-John, S., Lauffenburger, D.A. & Zandstra, P.W. Ligand/Receptor Signaling Threshold (LIST) Model Accounts for gp130-Mediated Embryonic Stem Cell Self-Renewal Responses to LIF and HIL-6. *Stem Cells* **20**, 119-138 (2002).
14. Keller, G.M. In vitro differentiation of embryonic stem cells. *Current Opinion in Cell Biology* **7**, 862-869 (1995).
15. Schuldiner, M., Yanuka, O., Itskovitz-Eldor, J., Melton, D.A. & Benvenisty, N. From the Cover: Effects of eight growth factors on the differentiation of cells derived from human embryonic stem cells. *PNAS* **97**, 11307-11312 (2000).
16. Discher, D.E., Mooney, D.J. & Zandstra, P.W. Growth factors, matrices, and forces combine and control stem cells. *Science* **324**, 1673 - 1677 (2009).
17. Hattori, K., Sugiura, S. & Kanamori, T. Microenvironment array chip for cell culture environment screening. *Lab on a Chip* (2011).
18. Anderson, D.G., Levenberg, S. & Langer, R. Nanoliter-scale synthesis of arrayed biomaterials and application to human embryonic stem cells. *Nat Biotech* **22**, 863-866 (2004).
19. Flaim, C.J., Chien, S. & Bhatia, S.N. An extracellular matrix microarray for probing cellular differentiation. *Nat Meth* **2**, 119-125 (2005).

20. Peerani, R., Onishi, K., Mahdavi, A., Kumacheva, E. & Zandstra, P.W. Manipulation of Signaling Thresholds in â€œEngineered Stem Cell Nichesâ€ Identifies Design Criteria for Pluripotent Stem Cell Screens. *PLoS ONE* **4**, e6438 (2009).
21. Abhyankar, V.V. & Beebe, D.J. Spatiotemporal Micropatterning of Cells on Arbitrary Substrates. *Analytical Chemistry* **79**, 4066-4073 (2007).
22. Sasaki, D. et al. Mass preparation of size-controlled mouse embryonic stem cell aggregates and induction of cardiac differentiation by cell patterning method. *Biomaterials* **30**, 4384-4389 (2009).
23. Soen, Y., Mori, A., Palmer, T.D. & Brown, P.O. Exploring the regulation of human neural precursor cell differentiation using arrays of signaling microenvironments. *Molecular systems biology [electronic resource].* **2**, 37 (2006).
24. Trkov, S., Eng, G., Di Liddo, R., Parnigotto, P.P. & Vunjak-Novakovic, G. Micropatterned three-dimensional hydrogel system to study human endothelial–mesenchymal stem cell interactions. *Journal of Tissue Engineering and Regenerative Medicine* **4**, 205-215 (2010).
25. Saha, S., Ji, L., de Pablo, J.J. & Palecek, S.P. Inhibition of human embryonic stem cell differentiation by mechanical strain. *Journal of Cellular Physiology* **206**, 126-137 (2006).
26. Sim, W.Y. et al. A pneumatic micro cell chip for the differentiation of human mesenchymal stem cells under mechanical stimulation. *Lab on a Chip* **7**, 1775-1782 (2007).
27. Weiner, L.P., Chen, Y. & Zhong, J.F. in Neural Stem Cells, Vol. 438 293-303 (Humana Press, 2008).
28. Zhong, J.F. et al. A microfluidic processor for gene expression profiling of single human embryonic stem cells. *Lab on a Chip* **8**, 68-74 (2008).
29. Tada, M., Takahama, Y., Abe, K., Nakatsuji, N. & Tada, T. Nuclear reprogramming of somatic cells by in vitro hybridization with ES cells. *Current Biology* **11**, 1553-1558 (2001).
30. Ying, Q.-L., Nichols, J., Evans, E.P. & Smith, A.G. Changing potency by spontaneous fusion. *Nature* **416**, 545-548 (2002).
31. Lee, P.J., Hung, P.J., Shaw, R., Jan, L. & Lee, L.P. Microfluidic application-specific integrated device for monitoring direct cell-cell communication via gap junctions between individual cell pairs. *Applied Physics Letters* **86**, 223902-223903 (2005).
32. Skelley, A.M., Kirak, O., Suh, H., Jaenisch, R. & Voldman, J. Microfluidic control of cell pairing and fusion. *Nat Meth* **6**, 147-152 (2009).
33. Frimat, J.-P. et al. A microfluidic array with cellular valving for single cell co-culture. *Lab on a Chip* (2010).
34. Gel, M. et al. Dielectrophoretic cell trapping and parallel one-to-one fusion based on field constriction created by a micro-orifice array. *Biomicrofluidics* **4**, 022808-022808 (2010).
35. Gel, M. et al. in Micro-NanoMechatronics and Human Science, 2009. MHS 2009. International Symposium on 517-5202009).
36. Karp, J.M. et al. Controlling size, shape and homogeneity of embryoid bodies using poly(ethylene glycol) microwells. *Lab on a Chip* **7**, 786-794 (2007).
37. Moeller, H.-C., Mian, M.K., Shrivastava, S., Chung, B.G. & Khademhosseini, A. A microwell array system for stem cell culture. *Biomaterials* **29**, 752-763 (2008).
38. Mohr, J.C., de Pablo, J.J. & Palecek, S.P. 3-D microwell culture of human embryonic stem cells. *Biomaterials* **27**, 6032-6042 (2006).
39. Khademhosseini, A. et al. Co-culture of human embryonic stem cells with murine embryonic fibroblasts on microwell-patterned substrates. *Biomaterials* **27**, 5968-5977 (2006).
40. Khademhosseini, A. et al. Cell docking inside microwells within reversibly sealed microfluidic channels for fabricating multiphenotype cell arrays. *Lab on a Chip* **5**, 1380-1386 (2005).
41. Kamei, K.-i. et al. Microfluidic image cytometry for quantitative single-cell profiling of human pluripotent stem cells in chemically defined conditions. *Lab on a Chip* **10**, 1113-1119 (2010).

42. Ong, S.-M. et al. A gel-free 3D microfluidic cell culture system. *Biomaterials* **29**, 3237-3244 (2008).
43. Rosenthal, A., Macdonald, A. & Voldman, J. Cell patterning chip for controlling the stem cell microenvironment. *Biomaterials* **28**, 3208-3216 (2007).
44. Aubin, H. et al. Directed 3D cell alignment and elongation in microengineered hydrogels. *Biomaterials* **31**, 6941-6951 (2010).
45. Tourovskaia, A., Figueroa-Masot, X. & Folch, A. Differentiation-on-a-chip: A microfluidic platform for long-term cell culture studies. *Lab on a Chip* **5**, 14-19 (2005).
46. Ni, X.F. et al. On-chip differentiation of human mesenchymal stem cells into adipocytes. *Microelectronic Engineering* **85**, 1330-1333 (2008).
47. Zhang, F., Sensébé, L., Zhou, Y.L., Lin, C.J. & Chen, Y. Osteogenic differentiation of human mesenchymal stem cells on chip: A comparison between two nutrient feeding methods. *Microelectronic Engineering* **86**, 1459-1461 (2009).
48. Gomez-Sjoberg, R., Leyrat, A.A., Pirone, D.M., Chen, C.S. & Quake, S.R. Versatile, Fully Automated, Microfluidic Cell Culture System. *Analytical Chemistry* **79**, 8557-8563 (2007).
49. Hwang, Y.-S. et al. Microwell-mediated control of embryoid body size regulates embryonic stem cell fate via differential expression of WNT5a and WNT11. *Proceedings of the National Academy of Sciences* **106**, 16978-16983 (2009).
50. Chung, B.G. et al. Human neural stem cell growth and differentiation in a gradient-generating microfluidic device. *Lab on a Chip* **5**, 401-406 (2005).
51. Park, J.Y. et al. Differentiation of Neural Progenitor Cells in a Microfluidic Chip-Generated Cytokine Gradient. *Stem Cells* **27**, 2646-2654 (2009).
52. Figallo, E. et al. Micro-bioreactor array for controlling cellular microenvironments. *Lab on a Chip* **7**, 710-719 (2007).
53. Cimetta, E., Figallo, E., Cannizzaro, C., Elvassore, N. & Vunjak-Novakovic, G. Micro-bioreactor arrays for controlling cellular environments: Design principles for human embryonic stem cell applications. *Methods* **47**, 81-89 (2009).
54. Futai, N., Gu, W., Song, J.W. & Takayama, S. Handheld recirculation system and customized media for microfluidic cell culture. *Lab on a Chip* **6**, 149-154 (2006).
55. Kim, L., Toh, Y.-C., Voldman, J. & Yu, H. A practical guide to microfluidic perfusion culture of adherent mammalian cells. *Lab on a Chip* **7**, 681-694 (2007).
56. Chin, V.I. et al. Microfabricated platform for studying stem cell fates. *Biotechnology and Bioengineering* **88**, 399-415 (2004).
57. Lindstrom, S. et al. High-Density Microwell Chip for Culture and Analysis of Stem Cells. *PLoS ONE* **4**, e6997 (2009).
58. Gilbert, P.M. & Blau, H.M. Engineering a stem cell house into a home. *Stem cell research & therapy* **2**, 3 (2010).
59. Yamada, K.M. & Cukierman, E. Modeling tissue morphogenesis and cancer in 3D. *Cell* **130**, 601 - 610 (2007).
60. Levental, K.R. et al. Matrix crosslinking forces tumor progression by enhancing integrin signaling. *Cell* **139**, 891 - 906 (2009).
61. LaBarge, M.A. et al. Human mammary progenitor cell fate decisions are products of interactions with combinatorial microenvironments. *Integr Biol (Camb)* **1**, 70 - 79 (2009).
62. Nur, E.K.A. et al. Covalently attached FGF-2 to three-dimensional polyamide nanofibrillar surfaces demonstrates enhanced biological stability and activity. *Mol Cell Biochem* **309**, 157 - 166 (2008).
63. Fan, V.H. et al. Tethered epidermal growth factor provides a survival advantage to mesenchymal stem cells. *Stem Cells* **25**, 1241 - 1251 (2007).

64. Mehta, G. et al. Synergistic effects of tethered growth factors and adhesion ligands on DNA synthesis and function of primary hepatocytes cultured on soft synthetic hydrogels. *Biomaterials* **31**, 4657 - 4671 (2010).
65. Beckstead, B.L., Santosa, D.M. & Giachelli, C.M. Mimicking cell-cell interactions at the biomaterial-cell interface for control of stem cell differentiation. *J Biomed Mater Res A* **79**, 94 - 103 (2006).
66. Engler, A.J., Sen, S., Sweeney, H.L. & Discher, D.E. Matrix elasticity directs stem cell lineage specification. *Cell* **126**, 677 - 689 (2006).
67. Georges, P.C., Miller, W.J., Meaney, D.F., Sawyer, E.S. & Janmey, P.A. Matrices with compliance comparable to that of brain tissue select neuronal over glial growth in mixed cortical cultures. *Biophys J* **90**, 3012 - 3018 (2006).
68. Saha, K. et al. Substrate modulus directs neural stem cell behavior. *Biophys J* **95**, 4426 - 4438 (2008).
69. Mei, Y. et al. Combinatorial development of biomaterials for clonal growth of human pluripotent stem cells. *Nat Mater* **9**, 768 - 778.
70. Majka, M. et al. Numerous growth factors, cytokines, and chemokines are secreted by human CD34+ cells, myeloblasts, erythroblasts, and megakaryoblasts and regulate normal hematopoiesis in an autocrine/paracrine manner. *Blood* **97**, 3075 (2001).
71. Gerber, H.P. et al. VEGF regulates haematopoietic stem cell survival by an internal autocrine loop mechanism. *Nature* **417**, 954-958 (2002).
72. Gabrilove, J.L. Angiogenic growth factors: autocrine and paracrine regulation of survival in hematologic malignancies. *The oncologist* **6**, 4 (2001).
73. Toda, H. et al. Stem cell-derived neural stem/progenitor cell supporting factor is an autocrine/paracrine survival factor for adult neural stem/progenitor cells. *Journal of Biological Chemistry* **278**, 35491 (2003).
74. Hu, X. et al. Transplantation of hypoxia-preconditioned mesenchymal stem cells improves infarcted heart function via enhanced survival of implanted cells and angiogenesis. *The Journal of thoracic and cardiovascular surgery* **135**, 799-808 (2008).
75. Kim, L., Vahey, M.D., Lee, H.-Y. & Voldman, J. Microfluidic arrays for logarithmically perfused embryonic stem cell culture. *Lab on a Chip* **6**, 394-406 (2006).
76. Schmierer, B. & Hill, C.S. TGF –SMAD signal transduction: molecular specificity and functional flexibility. *Nature Reviews Molecular Cell Biology* **8**, 970-982 (2007).
77. Ozil, J.P. et al. Egg activation events are regulated by the duration of a sustained [Ca2+] cyt signal in the mouse. *Developmental Biology* **282**, 39-54 (2005).
78. Corish, P. & Tyler-Smith, C. Attenuation of green fluorescent protein half-life in mammalian cells. *Protein Engineering* **12**, 1035-1040 (1999).
79. Williams, R.L. et al. Myeloid leukaemia inhibitory factor maintains the developmental potential of embryonic stem cells. *Nature* **336**, 684-687 (1988).
80. Desai, S.P., Freeman, D.M. & Voldman, J. Plastic masters-rigid templates for soft lithography. *Lab on a Chip* **9**, 1631-1637 (2009).
81. Nevill, J.T. et al. Vacuum soft lithography to direct neuronal polarization. *Soft Matter* **7**, 343-347.
82. Denn, M.M. Process fluid mechanics. (Prentice Hall, 1980).
83. Chin, V.I. et al. Microfabricated platform for studying stem cell fates. *Biotechnol Bioeng* **88**, 399 - 415 (2004).
84. PubChem.
85. Sigma-Aldrich.

86. Periasamy, N. & Verkman, A.S. Analysis of fluorophore diffusion by continuous distributions of diffusion coefficients: application to photobleaching measurements of multicomponent and anomalous diffusion. *Biophysical journal* **75**, 557-567 (1998).
87. Thomson, J.A. et al. Embryonic stem cell lines derived from human blastocysts. *Science* **282**, 1145 (1998).
88. Solter, D. & Knowles, B.B. Immunosurgery of mouse blastocyst. *Proceedings of the National Academy of Sciences of the United States of America* **72**, 5099 (1975).
89. Prokhorova, T.A. et al. Teratoma formation by human embryonic stem cells is site dependent and enhanced by the presence of Matrigel. *Stem Cells and Development* **18**, 47-54 (2009).
90. Shih, C.C., Forman, S.J., Chu, P. & Slovak, M. Human embryonic stem cells are prone to generate primitive, undifferentiated tumors in engrafted human fetal tissues in severe combined immunodeficient mice. *Stem Cells and Development* **16**, 893-902 (2007).
91. Lawrenz, B. et al. Highly sensitive biosafety model for stem-cell-derived grafts. *Cytotherapy* **6**, 212-222 (2004).
92. Gurdon, J.B. The developmental capacity of nuclei taken from intestinal epithelium cells of feeding tadpoles. *Journal of Embryology and Experimental Morphology* **10**, 622 (1962).
93. Takahashi, K. & Yamanaka, S. Induction of pluripotent stem cells from mouse embryonic and adult fibroblast cultures by defined factors. *Cell* **126**, 663-676 (2006).
94. Trond Aasen, A.R., Maria, J.B., Elena Garreta, A.C. & Federico Gonzalez, R.V. Efficient and rapid generation of induced pluripotent stem cells from human keratinocytes. *Nature biotechnology* **26**, 1276-1284 (2008).
95. Chambers, S.M. et al. Highly efficient neural conversion of human ES and iPS cells by dual inhibition of SMAD signaling. *Nature biotechnology* **27**, 275-280 (2009).
96. Park, I.H. et al. Reprogramming of human somatic cells to pluripotency with defined factors. *Nature* **451**, 141-146 (2007).
97. Huangfu, D. et al. Induction of pluripotent stem cells by defined factors is greatly improved by small-molecule compounds. *Nature biotechnology* **26**, 795-797 (2008).
98. Huangfu, D. et al. Induction of pluripotent stem cells from primary human fibroblasts with only Oct4 and Sox2. *Nature biotechnology* **26**, 1269-1275 (2008).
99. Yu, J. et al. Human induced pluripotent stem cells free of vector and transgene sequences. *Science* **324**, 797 (2009).
100. Kim, D. et al. Generation of human induced pluripotent stem cells by direct delivery of reprogramming proteins. *Cell Stem Cell* **4**, 472 (2009).
101. Soldner, F. et al. Parkinson's disease patient-derived induced pluripotent stem cells free of viral reprogramming factors. *Cell* **136**, 964-977 (2009).
102. Woltjen, K. et al. piggyBac transposition reprograms fibroblasts to induced pluripotent stem cells. *Nature* **458**, 766-770 (2009).
103. Jia, F. et al. A nonviral minicircle vector for deriving human iPS cells. *Nature methods* **7**, 197 (2010).
104. Lyssiotis, C.A. et al. Reprogramming of murine fibroblasts to induced pluripotent stem cells with chemical complementation of Klf4. *Proceedings of the National Academy of Sciences* **106**, 8912 (2009).
105. Yusa, K., Rad, R., Takeda, J. & Bradley, A. Generation of transgene-free induced pluripotent mouse stem cells by the piggyBac transposon. *Nature methods* **6**, 363-369 (2009).
106. Kaji, K. et al. Virus-free induction of pluripotency and subsequent excision of reprogramming factors. *Nature* **458**, 771-775 (2009).
107. Okita, K., Nakagawa, M., Hyenjong, H., Ichisaka, T. & Yamanaka, S. Generation of mouse induced pluripotent stem cells without viral vectors. *Science* **322**, 949 (2008).

108. Colman, A. & Dreesen, O. Pluripotent stem cells and disease modeling. *Cell Stem Cell* **5**, 244-247 (2009).
109. Saha, K. & Jaenisch, R. Technical challenges in using human induced pluripotent stem cells to model disease. *Cell Stem Cell* **5**, 584-595 (2009).
110. Lengerke, C. & Daley, G.Q. Disease models from pluripotent stem cells. *Annals of the New York Academy of Sciences* **1176**, 191-196 (2009).
111. Takahashi, K. et al. Induction of pluripotent stem cells from adult human fibroblasts by defined factors. *Cell* **131**, 861-872 (2007).
112. Yu, J. et al. Induced pluripotent stem cell lines derived from human somatic cells. *Science* **318**, 1917 (2007).
113. Amit, M. et al. Clonally derived human embryonic stem cell lines maintain pluripotency and proliferative potential for prolonged periods of culture. *Developmental Biology* **227**, 271-278 (2000).
114. Xu, C. et al. Feeder-free growth of undifferentiated human embryonic stem cells. *Nature biotechnology* **19**, 971-974 (2001).
115. Stojkovic, P. et al. Human Serum Matrix Supports Undifferentiated Growth of Human Embryonic Stem Cells. *Stem Cells* **23**, 895-902 (2005).
116. Braam, S.R. et al. Recombinant Vitronectin Is a Functionally Defined Substrate That Supports Human Embryonic Stem Cell Self Renewal via V 5 Integrin. *Stem Cells* **26**, 2257-2265 (2008).
117. Li, Y., Powell, S., Brunette, E., Lebkowski, J. & Mandalam, R. Expansion of human embryonic stem cells in defined serum free medium devoid of animal derived products. *Biotechnology and bioengineering* **91**, 688-698 (2005).
118. Amit, M., Shariki, C., Margulets, V. & Itskovitz-Eldor, J. Feeder layer-and serum-free culture of human embryonic stem cells. *Biology of reproduction* **70**, 837 (2004).
119. Yao, S. et al. (National Acad Sciences, 2006).
120. Ludwig, T.E. et al. Feeder-independent culture of human embryonic stem cells. *Nature methods* **3**, 637-646 (2006).
121. Ludwig, T.E. et al. Derivation of human embryonic stem cells in defined conditions. *Nature biotechnology* **24**, 185-187 (2006).
122. Rodin, S. et al. Long-term self-renewal of human pluripotent stem cells on human recombinant laminin-511. *Nature biotechnology* **28**, 611-615 (2010).
123. Li, Y.J., Chung, E.H., Rodriguez, R.T., Firpo, M.T. & Healy, K.E. Hydrogels as artificial matrices for human embryonic stem cell self renewal. *Journal of Biomedical Materials Research Part A* **79**, 1-5 (2006).
124. Gerecht, S. et al. Hyaluronic acid hydrogel for controlled self-renewal and differentiation of human embryonic stem cells. *Proceedings of the National Academy of Sciences* **104**, 11298 (2007).
125. Villa-Diaz, L.G. et al. Synthetic polymer coatings for long-term growth of human embryonic stem cells. *Nature biotechnology* **28**, 581-583 (2010).
126. Melkoumian, Z. et al. Synthetic peptide-acrylate surfaces for long-term self-renewal and cardiomyocyte differentiation of human embryonic stem cells. *Nature biotechnology* **28**, 606-610 (2010).
127. Wernig, M. et al. A drug-inducible transgenic system for direct reprogramming of multiple somatic cell types. *Nature biotechnology* **26**, 916-924 (2008).
128. Hockemeyer, D. et al. A drug-inducible system for direct reprogramming of human somatic cells to pluripotency. *Cell Stem Cell* **3**, 346-353 (2008).
129. Maherali, N. et al. A high-efficiency system for the generation and study of human induced pluripotent stem cells. *Cell Stem Cell* **3**, 340-345 (2008).

130. Yin, S. et al. CD133 positive hepatocellular carcinoma cells possess high capacity for tumorigenicity. *International journal of cancer* **120**, 1444-1450 (2007).
131. Castaigne, S. et al. All-trans retinoic acid as a differentiation therapy for acute promyelocytic leukemia. I. Clinical results [see comments]. *Blood* **76**, 1704 (1990).
132. Sell, S. Stem cell origin of cancer and differentiation therapy. *Critical reviews in oncology/hematology* **51**, 1-28 (2004).
133. Leszczyniecka, M., Roberts, T., Dent, P., Grant, S. & Fisher, P.B. Differentiation therapy of human cancer: basic science and clinical applications. *Pharmacology & Therapeutics* **90**, 105-156 (2001).
134. Hanahan, D. & Weinberg, R.A. The Hallmarks of Cancer. *Cell* **100**, 57-70 (2000).
135. Kucia, M. et al. Trafficking of Normal Stem Cells and Metastasis of Cancer Stem Cells Involve Similar Mechanisms: Pivotal Role of the SDF 1–CXCR4 Axis. *Stem Cells* **23**, 879-894 (2005).
136. Hermann, P.C. et al. Distinct populations of cancer stem cells determine tumor growth and metastatic activity in human pancreatic cancer. *Cell Stem Cell* **1**, 313-323 (2007).
137. Li, L. & Neaves, W.B. Normal stem cells and cancer stem cells: the niche matters. *Cancer research* **66**, 4553 (2006).
138. Wynn, R.F. et al. A small proportion of mesenchymal stem cells strongly expresses functionally active CXCR4 receptor capable of promoting migration to bone marrow. *Blood* **104**, 2643 (2004).
139. Li, C. et al. Identification of pancreatic cancer stem cells. *Cancer research* **67**, 1030 (2007).
140. Cariati, M. et al. Alpha 6 integrin is necessary for the tumourigenicity of a stem cell like subpopulation within the MCF7 breast cancer cell line. *International journal of cancer* **122**, 298-304 (2008).
141. Krystal, G.W., Hines, S.J. & Organ, C.P. Autocrine growth of small cell lung cancer mediated by coexpression of c-kit and stem cell factor. *Cancer research* **56**, 370 (1996).
142. Boccaccio, C. & Comoglio, P.M. Invasive growth: a MET-driven genetic programme for cancer and stem cells. *Nature Reviews Cancer* **6**, 637-645 (2006).
143. Bapat, S.A., Mali, A.M., Koppikar, C.B. & Kurrey, N.K. Stem and progenitor-like cells contribute to the aggressive behavior of human epithelial ovarian cancer. *Cancer research* **65**, 3025 (2005).
144. Kucia, M. et al. A population of very small embryonic-like (VSEL) CXCR4+ SSEA-1+ Oct-4+ stem cells identified in adult bone marrow. *Leukemia* **20**, 857-869 (2006).
145. Chiou, S.H. et al. Positive correlations of Oct-4 and Nanog in oral cancer stem-like cells and high-grade oral squamous cell carcinoma. *Clinical Cancer Research* **14**, 4085 (2008).
146. Hart, A.H. et al. The pluripotency homeobox gene NANOG is expressed in human germ cell tumors. *Cancer* **104**, 2092-2098 (2005).
147. Spira, A.I. & Carducci, M.A. Differentiation therapy. *Current Opinion in Pharmacology* **3**, 338-343 (2003).
148. Beere, H.M. & Hickman, J.A. Differentiation: a suitable strategy for cancer chemotherapy? *Anti-cancer drug design* **8**, 299 (1993).
149. Kawamata, H., Tachibana, M., Fujimori, T. & Imai, Y. Differentiation-inducing therapy for solid tumors. *Current pharmaceutical design* **12**, 379-385 (2006).
150. Dean, M., Fojo, T. & Bates, S. Tumour stem cells and drug resistance. *Nature Reviews Cancer* **5**, 275-284 (2005).
151. Eyler, C.E. & Rich, J.N. Survival of the fittest: cancer stem cells in therapeutic resistance and angiogenesis. *Journal of Clinical Oncology* **26**, 2839 (2008).
152. Donnenberg, V.S. & Donnenberg, A.D. Multiple drug resistance in cancer revisited: the cancer stem cell hypothesis. *The Journal of Clinical Pharmacology* **45**, 872 (2005).
153. Gottesman, M.M. Mechanisms of cancer drug resistance. *Annual review of medicine* **53**, 615-627 (2002).

154. Bao, S. et al. Glioma stem cells promote radioresistance by preferential activation of the DNA damage response. *Nature* **444**, 756-760 (2006).
155. Smalley, M. & Ashworth, A. Stem cells and breast cancer: a field in transit. *Nature Reviews Cancer* **3**, 832-844 (2003).
156. Salama, P. & Platell, C. Colorectal cancer stem cells. *ANZ Journal of Surgery* **79**, 697-702 (2009).
157. Wulf, G.G. et al. A leukemic stem cell with intrinsic drug efflux capacity in acute myeloid leukemia. *Blood* **98**, 1166 (2001).
158. Feuring-Buske, M. & Hogge, D.E. Hoechst 33342 efflux identifies a subpopulation of cytogenetically normal CD34+ CD38- progenitor cells from patients with acute myeloid leukemia. *Blood* **97**, 3882 (2001).
159. Szotek, P.P. et al. Ovarian cancer side population defines cells with stem cell-like characteristics and Mullerian Inhibiting Substance responsiveness. *Proceedings of the National Academy of Sciences* **103**, 11154 (2006).
160. Chiba, T. et al. Side population purified from hepatocellular carcinoma cells harbors cancer stem cell–like properties. *Hepatology* **44**, 240-251 (2006).
161. Hirschmann-Jax, C. et al. A distinct "side population" of cells with high drug efflux capacity in human tumor cells. *Proceedings of the National Academy of Sciences of the United States of America* **101**, 14228 (2004).
162. Setoguchi, T., Taga, T. & Kondo, T. Cancer stem cells persist in many cancer cell lines. *Cell Cycle* **3**, 414-415 (2004).
163. Shen, G. et al. Identification of cancer stem-like cells in the C6 glioma cell line and the limitation of current identification methods. *In Vitro Cellular & Developmental Biology-Animal* **44**, 280-289 (2008).
164. Ho, M.M., Ng, A.V., Lam, S. & Hung, J.Y. Side population in human lung cancer cell lines and tumors is enriched with stem-like cancer cells. *Cancer research* **67**, 4827 (2007).
165. Mitsutake, N. et al. Characterization of side population in thyroid cancer cell lines: cancer stem-like cells are enriched partly but not exclusively. *Endocrinology* **148**, 1797 (2007).
166. Wang, J., Guo, L.P., Chen, L.Z., Zeng, Y.X. & Lu, S.H. Identification of cancer stem cell–like side population cells in human nasopharyngeal carcinoma cell line. *Cancer research* **67**, 3716 (2007).
167. Patrawala, L. et al. Side population is enriched in tumorigenic, stem-like cancer cells, whereas ABCG2+ and ABCG2- cancer cells are similarly tumorigenic. *Cancer research* **65**, 6207 (2005).
168. Goodell, M.A., McKinney-Freeman, S. & Camargo, F.D. Isolation and characterization of side population cells. *METHODS IN MOLECULAR BIOLOGY-CLIFTON THEN TOTOWA*- **290**, 343-352 (2005).
169. Yuan, X. et al. Isolation of cancer stem cells from adult glioblastoma multiforme. *Oncogene* **23**, 9392-9400 (2004).
170. Jensen, J. & Parmar, M. Strengths and limitations of the neurosphere culture system. *Molecular Neurobiology* **34**, 153-161 (2006).
171. Reynolds, B.A. & Weiss, S. Generation of neurons and astrocytes from isolated cells of the adult mammalian central nervous system. *Science* **255**, 1707-1710 (1992).

APPENDIX A: SUPPLEMENTAL DEVICE CHARACTERIZATION

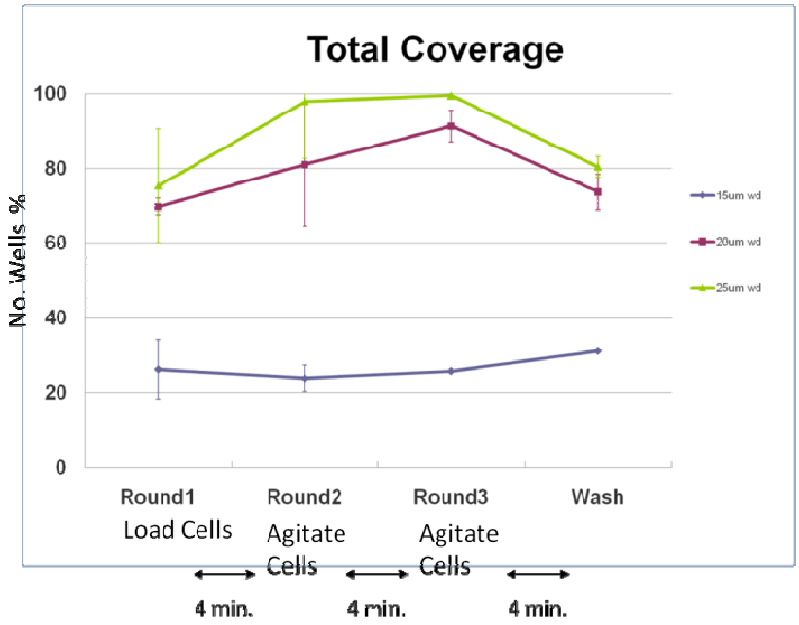

Figure 35. Effect of agitation on cell loading efficiency. One or two rounds of agitation is enough to almost completely fill larger microwells (20x20µm and 25x25µm). All wells are 30µm deep.

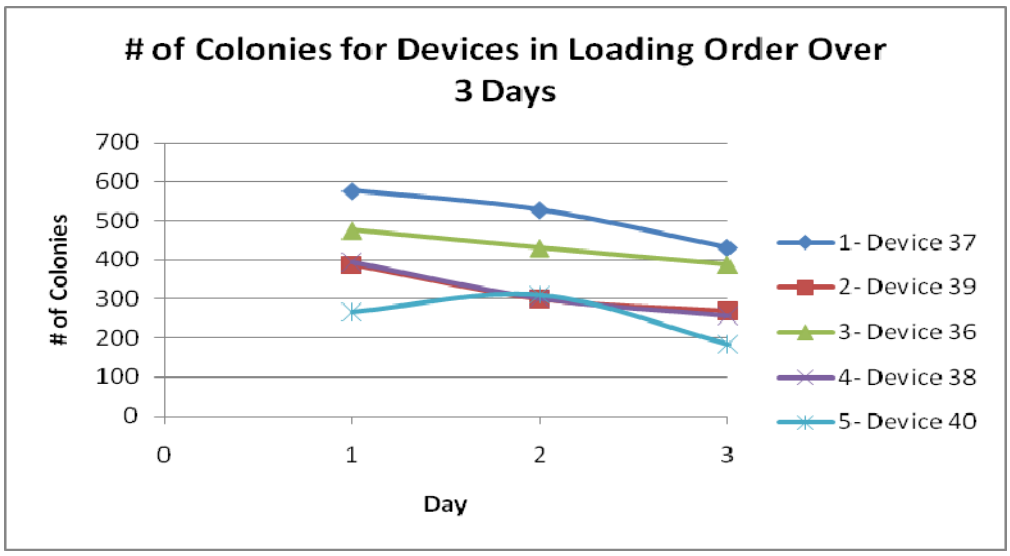

Figure 36. Number of mouse stem cell colonies for devices 37, 39, 36, 38, and 40 [in loading order] over the first three days of culture. The same stem cell suspension was used for all five devices. The devices were loaded in sequential order. Please note that last device loaded has only half as many surviving colonies by Day 3 as the first device loaded, indicating temperature sensitivity of the mouse ES cells.

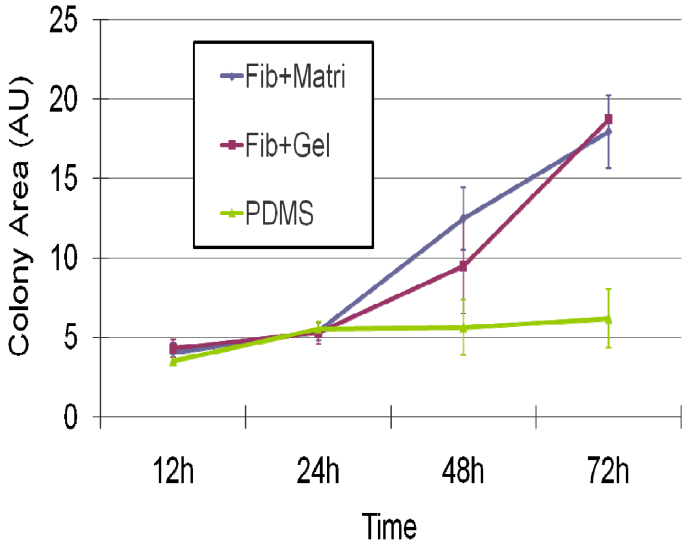

Figure 37. Comparison of various ECM substrates and effect on mouse embryonic stem cell growth. Matrigel 500:1 and 0.2% gelatin both showed comparable growth rates in agreement with previously published data.

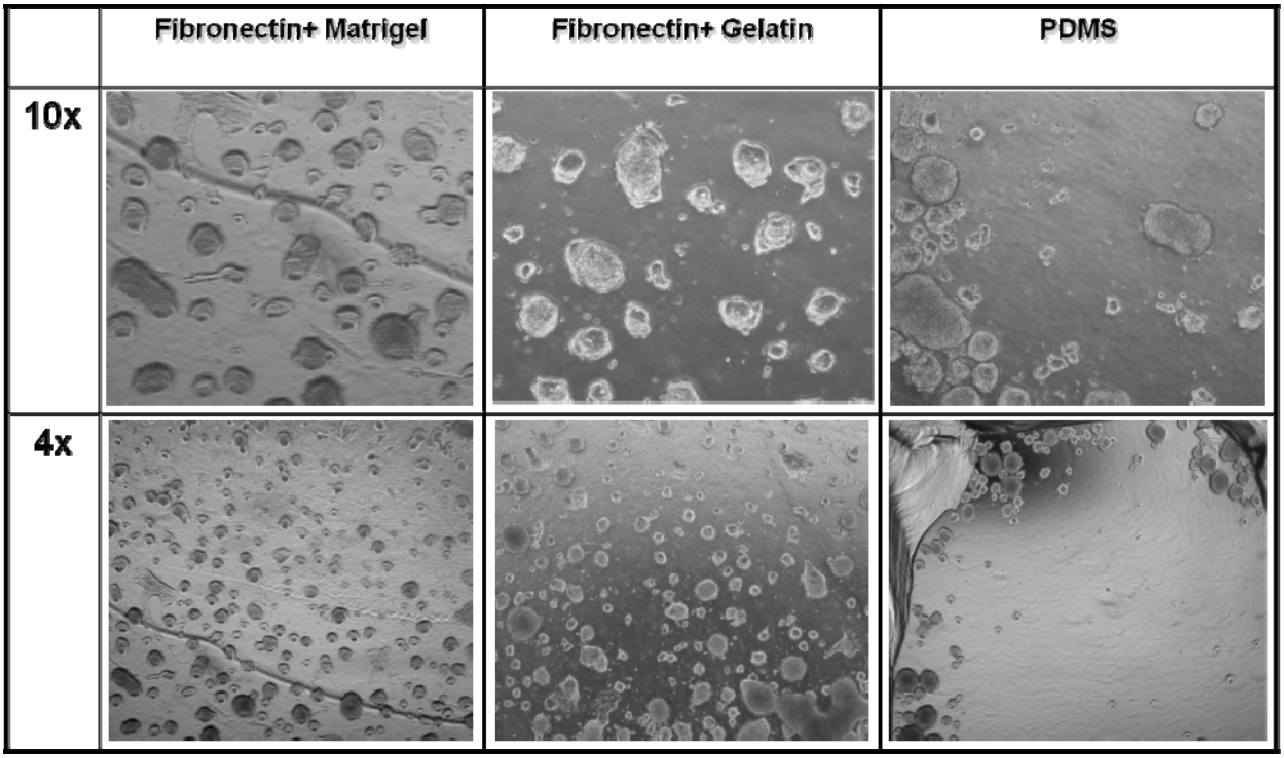

Figure 38. PDMS devices could be coated with Matrigel or gelatin directly without the use of fibronectin as an adhesion layer, but glass substrates required an adhesion coating of fibronectin to effectively coat Matrigel or gelatin as growth substrates. Bare PDMS shows very little stem cell adhesion and was discounted as a suitable culture substrate.

APPENDIX B: CANCER STEM CELL BIOLOGY

Introduction

Metastasis in cancer accounts of over 90% of lethality in cancer patients, yet scientists do not have a comprehensive metastasis model on which to perform research. One promising metastatic model candidate is the existence of cancer stem cells. While these cells comprise a tiny portion of the tumor's mass, these special tumor cells are 1000-10,000 times as tumorigenic and able to form new tumors within mouse models easily.[130] Since cancer stem cells are especially resistant to standard chemo- and radiotherapy, one approach to killing these key stem cells is to use a drug to induce them to terminally differentiate, effectively removing the tumor's proliferative and metastatic abilities.[64, 131-133] The absolute biggest challenge facing the field of cancer stem cell research is the relative scarcity of these cells; simply put, it is hard to accumulate enough cancer stem cells to do research on them using the standard tissue culture technique that has been used for the last 100 years. We propose to innovate cancer stem cell research through a microfluidic platform which can generate more data points than conventional techniques, but requires only 1/100 the normal number of cells, opening up the possibility of doing research on actual patient biopsy samples. The lab-on-a-chip platform also integrates on-chip cell trapping, drug concentration gradient generation, and real-time monitoring abilities which are difficult to achieve using culture plates.

Clinical Therapy of Cancer Stem Cells

Cancer is one of the leading causes of death in the United States. And in particular, metastases account for over 90% of the lethality in cancer patients.[134] Since metastasis is one of the main thrusts of cancer research, a lot of attention has been focused on finding appropriate models for research. One of the proposed models for the study of metastasis is the existence of cancer stem cells (CSC). These so called cancer stem cells are named that way because they share many biological characteristics with embryonic stem cells, which have been under study for much longer. These special subpopulations seem to drive tumor growth and recurrence. While these cells comprise only 0.1-1% of the tumor mass, they have 1000 to 10,000 times the tumorigenicity of the rest of the tumor.[130] This implies that cancer stem cells have special characteristics which make them especially suited to survive in a foreign tissue and start proliferating. To provide further evidence that cancer stem cells may be the key cells behind metastasis, these stem cells are known to express surface markers that are either identified as stem cell markers or are associated with homing and metastasis (CXCR4, CD133, α6 integrin, c-kit, c-met, LIF-R).[135-144] And of particular interest to our research, cancer stem cells express key transcription factors, such as Nanog, which promote pluripotency and immortality (Figure 39). While the existence of

cancer stem cells is gaining credence in literature, their origins *in vivo* are unknown (Figure 40).

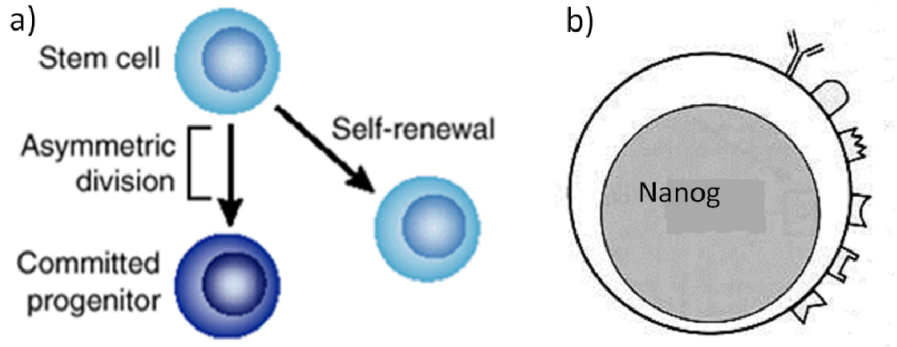

Figure 39. Cancer stem cells exhibit many of the characteristics of embryonic and adult stem cells such as a) the capacity for self-renewal, and b) expression of key transcription factors which promote pluripotency and immortality such as Nanog.

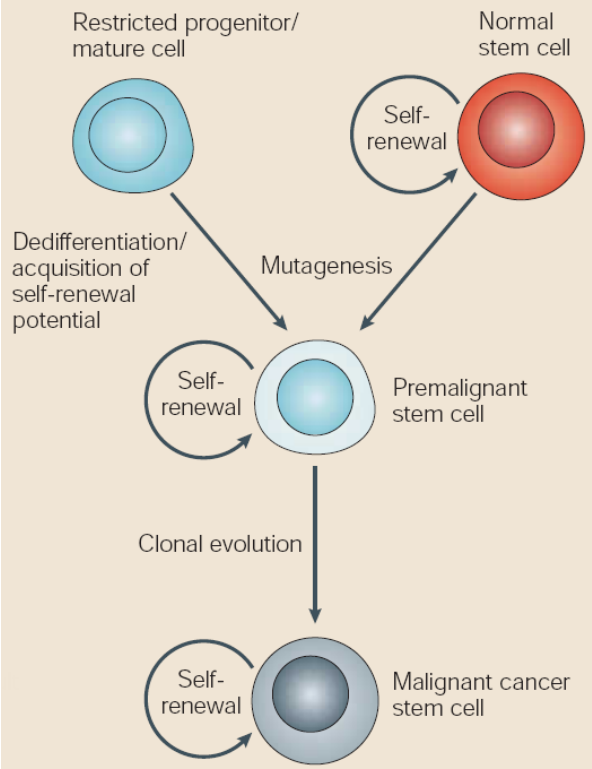

Figure 40. Proposed acquired mutagenesis steps which can generate a cancer stem cell from a mature cell or a normal stem cell. *in vivo* origins are still under debate.

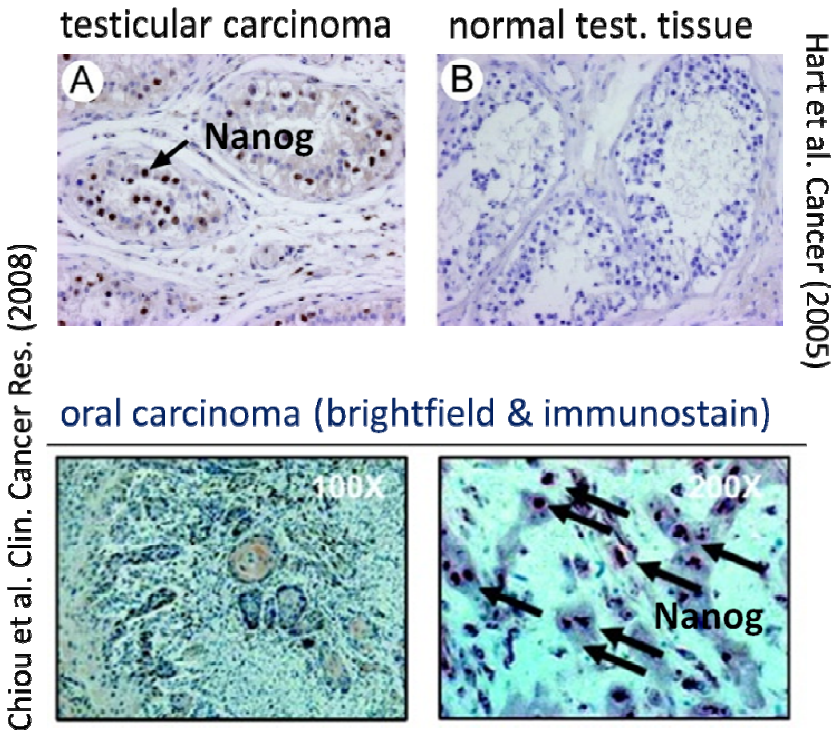

Figure 41. Tissue biopsy samples from patient tumors immunostained for Nanog protein. The presence of Nanog+ cells supports the hypothesis that clinical tumors contain cancer stem cells which express Nanog.[145, 146]

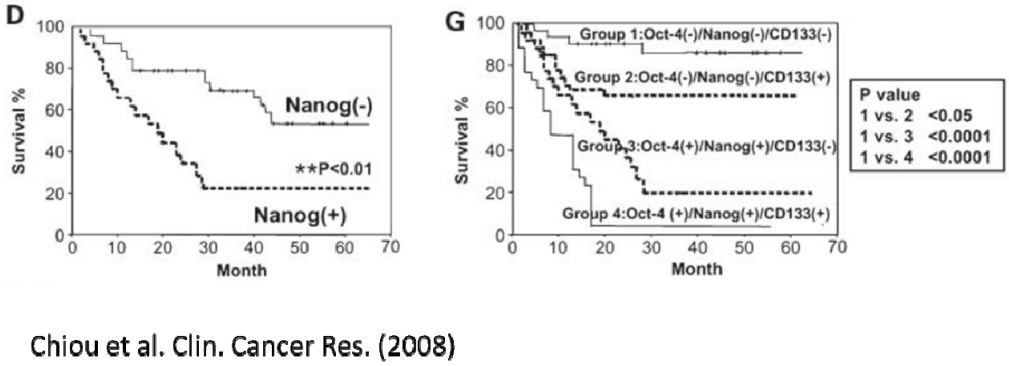

Figure 42. Kaplan-Meier analyses demonstrated that Nanog/Oct-4/CD133 triple-positive patients predicted the worst survival prognosis of the 52 oral cancer patients.[145]

If cancer stem cells are truly the key cells behind the development of metastases, then the way we think of patient treatment has to be reevaluated. Standard chemotherapy and radiation therapy focus on killing rapidly proliferating cells by inducing sufficient amounts of DNA damage such that the cells are driven to commit suicide through apoptosis. If the chemotherapy does not kill the cancer stem cells even though the bulk of the tumor is removed, the cancer stem cells will regrow the tumor once treatment is stopped and the patient relapses (Figure 43). If we instead focus in

targeting the cancer stem cells within a tumor, we can kill the proliferative engine of the tumor and then work on forcing the cancer into remission through surgery and chemotherapy.[131-133, 147-149]

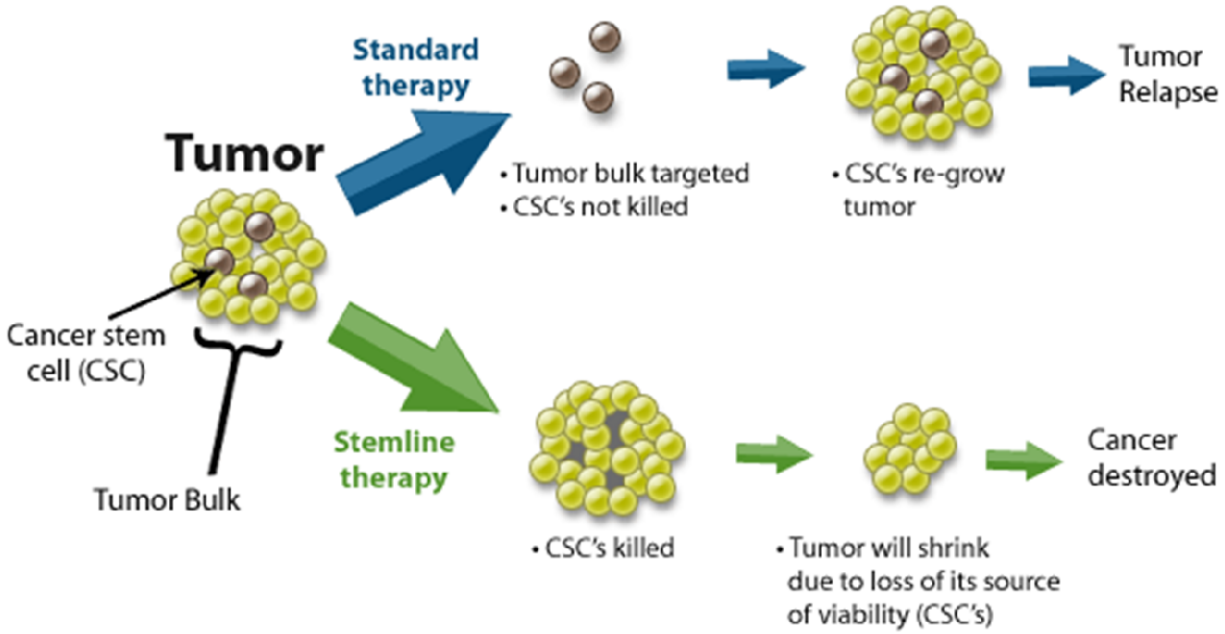

Figure 43. Proposed changes to clinical therapy of cancer patients where the cancer stem cells are targeted instead of all rapidly proliferating cells.

The reason standard cancer therapy seems to not be as effective against cancer stem cells is that they have multiple natural defenses against DNA damage including specialized membrane drug pumps to pump out the toxins,[150-153] high levels of DNA repair proteins,[154] and a slower rate of division than their daughter cells which make up the bulk of the tumor mass.[155, 156] All these factors greatly decrease the effect chemo- and radiotherapy have on the survival of these special cancer cells. Since cancer stem cells are so unresponsive to conventional treatment, we will need to think outside the box. One hypothesis for targeting cancer stem cells is differentiation therapy. The premise of differentiation therapy is that we induce the cancer stem cells to terminally differentiate, *i.e.* to lose their stem cell properties and behave like normal cells. Once the cancer stem cells are differentiated, they will lose their ability to proliferate without control as well as most of their natural defenses against standard chemotherapy (Figure 44). The loss of its cancer stem cells for a tumor is like removing its engine: proliferation stops, and the ability to seed new tumors as metastases is taken away. The tumor is essentially benign and can be treated through surgery and standard chemotherapy. Patient mortality is greatly reduced as the cancer is regressed back to a pre-metastatic stage.

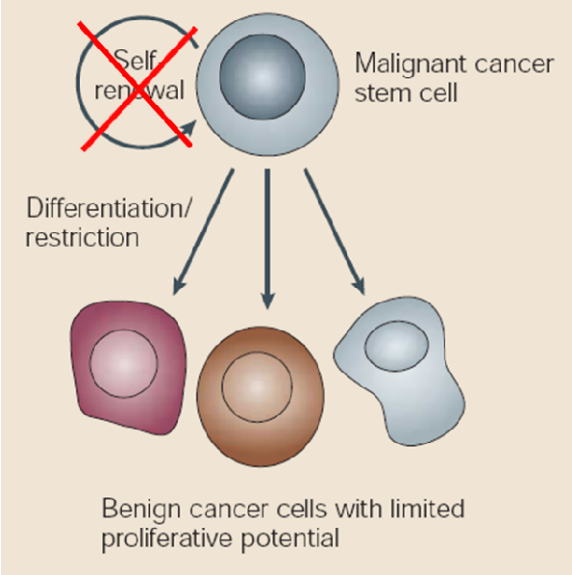

Figure 44. Effect of differentiation therapy is to eliminate the cancer stem cell's ability to self-renew and proliferate by pushing the cancer stem cell towards a terminally differentiated state, thus making the cell more receptive to standard chemotherapy drugs.

Current Challenges and Possible Contributions

While cancer stem cells (CSC) are a hot new field in cancer biology, there exist several key challenges which must be overcome. The first is the difficulty researchers face in purifying and enriching a cell sample to study. Currently, there are three methods commonly employed for the isolation of cancer stem cells: (1) flow cytometry based on Hoescht dye efflux, (2) flow cytometry based upon cell surface marker expression, and (3) sphere culture. These methods lead to varying degrees of enrichment of CSCs, and each has its advantages and limitations. Hoescht exclusion sorting has been able to identify side populations which are relevant to a variety of tumors,[157-168] but it is generally agreed that the side populations isolated do not represent a homogenous population of CSCs. Furthermore, there have been reports that the Hoescht dye can have deleterious effects on cells.[164] The next method, sphere culture, takes advantage of the fact that some CSCs can naturally give rise to spheres in culture. Although culturing for spheres is an easier method of enrichment compared with the other two methods which requires FACS, the resulting spheres still represent a heterogeneous population with only a portion of the cells capable of self-renewal. [169, 170] The last method, sorting by cell surface markers, is the most common method used to sort out relevant side populations since it has the most precision in sorting out a homogenous population, but there are key limitations. The number of CSCs usually identified by this method is always low, requiring a large number of cells to be sorted. This is especially problematic when isolating cells from tumor samples that are often small in size (~300-1000 CSCs per small animal). Also, isolation of CSCs from tissues requires the cells to be enzymatically dissociated, which can damage some of the surface antigens expressed.[171]

Once a homogenous cancer stem cell population has been sorted out, the next step would optimally be expansion of that cell population to maximize the number of experiments which could be performed, however expansion of adherent CSCs is currently a difficult problem. For that reason, leukemia is the most well-studied branch of CSCs since blood cells do not require a solid substrate for expansion. To expand research into carcinomas, which encompass the large majority of clinical cancers, several labs are performing high-throughput screening of extracellular matrix combinations to find the optimal growth substrate. Linked to the screening of appropriate growth substrates is screening for the appropriate medium formulation necessary to maintain cancer stem cells long-term. These are all works in progress by leading researchers in the field of cancer stem cells.

Multiple papers have used cancer stem cells purified from actual patient tumors to show that these stem cells merit intense attention, but patient samples yield only enough cells for very preliminary key studies. Our proposed microfluidic platform will overcome the cell scarcity challenge by being able to harvest large amounts of data out of each experiment. Since our device is engineered to treat every single stem cell as a complete data set (spatial and temporal data), research can even be performed on patient tumor biopsy samples which generally only yield a few thousand cells at the most. For another facet of research, our microfluidic platform can also be used by pharmaceutical companies to quickly screen their small molecule libraries for promising drug candidates. Also, since every cancer patient is unique, personalized testing of drug candidates on actual patient samples would greatly decrease the amount of time wasted on treatments which don't work. In addition to testing a concentration spectrum of just one drug, our microfluidic device can also handle drug combinatorial gradients and thus highlight promising drug regimens for the doctors to try. The ability to screen drug candidates on the large scale is currently out of reach.